

Diagnostic assessment on urban floods using satellite data and hydrologic models in Kigali, Rwanda.

MARC MANYIFIKA

February, 2015

SUPERVISORS:

Dr. Ing. T.H.M. RIENTJES (Tom)

Ir. G.N. PARODI (Gabriel)



Diagnostic assessment on urban floods using satellite data and hydrologic models in Kigali, Rwanda.

MARC MANYIFIKA

Enschede, The Netherlands, February, 2015

Thesis submitted to the Faculty of Geo-Information Science and Earth Observation of the University of Twente in partial fulfilment of the requirements for the degree of Master of Science in Geo-information Science and Earth Observation.

Specialization: Water Resources and Environmental Management.

SUPERVISORS:

Dr. Ing. T.H.M. RIENTJES (Tom)

Ir. G.N. PARODI (Gabriel)

THESIS ASSESSMENT BOARD:

Dr. Ir. C. van der Tol (Chair)

Prof. Dr. P. Reggiani University of Siegen - Germany

Dr. Ing. T.H.M. RIENTJES (Tom) first supervisor

Ir. G.N. PARODI (Gabriel) second supervisor

DISCLAIMER

This document describes work undertaken as part of a programme of study at the Faculty of Geo-Information Science and Earth Observation of the University of Twente. All views and opinions expressed therein remain the sole responsibility of the author, and do not necessarily represent those of the Faculty.

ABSTRACT

The Nyabugogo commercial hub, downtown Kigali is a historically key commercial center of Kigali city and it is located geographically between the Mont Kigali and Mont Jali in a bottleneck manner. In the past few years, the area has been characterized with frequent flooding events for which no records once or ever were taken. Additionally, the hydrological knowledge on the causes and routing of water leading to flooding was lacking. In this study, an analysis of the frequent flooding was done and to overcome the significant problem of data scarcity satellite data, rainfall-runoff modelling and hydrodynamic flood modelling were applied. The CMORPH 8km 30min which were time variably bias corrected were used to identify and analyse the extreme rainfall events susceptible of causing flooding in the study area. The HEC-HMS NRCS CN model, the Muskingum routing model and the baseflow recession model were applied to estimate the upstream runoff which were used as boundary inflows to the flood model. The developed rainfall-runoff models of the gauged sub catchments were calibrated and the resulting optimum parameter values were locally regionalized to estimate the unknown parameter values of the ungauged sub catchments. This regionalization was based on the principles of area conversion, main channel length conversion and the gauged sub catchments proximity factor. An overall calibration of the entire Nyabugogo catchment rainfall-runoff model set up was done using the flow measurements of the Nemba gauging station. The calibration used three objective functions which were the Peak weighted root mean square error (PWRMSE), the relative volumetric error (RVE) and the Nash-Sutcliffe (NS) allowing the control of the peak simulation, the volume and the hydrograph shape respectively. A PWRMSE of 3.4, a RVE of -4.9 and a NS of 0.6 were obtained after the model calibration. Four extreme rainfall events were selected in this study and their spacial-temporal patterns were analysed. It was found that a horizontal movement from east to west was common to all the selected events and higher rainfall amount were observed during the periods of March-April-May and October-November-December corresponding to the two yearly rainfall seasons in the region. It was also found that the sub catchments of Karuruma, Mpazi, Muhazi, Nyacyonga, Rufigiza, Rugunga and Yanze contributed higher amount of runoff in the Nyabugogo river during the selected flooding events. The resulting upstream runoff were forced into the flood model set up in Sobek 1D2D. The effect of the DEM resolution, building representation and surface roughness were analysed during the stepwise set up of the flood model. A 10m resolution DTM, locally available, was used to interpolate the different resolutions used in this study. It was found that coarser resolutions led to larger inundation areas, higher maximum depths and flood durations. It was also found that fine resolutions required very long simulation periods (more than 3 days for a 5m resolution). The flood model was found to be significantly sensitive to the surface roughness. The simulations of the selected events in Sobek revealed strong backwater effects at the confluence points of the Nyabugogo river and its tributaries Yanze and Mpazi.

Keywords: CMORPH, extreme rainfall events, rainfall-runoff modelling, HEC-HMS, regionalization, hydrodynamic flood modelling, Sobek 1D2D.

ACKNOWLEDGEMENTS

First and foremost, all thanks go to the Almighty God.

I would like to express my sincere gratitude to the Government of The Netherlands through the Netherlands Fellowship Program (NFP) for the opportunity offered to me to pursue my master of science studies in the Netherlands. I would like also to thank the Government of Rwanda through the Ministry of Natural Resources (MINIRENA) and the Rwanda Natural Resources Authority/Integrated Water Resources Management Department (IWRMD) for allowing me to pursue my study and granting me a study leave.

I would like to also thank the University of Twente through its Faculty of Geo-information Science and Earth observation and the Water Resources department for all the help in increasing my knowledge and academic curriculum. Many thanks to all the lecturers and staff for making my stay pleasant and instructive.

Special thanks to my supervisor Dr. Ir. Tom Rientjes for his dedication and critical comments on my work. Your guidance and advices were of significant help in the completion of this thesis.

Special thanks to my work supervisor Mr. Vincent de Paul KABALISA and the Integrated Water Resources Management department for encouraging me to do this, for supporting my fieldwork and providing me all the necessary equipments needed. Mr. Davis BUGINGO, my friend, I am very grateful for all your help in my fieldwork, may you and your family be blessed for ever.

Special thanks to my colleagues and classmates for their friendship and support throughout my stay at ITC. It was an honor to spend 18 months in your company. May you for ever be blessed.

Special thanks to the Rwandan community in ITC (Fred, Gilbert, Elias, Ignace, Appolonie and Dominique) and in Enschede. Aime Olivier N. thanks for your friendship. Guys, I will forever cherish the memories we shared during these 18 months.

Special thanks to my family for their encouragement and moral support. To my Dad, my Mum, my sisters and brothers, and my Uncle (Vavo). The distance between us did mean nothing. I hope I made you guys proud.

Last but not least, special thanks to my lady (boo) for your love, encouragement and support. You were always there despite the distance...and yes “*azoca uwambaye*”.

TABLE OF CONTENTS

1. INTRODUCTION	1
1.1. BACKGROUND	1
1.2. PROBLEM STATEMENT	3
1.3. RATIONAL OF THE RESEARCH	3
1.4. RESEARCH OBJECTIVES AND QUESTIONS	3
1.4.1. Main objective	4
1.4.2. Specific objectives	4
1.4.3. Research questions	4
1.5. THESIS STRUCTURE	4
2. LITERATURE REVIEW	7
2.1. FLOOD MODELLING	7
2.1.1. Topographical representation	9
2.1.2. Surface roughness	9
2.1.3. Boundary conditions	10
2.2. RAINFALL-RUNOFF MODELLING	10
2.3. SATELLITE RAINFALL ESTIMATES	11
2.4. SOURCES OF ERRORS IN HYDROLOGIC MODELLING	11
3. STUDY AREA	13
3.1. STUDY AREA CONCEPTUALIZATION	13
3.2. TOPOGRAPHY AND CLIMATE	14
3.3. SOIL, LAND USE/LAND COVER	15
4. DATA COLLECTION AND PRE-PROCESSING	16
4.1. RAINFALL DATA	16
4.1.1. Data collected	16
4.1.2. Data processing	17
4.2. DISCHARGE DATA	20
4.2.1. Data collected	20
4.2.2. Stage discharge relationship	23
4.2.3. Consistency check of discharge data	25
4.2.4. Corrected hydrographs	27
4.2.5. Lake Muhazi sub catchment	28
4.3. TOPOGRAPHICAL DATA ACQUISITION	29
4.4. RIVER GEOMETRY	29
4.5. OBSERVED FLOOD DEPTHS	30
4.6. SATELLITE RAINFALL DATA	30
5. RESEARCH METHODOLOGY AND MATERIALS	32
5.1. CONCEPTUAL FRAMEWORK	32
5.2. SATELLITE RAINFALL ESTIMATES	32
5.2.1. Extreme rainfall events	32
5.2.2. Bias correction	33
5.3. RAINFALL-RUNOFF MODELLING	33
5.3.1. Sub catchments geomorphological parameters	33
5.3.2. HEC-HMS model development	34
5.3.3. Calibration of the HEC-HMS model	38

5.3.4.	Regionalization of the local parameters	38
5.4.	FLOOD MODELLING	38
5.4.1.	Digital terrain modelling.....	38
5.4.2.	River geometry	39
5.4.3.	Sobek 1D2D model development	40
5.4.4.	Surface roughness	43
6.	RESULTS AND DISCUSSION.....	45
6.1.	GEOMORPHOLOGICAL PARAMETERS	45
6.2.	EXTREME RAINFALL EVENTS.....	46
6.2.1.	Rainfall coverage per sub catchments	46
6.2.2.	Extreme rainfall pattern.....	49
6.3.	RAINFALL-RUNOFF MODEL.....	51
6.3.1.	Gauged sub catchments rainfall-runoff model outputs	51
6.3.2.	Regionalization of local parameters.....	52
6.3.3.	Lake Muhazi sub catchment rainfall-runoff model output	53
6.3.4.	Nyabugogo catchment model output.....	53
6.3.5.	Inflow boundaries of the flood model.....	54
6.4.	FLOOD MODEL.....	57
6.4.1.	River profile	57
6.4.2.	Effect of DEM resolution.....	57
6.4.3.	Surface roughness	59
6.4.4.	Building representation.....	60
6.4.5.	Simulation results.....	60
7.	CONCLUSION AND RECOMMENDATIONS.....	62
7.1.	CONCLUSION	62
7.2.	RECOMMENDATIONS	63

LIST OF FIGURES

Figure 1-1: Typical flash flood hydrograph observed in the Mpazi channel (left) source: (SHERIngénieurs-Conseils, 2013), example of the flooding process in the Nyabugogo commercial hub (right).....	2
Figure 1-2: Flow chart of the research approach.....	3
Figure 2-1: Real world representation in hydrodynamic models.	7
Figure 2-2: Typical computation procedure of flood models.	8
Figure 3-1: Study area.....	13
Figure 3-2: Study area conceptualization.	14
Figure 3-3: Nyabugogo topographical map.....	14
Figure 3-4: Nyabugogo soil map.	15
Figure 3-5: Nyabugogo LULC map.....	15
Figure 4-1: Rainfall stations influence area and descriptions.....	16
Figure 4-2: Example of double mass curves.	18
Figure 4-3: Filled in and corrected rainfall data.	18
Figure 4-4: Altitude and Rainfall relationship.	19
Figure 4-5: Rusumo River cross section measurement and manual schematization.	20
Figure 4-6: Rusumo River water stages (left) and Rusumo River stage discharge relationship (right).....	21
Figure 4-7: Yanze River cross section measurement and automatic schematization using ArcGIS software.	21
Figure 4-8: Yanze River water stages (left) and Yanze River stage discharge relationship (right).....	21
Figure 4-9: Nyabugogo River cross section measurement and automatic schematization using an ADCP device.	22
Figure 4-10: Nyabugogo River water stages (left) and Nyabugogo River stage discharge relationship (right).	22
Figure 4-11: Lake Muhazi outlet dyke (top left), lake gauging scale (bottom left) and vegetation covering the outlet of the lake (right).	23
Figure 4-12: Rusumo River corrected water stages.....	24
Figure 4-13: Rusumo River discharge.	24
Figure 4-14: Yanze River discharge.	25
Figure 4-15: Nyabugogo River discharge.....	25
Figure 4-16: Rusumo sub catchment change ratios.	26
Figure 4-17: Yanze sub catchment change ratios.....	26
Figure 4-18: Nyabugogo catchment change ratios.....	27
Figure 4-19: Rusumo River Hydrograph.	27
Figure 4-20: Yanze River hydrograph.	27
Figure 4-21: Nyabugogo River hydrograph.....	28
Figure 4-22: Lake Muhazi hydrograph.	28
Figure 4-23: Nyabugogo River topographical points.....	30
Figure 4-24: Flood depth observations.	30
Figure 4-25: ISOD toolbox main screen.	31
Figure 5-1: Conceptual framework.	32
Figure 5-2: Typical watershed runoff representation (Arlen D. Feldman, 2000).....	35
Figure 5-3: HEC-HMS applied components.	35
Figure 5-4: Muskingum reach schematization.	37
Figure 5-5: Hill shades of the elevation grid at different resolutions.	39

Figure 5-6: schematization in Sobek 1D2D.....	42
Figure 5-7: Cross section input window in NETTER.	43
Figure 5-8: Roughness coefficient map.	44
Figure 6-1: HSG and CN maps.....	45
Figure 6-2: Extreme rainfall events susceptible of causing floods in the Nyabugogo commercial hub, downtown Kigali.	48
Figure 6-3: Typical rainfall event pattern.....	50
Figure 6-4: Set up screens of Rusumo and Yanze sub catchments.....	51
Figure 6-5: Rusumo (top) and Yanze (bottom) simulated hydrograph.	51
Figure 6-6: Lake Muhazi sub catchment model set up main screen and simulated hydrograph.....	53
Figure 6-7: Nyabugogo catchment schematization in HEC-HMS.....	54
Figure 6-8: Nyabugogo catchment simulated hydrograph.	54
Figure 6-9: Upstream inflow boundary hydrograph to the flood model.....	56
Figure 6-10: Nyabugogo river longitudinal profiles for different spatial resolutions.	57
Figure 6-11: Maximum depth maps for different DEM resolutions.	58
Figure 6-12: Surface roughness sensitivity analysis plot.....	59
Figure 6-13: Building representations effects on the model outputs. A similar figure is shown in A.T. Haile (2005).....	60
Figure 6-14: Maximum flood depth per event.....	61
Figure 6-15: Maximum velocity per event.....	61

LIST OF TABLES

Table 4-1: Missing and erroneous data per rainfall stations.	17
Table 5-1: Performance criteria.	38
Table 5-2: Roughness coefficient adapted from Tennakoon (2004).	43
Table 6-1: Sub catchments geomorphological parameters.	46
Table 6-2: Sub catchments receiving much water.	48
Table 6-3: Optimum parameters and Objective functions values for Rusumo and Yanze sub catchments rainfall-runoff models.	52
Table 6-4: Ratios used for estimating missing parameters.	52
Table 6-5: Sub catchment contributing much water to flooding.	56
Table 6-6: Model outputs for different resolutions.	58

1. INTRODUCTION

1.1. Background

Literatures provide different flood definitions and classifications. For example, Douben (2006) provided a separation between the definition of floods and flooding with three flood severity classifications. In their MSc thesis for example, Palmirino-Reganit (2005) used a flood definition and classification based on the source (or water body) of excess water; and Tarekegn (2009) used a flood definition based on the flood's induction nature (natural or human) while classifying floods based on their physical characteristics like formation speed, coverage area and location among others. The vantage point of all these definitions is that flood is the overflowing or inundation of water from its natural or artificial confinement to normally dry lands. According to Douben (2006), flooding are caused by extreme wet climatic conditions like heavy long-lasting rains (65%), torrential rains (15%), tropical cyclones (10%) and monsoon rains (5%).

Flooding belongs to the most common and damaging hazards (Sanders, 2007) usually experienced in forms of death, displacement, evacuation, homelessness, injury, etc. Urban areas are often the most vulnerable since industrial and urban settlements developments are often located in flood prone areas. Consequently, risks by extreme flood events increase with ongoing increasing population and economic development pressure (Padi, Baldassarre, & Castellarin, 2011). In the African context, many factors are behind flood risks increments. For example, the climate trend from the 20th to the early 21st century is toward increasing with more frequent monsoon rains (Douben, 2006), causing increased river flows and consequently flooding risks across the continent (Jury, 2013). Also, the often high rate of population density partly attributed to informal and illegal urbanization in floodplains contribute to flooding risks increment, etc.

In Rwanda, frequent floodings have become among the major problems nowadays, especially in Kigali city due to population densification and rapid urbanization growth (REMA, 2009). Few studies on flooding issues in Kigali city are reported. For example, an analysis of the flood exposure and vulnerability of the city of Kigali, using a flood risk analysis model adapted to the city's situation is provided by Bizimana and Schilling (2010). The study influenced few urban planning like the relocation of the former Kiruhura market and the restriction of building in floodplains. Recently, the Government of Rwanda through the RNRA/IWRMD¹, conducted a special investigation on the flooding issues of the Nyabugogo commercial hub, downtown Kigali city. The major outcomes of this investigation were the observation of rapid hydrologic responses of highly urbanised sub catchments like the Mpazi sub catchment as illustrated on figure 1-1. Also poor management and upgrade of existing urban structures leading to the reduction of water conveyance capacity was highlighted. The investigation also indicated a lack of knowledge and practice in the country towards flood prediction and management. The latter was reflected in the scarcity of data for flood studies and management during the course of this study.

The Nyabugogo commercial hub, downtown Kigali is the area of interest of this study. The lack of knowledge of the causes of frequent flooding in the area, the scarcity of data for flood studies and the socio economic value of the area are the major reasons for selecting the Nyabugogo commercial hub, downtown Kigali as the area of interest for this study. Historically, this area has always been a key

¹ Rwanda Natural Resources Authority/Integrated Water Resources Department

commercial centre of Kigali city and a transit hub where most of the national roads intersect (Kigali-Gatuna, Kigali-Gitarama and Kigali-Musanze). The area's economic and transport vitality has led to the area growth in use, causing increased flooding risk and vulnerability over time. MININFRA/RTDA² described the area as the most vulnerable area in Kigali city, despite its historical importance. The observed settlement densification around the commercial hub is believed influenced by its geographical location in relation to the city of Kigali, where people want to be close to economic opportunities. The latter results in informal settlements developing on steep slopes surrounding the area with increasing overflow, runoff of rain and sanitary water discharges in the area.

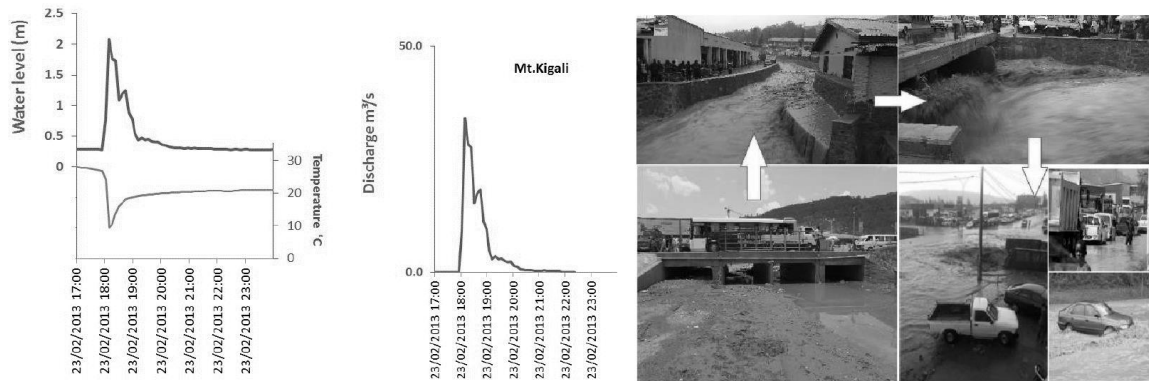


Figure 1-1: Typical flash flood hydrograph observed in the Mpazi channel (left) source: (SHERIngénieurs-Conseils, 2013), example of the flooding process in the Nyabugogo commercial hub (right).

The flood prone urban area in the Nyabugogo catchment outlet (refer to figure 3-2) located in an extremely vulnerable flat wetland area, surrounded by rippling hills. It is crossed by the Nyabugogo River at the entry of a narrow valley between the Mont Kigali and the Mont Jali. The area is characterized by poorly maintained urban drainage structures with insufficient conveyance capacities. On top of that, both transit growth demand and flooding have exacerbated its reduced transit and road infrastructure capacity to cope with flooding. The resulting inundation zone extends to Muhima market upstream the central bus park until downstream at the confluence with the Nyabugogo River. At the proximity of the Muhima market, the Rugunga tributary discharges in the Nyabugogo river in the eastern Muhima wetland while the Mpazi sub catchment discharges the Mont Kigali flow in the south through a steep channel crossing the commercial hub. Rugunga and Mpazi both drain densely urbanized sub catchments. The complex hydrological behavior of this system is not well understood and is a focal point of this study.

The increasing potential damages by flooding mark the need for protective measures to man and the environment (Douben, 2006). Increasing availability of higher accuracy remote sensing data, computational capacity and increasing understanding of hydrological processes (Paiva, Collischonn, & Tucci, 2011), have made hydrological models especially hydrodynamic models effective tools for flood simulation providing reliable information about the flood characteristics and propagations (Tarekegn, Haile, Rientjes, Reggiani, & Alkema, 2010). However, these models must be undertaken with precaution to avoid committing large errors in flood estimations (Leauthaud et al., 2013).

² Ministry of Infrastructure/ Rwanda Transport Development Agency.

1.2. Problem statement

This study conducted a diagnostic assessment of the flood behaviour of the poorly gauged Nyabugogo catchment shown on figure 3-1. The understanding of the causes of the frequent flooding in the downstream area of the catchment was the main driver to this research since this was unknown. Moreover, flooding in the downstream urban area commonly develop over very short time period (<15min) adding complexity to understand the system flash flood behaviour (see figure 1-1). The challenge to this study was to optimally and effectively parameterize the system for 1D2D hydrodynamic flood modelling, knowing that required data were scarce in the area such as the system geometry, the land cover roughness, inadequate gauging network, no flooding inundation records, etc. To overcome the problem of the real world data scarcity, applications of satellite remote sensing products for rainfall representation as well as rainfall-runoff modelling and hydrodynamic flood modelling were explored. Data model integration was inherent and a scientific challenge in this study.

1.3. Rational of the research

This study was aiming at understanding the causes and modelling the frequent flash floods in the Nyabugogo commercial hub, downtown Kigali. For this purpose a 1D2D hydrodynamic flood model of the area was developed (see figure 3-2). The flood model needed rainfall-runoff inputs for simulation of inflows at the model boundary which was handled by means of numerical boundary conditions. Since the data required to adequately estimate the runoff from upstream areas at required temporal resolution was limited, a rainfall-runoff model of the upstream area was developed. In order to increase the spatial-temporal resolution of the rainfall measurements so to enable representation and simulation of the observed high intensity rainfall events, satellite rainfall data were used. The resulting rainfall events at required spatial-temporal resolution served as input to the rainfall-runoff model.

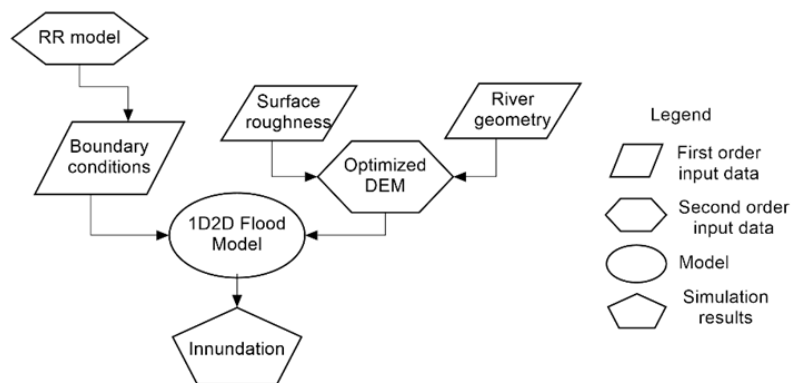


Figure 1-2: Flow chart of the research approach.

1.4. Research objectives and questions

This study was primarily focused on studying the frequent flash floodings in Kigali city, particularly the Nyabugogo commercial hub around the central bus park. Very little knowledge was available about the origin of the flood runoff discharge but also the data required to conduct the study in the area were very scarce. An attempt to develop a flash flood model for the frequently flooded small scale area was the target in this research. A combination of the available data, remote sensing products and hydrologic models was applied to overcome the data scarcity problem.

1.4.1. Main objective

The main objective of this study is to develop a flash flood model of the data scarce Nyabugogo commercial hub in Kigali city, using remote sensing data, a rainfall-runoff and a 1D2D hydrodynamic flood model.

1.4.2. Specific objectives

A number of steps were taken in this research to develop the flood model of the Nyabugogo commercial hub. Runoff from the upstream areas that served as inflow to the flood model were estimated using a rainfall-runoff model and satellite rainfall remote sensing. A step wise development of the flood model, ensuring optimized parameterization with the available data was done. The hydrological behaviour of study area was then analysed using all the tools and data available. The specific objectives of this research are:

- To develop a rainfall-runoff model of the entire Nyabugogo catchment to estimate the runoff from upstream areas,
- To explore the applicability of satellite rainfall products to represent the rainfall events causing floodings,
- To establish numerical boundary inflows to the 1D2D hydrodynamic flood model,
- To develop a 1D2D hydrodynamic flood model of the Nyabugogo commercial hub in the city of Kigali to assess flood characteristics like flood extent and duration.

1.4.3. Research questions

This study was interested in the rainfall distribution and the runoff routing leading to flooding as well as the hydrologic model parameterization required to meet the research objectives despite the data scarcity problem faced. The questions addressed in this research were:

- Can rainfall remote sensing data be used to estimate and represent rainfall in the study area at required spatial-temporal resolution?
- Are there specific rainfall pattern and distributions that can be related to the recurrent floodings?
- What is the sub basins runoff contributions to flooding?
- What is a suitable DEM spatial resolution for flood modelling in the study area?
- How can the surface roughness be parameterized for the Nyabugogo commercial hub area?

1.5. Thesis structure

The outline of this thesis report is composed of seven chapters and is as follows:

The first chapter provides the introduction of this study. The second chapter provides a literature review which illustrates the state of the art as far as studies like this one are concerned. The third chapter provides a description of the study area. The fourth chapter presents the data used for this study with a discussion on their inaccuracies and gaps, their pre-processing is also discussed. The fifth chapter provides the research methodology. The sixth chapter presents and discuss the results. The seventh chapter provides a conclusion and few recommendations.

2. LITERATURE REVIEW

Information about flood behaviour and risk are provided by many flood studies. Such studies help in quantifying the impact of floods on proposed development projects, in floodplain planning as well as in water quality assessment. Nowadays, with the advances in data collection technique, computational facilities and theoretical developments, wide use of flood models is done for flood studies.

2.1. Flood modelling

In hydrology, many definitions (Gupta, 2010; Tom Rientjes, 2014) of the word “model” exists but all agree on the fact that a model is a representation of the real world, mostly for a specific purpose. Since the level of complexity of observable hydrological processes is very high, simplified representation are mostly adopted in order to simulate the processes considered as the most dominant in the natural phenomenon being studied. Artan et al. (2007) defined flood models as hydrologic and hydraulic processes representations in river channels and floodplains.

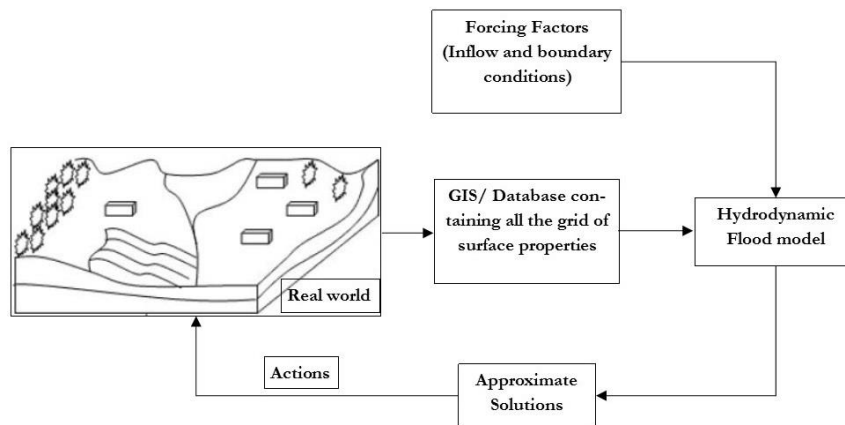


Figure 2-1: Real world representation in hydrodynamic models.

The existence of many flood models, from lumped to distributed, are acknowledged by Leauthaud et al. (2013) with their differences in physical basis, complexity and data requirements. These models, according to Hunter, Bates, Horritt, and Wilson (2007), require sufficient ground measurements and historical observations for effectiveness, otherwise remote sensing products may be used like DEMs³ (which are extremely important in this case), land cover images, rainfall estimates, etc. Furthermore, recent applications for ungauged catchment flood estimation approaches rely on more simplified parsimonious approaches like lumped models coupled with satellite data to overcome the problem of data scarcity, like Leauthaud et al. (2013), Sanyal, Densmore, and Carbonneau (2014) and Smithers, Chetty, Frezghi, Knoesen, and Tewelde (2013), among others.

The approach of flood models computation can either be 1D⁴, 2D⁵ or coupled 1D2D. The 1D approach principle, according to Alemseged and Rientjes (2007), is that flow properties like water level, velocity and discharge only varies in the direction of the stream while they are ignored in any other direction. The 2D

³ Digital Elevation Models.

⁴ One dimensional

⁵ Two dimensional

approach principle is that flow characteristics vary along 2 directions (i.e. x and y directions) based on the georeferenced grid defined by the DEM. Finally, the coupled 1D2D approach, simulates the river flow using a 1D representation and floodplain flow using a 2D representation.

A lot of works are available on the coupling of 1D and 2D approaches for flood modelling. Some using the finite volume method (Bladé et al., 2012; Fernández-Nieto, Marin, & Monnier, 2010; Finaud-Guyot, Delenne, Guinot, & Llovel, 2011), others using the finite difference method (Tarekegn et al., 2010; Zhang, Han, Wang, & Huang, 2014), where a coupled 1D2D hydrodynamic model was applied. The coupling of 1D2D lied on the combination of the 1D flow in river channels solving the Saint-Venant equation for flow propagation and the 2D flow in the floodplain solving the shallow-water equation (the vertically integrated Navier-Stokes equations).

In flood modelling, many decisions have to be made. These range from selecting the flow governing equations, discretising them over time and space, selecting a numerical model approach so that its solver may provide model outcomes that are approximate solution of the problem, defining initial and boundary condition, etc. Figure 2-2 illustrates a summary of the solving procedures of flood models as reported by Alemseged and Rientjes (2007).

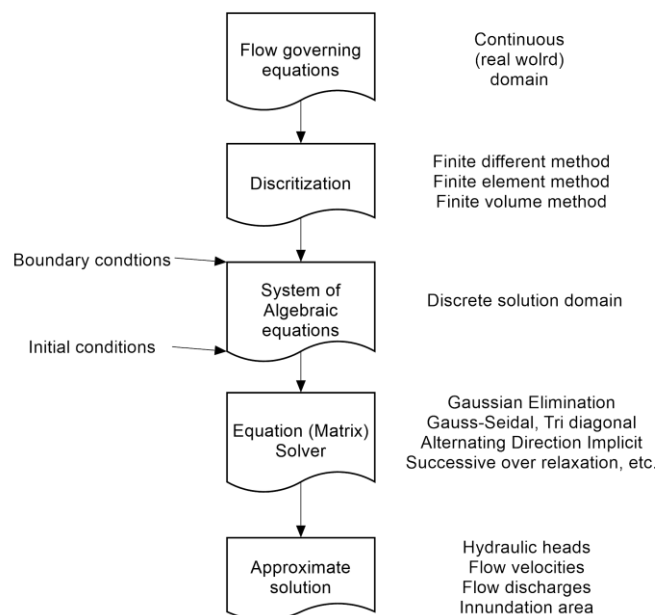


Figure 2-2: Typical computation procedure of flood models.

The real world characteristics are implemented in flood models by means of parameterization. The major input parameters to a flood model are the surface roughness mainly depending on the land cover conditions of the floodplain as well as the type of river bed materials, the floodplain and channel topography mainly obtained from field survey, contour maps or from remote sensing products such as LIDAR⁶, ASTER⁷ or SRTM⁸ for example; and finally the initial and boundary conditions.

⁶ Light detection and ranging.

⁷ Advanced Spaceborne Thermal Emission and Reflection Radiometer.

⁸ Shuttle Radar Topography Mission.

2.1.1. Topographical representation

Mukherjee et al. (2013) states that quantitative representations of the terrain elevation by means of a Digital Elevation Model (DEM) is essential for hydrologic models application. In their study, Md Ali, Solomatine, and Di Baldassarre (2015) indicated that DEMs are derived from different sources like remote sensing (spaceborne or airborne imagery) or traditional methods (ground survey) and are fundamental input data to flood models as they provide a representation of the floodplain terrain and river channel layout and ideally geometry.

The vertical accuracy of open source DEM was assessed by Mukherjee et al. (2013) who compared their derived attributes (river length, area delineation, etc.) using postings CartoSat DEM and survey of India (SOI) height information. The study found that DEM's of coarser resolution affected the representation of terrain characteristics. Also it is indicated that the terrain morphology strongly influences the DEM accuracy. An extensive review on studies on topographic data accuracy and precision evaluation is provided by Md Ali et al. (2015). The main findings from all the reported studies were that the flood extent estimation increases with coarser DEMs, flood wave travel times are strongly related to the model resolution used, there are potential problem using satellite remotely sensed topographic data in flood hazard assessment for small areas, for large homogenous floodplain the use of SRTM may be envisaged, etc.

According to Casas, Lane, Yu, and Benito (2010), the topographical representation adequately must represent the terrain irregularities over which water is flowing at an adequate discretization scale in order to capture the flow process of interest. In this study, a DGPS⁹ based aerial image DTM was used for topographical representation in the flood model while the river geometry was obtained from ground survey also the open source SRTM was used for the parameterization of the rainfall-runoff model.

2.1.2. Surface roughness

GIS database management systems help much in hydrologic and hydraulic modelling. The data preparation and processing using GIS like topographic and drainage information extraction, soil and land cover data, etc. which constitutes major inputs to the flood model is facilitated as well as the dissemination of model outputs (A.T. Haile, 2005). Many functions of GIS for hydrology are provided by (Band & Moore, 1995). These are for example the determination of spatial patterns of surface attributes at scale and resolution appropriate for water routing, the representation of spatial dependence of certain hydrological processes, the delineation of the catchment area with its stream network, the construction and sampling of key statistical variables, the determination of scale effects on the distribution functions of key land surface variables and their correlation, the optimal partitioning of the surface into sufficiently homogeneous land units, etc.

The roughness parameter is an effective parameter for distributed models obtained mostly through calibration procedure because of its complex parameterization. A relation between roughness parameter and topography is acknowledge by Casas et al. (2010) through the definition and use of floodplain roughness elements comprising both ground surface irregularities (i.e topographic variability) and vegetation elements (like trees, grass, etc.). Also, floodplain roughness parameterization, sometimes parameterized by a single value or derived from remote-sensing based land cover map, may constitutes an important source of uncertainties in a flood model (Straatsma & Huthoff, 2011). A distributed flood model therefore requires an adequate map of these roughness elements over the flood model domain.

⁹ Differential Global Positioning System.

A lot of researches on roughness parameterization have been done over the years. For example Casas et al. (2010) worked on roughness parameterization using LIDAR derived land cover data while defining the roughness height (Z_0) as a function of the topographic amount in the mesh (or grid used). By connecting the topography and the roughness parameterization, a relation between the roughness parameter and flow prediction was found by the study with additional complexity of the parameterization. Also Straatsma and Huthoff (2011) assessed the uncertainties of 2D hydrodynamic models due to errors in the roughness parameterization using the WAQUA hydrodynamic model and surface roughness derived manually from high resolution aerial images (ecotope maps). The study found that an image classification accuracy of 69% led to simulated water levels errors in the order of centimeters.

For this study, the floodplain roughness elements, were defined by overlapping a map of the surface roughness coefficient (obtained from the digitization of the flood model domain orthophoto with a 0.25m resolution) and the elevation grid of the flood model domain (obtained from a 10 m resolution DTM). Note that the maps had the same spatial dimensions and grid resolution.

2.1.3. Boundary conditions

Hydrodynamic flood models require model boundary inflow discharges for flow simulation. Since flows for the study area is runoff from upstream catchment, numerical boundary conditions are used as a mean to regulate these flow fields like inflow/outflow discharges and water levels in the flood model domain. According to Tom Rientjes (2014), boundary conditions are mathematical statements at the lateral boundaries of the model domain that serve to simulate the hydrological influences of the real world. This means inflow and outflow discharges and water levels are imposed by boundary conditions (Tarekegn et al., 2010). These boundary fluxes are expressed in terms of mass and momentum exchanges (Alemseged & Rientjes, 2007). In this study, the boundary conditions applied were the Neumann condition (or specified flow boundary) regulating the upstream inflows in the flood model domain and the Dirichlet condition (or specified head free flow boundary) regulating the model outflow condition.

2.2. Rainfall-runoff modelling

It is common practice to use different methods to estimate the upstream inflows in data scarce regions like rainfall-runoff models for example. These are commonly lumped conceptual models providing the relation between rainfall and runoff by simplifying the major hydrological processes (THM Rientjes, Perera, Haile, Reggiani, & Muthuwatta, 2011). Many applications of rainfall-runoff modelling are available in literatures.

Recently, Abushandi and Merkel (2013) applied the HEC-HMS and IHACRES rainfall-runoff models for a single streamflow event simulation in Wadi Dhuliel catchment. Application of satellite-derived rainfall dataset (GSMaP-MVK+) to locate the rainfall storm was made. The study found that the HEC-HMS SCS-CN method performed well compared to IHACRES model as a better fit was obtained. Also Laouacheria and Mansouri (2015) successfully applied rainfall-runoff modelling combining HEC-HMS linear reservoir model and WBNM parallel cascades model to predict a 50 years return period event catchment response. The study highlighted as its main finding the potential of hydrologic modelling for studies of effects of urban development on storm runoff.

In this study, a rainfall-runoff model was developed to enable the estimation of the catchment runoff using the HEC-HMS software. The simulated and aggregated runoff from the upstream sub catchments served as inflows to the flood model of the study area.

2.3. Satellite rainfall estimates

Remote sensing constitutes an important source for data acquisition providing spatial-temporal coverages that may be used in flood models. Remote sensing provide data on meteorological variables like rainfall data among others, however attention on the temporal and spatial resolution is required as well as potential biases.

According to Alemseged Tamiru Haile, Habib, Elsaadani, and Rientjes (2013) satellite rainfall estimates provide alternatives of rainfall properties assessment over large area at sub daily time scales, especially for poorly gauged catchments with low observation frequency. The study did a comparison of satellite rainfall products (TRMM¹⁰ 3B42RT, TRMM 3B42PRT and CMORPH) diurnal cycle representation over the lake Tana basin and lake Victoria basin. The main findings was that the rainfall product performance was affected by the geographic features, also that the performance difference between rainfall products was small and favourable over the lake Victoria basin and finally that the CMORPH product was the overall best performer. Also in their study, Habib, Haile, Sazib, Zhang, and Rientjes (2014) evaluated the effects of satellite rainfall bias correction on runoff simulations using the CMORPH product and the HBV¹¹ rainfall-runoff model. The study found among others that accounting for temporal variation in the bias reduces the rainfall bias up to 50 percent. Another study by Habib, Haile, Tian, and Joyce (2012) evaluated the performance of the CMORPH available at fine space-time resolutions (1hr and 8km). The study found the product to have high detection skills and ability to reduce rapidly its random errors when aggregated in space or in time, and so forth. Furthermore, Maggioni et al. (2013) found that the bias corrected CMORPH was the most accurate product in predicting runoff variability compared to the TRMM 3B42RT and the MPE¹² rainfall estimates.

In this study, the CMORPH product available at fine space-time resolution (8km and 30min) was used as forcing factor for the rainfall-runoff model in order to estimate the upstream inflows used as input flows to the flood model.

2.4. Sources of errors in hydrologic modelling

The recent development in hydrologic modelling has seen arising concerns about the reliability of the models outputs. These concerns are due to errors observed in the modelling results expressed as the deviation between simulated outputs and the real world observations. The origins of errors in hydrological modelling are reported by Alemseged and Rientjes (2007) to be from six different sources as follows:

- Random or systematic errors in the forcing data (ϵ_i), for e.g. precipitation;
- Random or systematic errors in the recorded state data (ϵ_r), for e.g. water levels;
- Errors due to non-optimal parameters values (ϵ_{no});
- Errors due to the incompleteness and use of biased model structure (ϵ_s);
- Errors due to time-space model domain discretization (ϵ_d);
- Errors due to rounding off (ϵ_{ro}).

The total error (ϵ_t) will then be the sum of all the above.

$$V_{sim} - V_{obs} \equiv \epsilon_t = \epsilon_i + \epsilon_r + \epsilon_{no} + \epsilon_s + \epsilon_d + \epsilon_{ro}, \quad 2-1$$

¹⁰ Tropical Rainfall Monitoring Mission.

¹¹ Hydrologiska Byråns Vattenbalansavdelning model.

¹² Multisensor Precipitation Estimates.

Further error descriptions for numerical approaches are provided by Tom Rientjes (2014). These range from physical system errors (caused by inappropriate hydrological processes simplifications and incorrect schematizations), mathematical errors (caused by wrong differential equations expressions), to numerical errors (caused by truncation residuals in calculations) and computational errors (mainly caused by round off errors due to computer limitations in representing digits).

3. STUDY AREA

“Rwanda”:

Literatures such as Munyaneza (2014) and Mikova, Wali, and Nhapi (2010) have reported Rwanda to be a small, mountainous, landlocked country commonly known as the “land of 1,000 hills”. The country’s area is of 26,338 square kilometres with 2,175 square kilometres covered by water, and it is also considered to be the most densely populated African country. The country is located between 1 degree and 3 degrees south of the equator, 29 degrees and 31 degrees east of Greenwich.

The Nyabugogo catchment, on figure 3-1, is a major sub catchment of the Nyabarongo downstream catchment spreading over the central, eastern and northern parts of Rwanda. It is the most densely populated and urbanized catchment (but also having rural areas) in Rwanda as it covers a major portion of the capital city of Kigali as well as few other districts. Its area is around 1,540 square kilometers including the Lake Muhazi which drains the upstream part with a catchment area of 878.7 square kilometers.

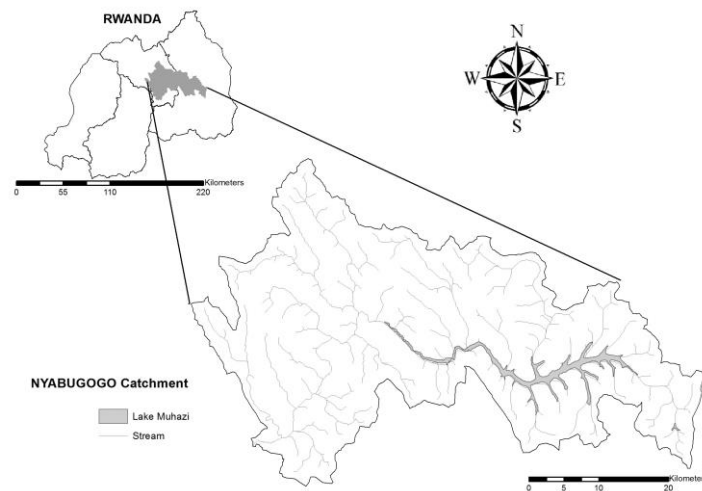


Figure 3-1: Study area.

3.1. Study area conceptualization

As described in the rational of the research, two hydrologic models were developed in this research. Each of the model had a different approach and purpose that led to the conceptualization shown on figure 3-2. The flood model domain only covers the frequent flooded area of the Nyabugogo commercial hub downtown Kigali up to the Nyabugogo river gauging station (at the Nemba station downstream) below the Gisenyi road bridge. Attention was taken in delimitating the flood model domain to enable the river flood plain to be represented completely. The observation of all the upstream area effects without backwater effects affecting the downstream boundary was achieved within the flood model delimitation used in this study. Since the upstream area inflows were estimated using a rainfall-runoff model, the entire Nyabugogo catchment was divided into sixteen sub catchments (including the flood plain itself) directly discharging in the Nyabugogo River to allow the assessment of the sub catchments contributions. The following is illustrated on figure 3-2.

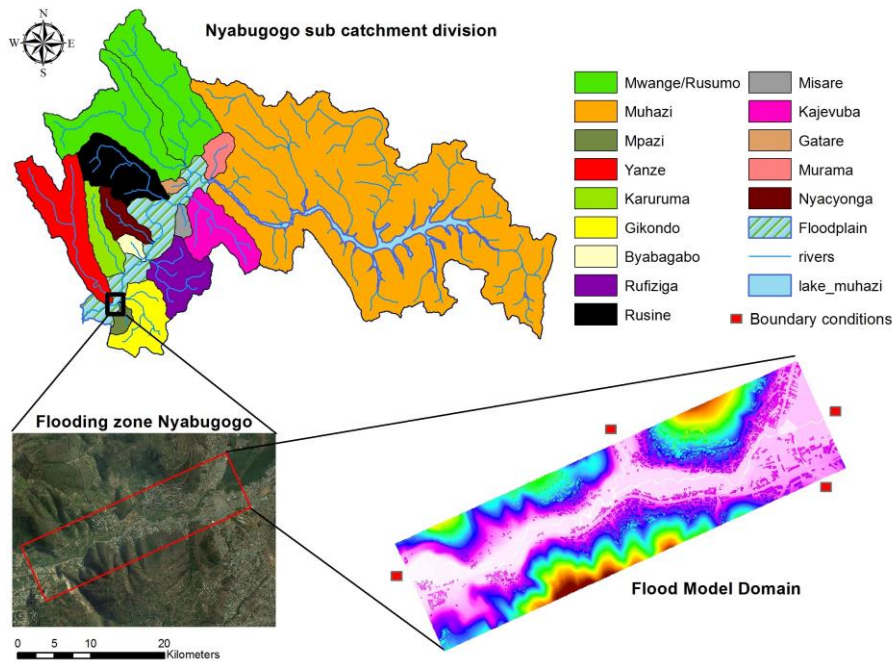


Figure 3-2: Study area conceptualization.

3.2. Topography and climate

The topography of the Nyabugogo catchment varies between 1,350 and 2,300 m a.s.l. and it is characterized by abrupt changes on short distances in the northern, western and few areas in the southern parts. The central and eastern parts of the catchment is more or less flat and gentle (i.e. the Nyabugogo river flood plain and lake Muhazi).

The climate of the Nyabugogo catchment is similar to the country’s which is a tropical temperate climate. The average precipitation per annum in the Nyabugogo catchment is observed below 1,200 millimeters with temperature varying between 19 and 21 degree Celsius (MUSONI, 2009).

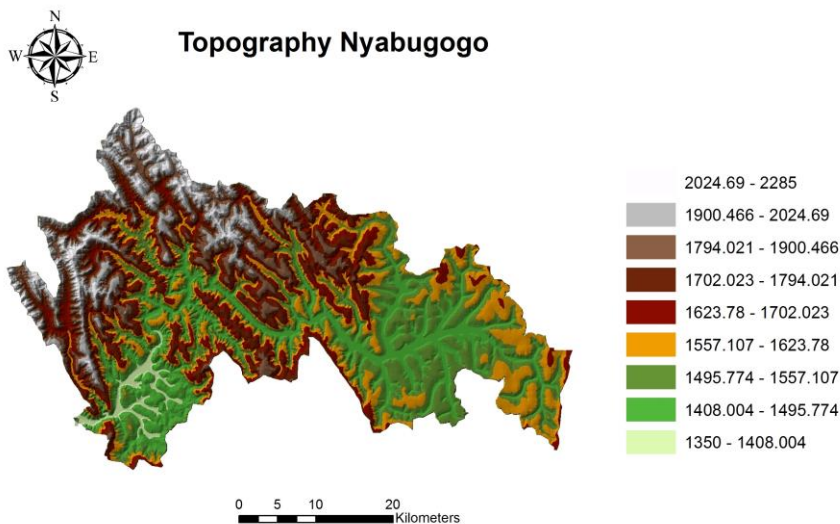


Figure 3-3: Nyabugogo topographical map.

3.3. Soil, Land Use/Land Cover

An overall description of the Nyabugogo catchment lithology was provided by SHERIngénieurs-Conseils (2014). Predominant shale material in the western part, schist and quartzite alteration with significant granite and pegmatite in the center and east were reported. All of the valley bottom throughout the catchment contain alluvial material. Soil classes predominantly found in the catchment are nitosol, acricol, alisol and lixisol with ferralsols in the eastern part around the lake Muhazi and the western part at some location. In the western part, a spread of camisole is found. The central part and valley bottom of the catchment are characterized by low infiltration clay soils and a flat topography.

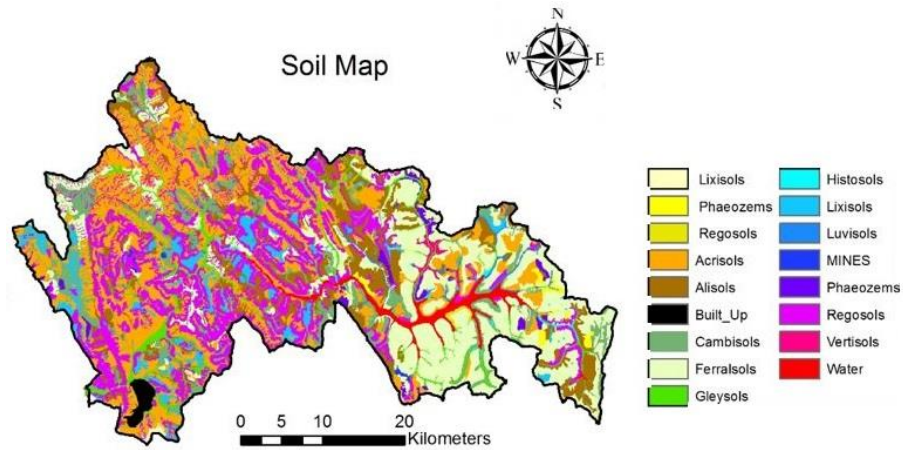


Figure 3-4: Nyabugogo soil map.

Rain fed agriculture dominate the land use where irrigated/ agricultural wetland are observed. The center and eastern part of the catchment contain small forest plantation plots as well as small natural open lands (SHERIngénieurs-Conseils, 2014). A significant built up area is observed in the catchment because of the city of Kigali. A single small area of natural forest in the west is observed also.

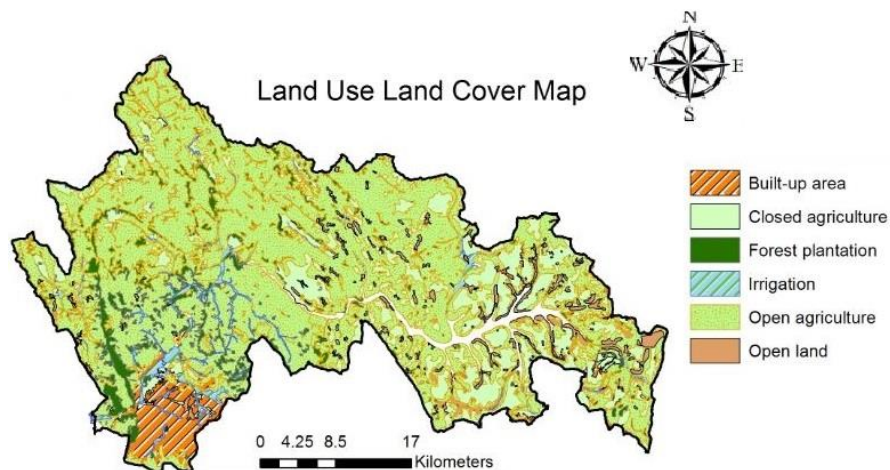


Figure 3-5: Nyabugogo LULC map.

4. DATA COLLECTION AND PRE-PROCESSING

For recent years (2011, 2012 and 2013) frequent floodings have been reported the Nyabugogo commercial hub in the downtown Kigali around the central bus park (figure 3-2). No specific records of any kind of these events were available except in people's memories. Since this study was focused on understanding the causes of these flooding as stated previously, among all the data collected (as far as the meteorological and hydrological data were concerned), only the data for the years 2011, 2012 and 2013 were selected, processed and used in this research. The meteorological data were obtained from the RMA¹³ and the hydrological data from the RNRA/IWRMD¹⁴.

The following chapter provides a description of the data collected and all the methods used for their processing.

4.1. Rainfall data

4.1.1. Data collected

The available rainfall data collected were daily measurements. Among all the available rainfall stations collected, only 10 stations were used because their area of influence include the Nyabugogo catchment as illustrated in figure 4-1.

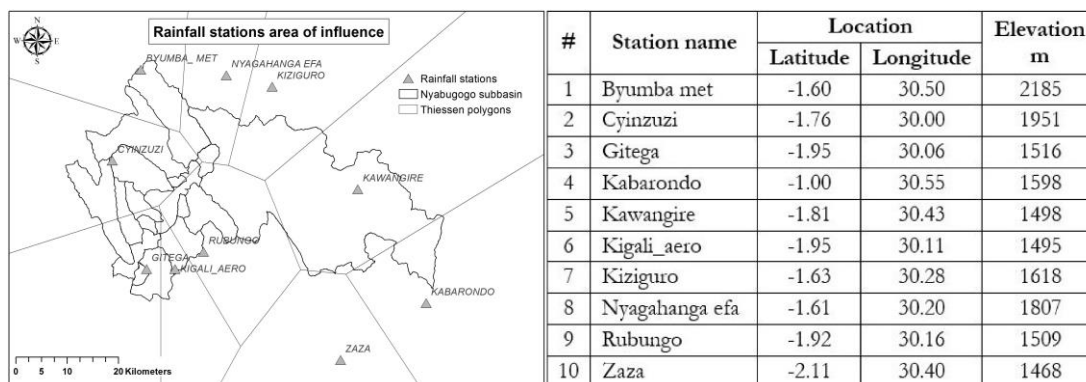


Figure 4-1: Rainfall stations influence area and descriptions.

A preliminary visual inspection revealed missing data for certain dates per station (these are indicated by a minus 8 on the charts provided in annex A) and few recordings considered erroneous. Cyinzuzi and Kiziguro rainfall stations were found with many days of missing data (more than 200 indicated by a green arrow in annex A) compared to other stations. However, Kigali airport and Gitega rainfall stations had no missing data. Few erroneous data were detected on Gitega and Cyinzuzi rainfall stations (indicated by a red arrow in annex A). Table 4-1 provides a summary of these findings.

¹³ Rwanda Meteorology Agency.

¹⁴ Rwanda Natural Resources Authority/ Integrated Water Resources Management Department.

#	Station name	Missing dates	Erroneous dates
1	Byumba met	20	0
2	Cyinzuzi	242	29
3	Gitega	0	1
4	Kabarondo	23	0
5	Kawangire	26	0
6	Kigali_aero	0	0
7	Kiziguro	300	0
8	Nyagahanga efa	95	0
9	Rubungo	31	0
10	Zaza	19	0

Table 4-1: Missing and erroneous data per rainfall stations.

Gitega rainfall station had only a day considered as erroneous (indicated with a red arrow in the annex A). December 17th, 2013 had a record of 117.4 mm of rainfall. The fact that this station is relatively close to the frequently flooded area, a record like that would make no sense because it would have led to a massive flooding which would have been reported somehow (local news, etc.). Additionally, all the surrounding stations recorded rainfall was very low. Cyinzuzi rainfall station had 29 successive daily measurements which must be considered erroneous (indicated with a red arrow in annex A) mostly due to their unusual pattern. The station recorded a succession of 29 rainfall events of magnitude varying between 20 to 23 mm of rainfall. Knowing the rapid responses of the sub catchments of Nyabugogo, this expectedly would have led to a flooding but extended for more than a day which has never happened. Also, all other surrounding stations used, exhibited a different rainfall pattern during that period.

4.1.2. Data processing

This section provides a summary of the processing of the collected rainfall data. It describes firstly the rainfall data consistency check prior to filling in and correcting them. It then describes the altitude-rainfall relationship analysis prior to aerial estimation of rainfall.

From the previous visual inspection, a necessity of filling in and correcting the rainfall data prior to modelling application was found. However, before filling in and correcting the rainfall data, a consistency check of the rainfall data was done. The consistency of the rainfall stations records were tested in order to assess their degree of similarity. The double mass curve analysis (Searcy & Hardison, 1950) based on daily cumulative of rainfall per station against the average daily cumulative of the surrounding stations was used. Figure 4-2 provides examples of the double mass curves of Cyinzuzi and Kiziguro rainfall stations. The observed irregularities on these curves were due to the large number of missing data (characterised by a prolonged horizontal line on the curve) as well as erroneous records for the case of Cyinzuzi rainfall station (characterised by a prolonged vertical line on the curve). However, despite these few irregularities, these 2 stations like all the other rainfall stations (refer to annex B) used for this research, have proven to be very consistent with very high regression coefficients ($R^2 > 0.9$). Once this test was complete, the filling in and correction of rainfall data was done.

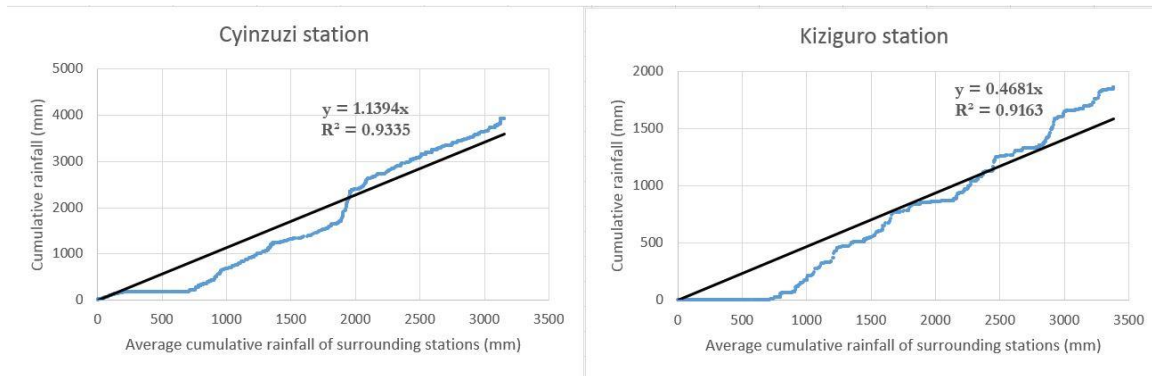


Figure 4-2: Example of double mass curves.

Based on the high consistency of rainfall stations records, two methods of rainfall data completion were adopted simultaneously in this study. These methods were:

For gaps less than a week, where the level of errors (or noise/diversity in the observations) were considered negligible the simple linear regression method (Helsel & Hirsch, 1992) was used. A description of this method is provided in the annex C1 as reported by Perera (2009) and Gumindoga (2010). As the method links an incomplete station to a complete one, the rainfall station of Kigali airport (which is among the WMO¹⁵ global network) was used to complete these small gaps in the surrounding stations.

For gaps larger than a week, the modified normal ratio method was used because the level of diversity in rainfall estimates was considered not negligible. This method was recommended by Tang, Kassim, and Abubakar (1996). The author did an evaluation of different methods of filling in missing rainfall data taking into account the temporal and spatial characteristics of the raw data. The study concluded that the most appropriate method for filling in missing daily rainfall data is the modified normal ratio (a description of the method is given in the annex C2). On figure 4-3 the filled in and corrected rainfall records are shown.

Rainfall data

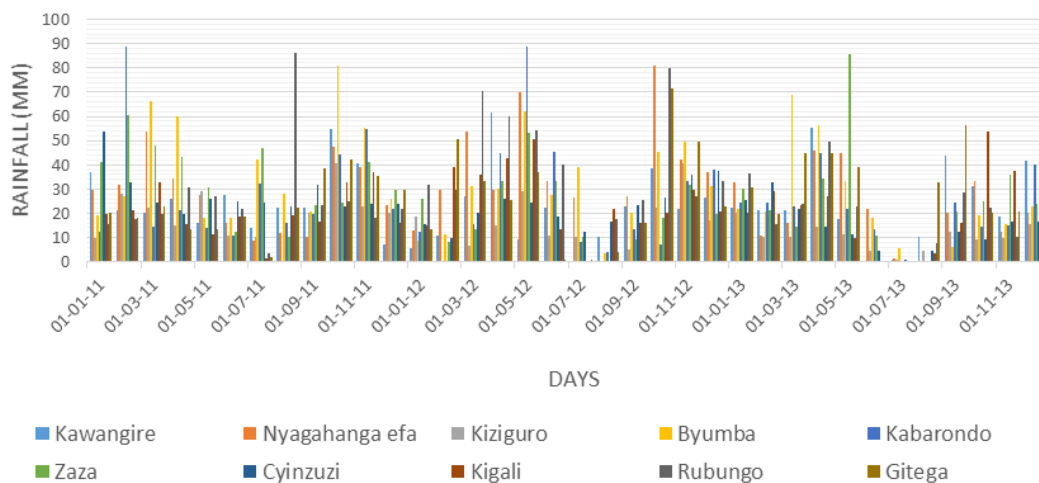


Figure 4-3: Filled in and corrected rainfall data.

¹⁵ World Meteorological Agency.

A quality assessment of the filled rainfall data was done. A comparison of the annual rainfall data per station was done in order to assess the strength of the method adopted, since the annual rainfall are considered independent. According to Debru (2010), a large discrepancy between annual rainfall per catchment implies that the method used was not adequate. In this research, only 3 years of rainfall per station were used and the annual rainfall per year per station were found to be in the same range. Therefore, the filled in and corrected data were considered adequate.

After filling in and correcting the rainfall data, the relationship between altitude and rainfall in the Nyabugogo catchment was analysed. Figure 4-4 illustrates this relationship. Based on the work of Lloyd (2005), the regression coefficient (r^2) of 0.54 in the Nyabugogo catchment was found small. It was therefore concluded, for the case of the Nyabugogo catchment, that simple methods of aerial estimation of rainfall could be used since there was no need of including the altitude as a second variable in estimating the areal rainfall. The accuracy of the rainfall estimates using simple methods in this case was considered of acceptable accuracy.

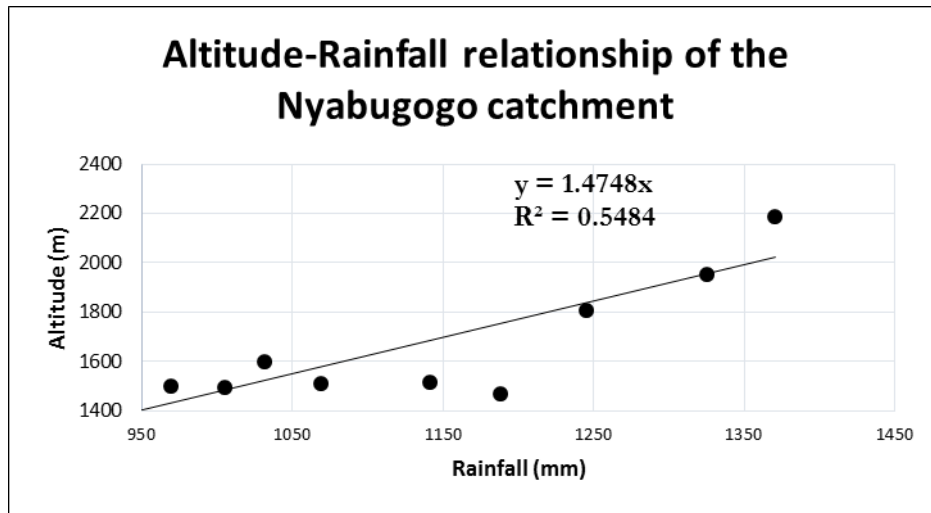


Figure 4-4: Altitude and Rainfall relationship.

The aerial estimation of rainfall per sub catchments were done using the Thiessen polygon method as described and reported by many authors (Gupta, 2010; Searcy & Hardison, 1950; Wanielista, Kersten, & Eaglin, 1997). The following is illustrated in figure 4-1. These estimations were used in the discharge data analysis as well as in the Rainfall-runoff model setup in the following sections. The influence area of a Thiessen polygon divided by the target catchment area constitutes the weight of the rainfall station in the target catchment. Mathematically, this is written as:

$$\bar{P} = \frac{1}{A} \sum_{s=1}^n (A_s P_s), \quad 4-1$$

Where \bar{P} and P_s are the average rainfall and stations rainfall respectively. A is the target catchment area, A_s is the station's influence area in the target catchment and n is the number of rainfall stations influencing the target catchment.

4.2. Discharge data

It is of significant importance to have adequate catchment runoff time series. The latter is considered as an integrated response function of all upstream processes of a hydrological system. Therefore the quality of the runoff data was checked using graphical method and by comparing the change in the rainfall and the runoff (Hoyos Goez, 2011). In this study, no river rating curve were available, therefore the few available field measurements of discharge were used along with the water stages to estimate the flow which was then qualitatively assessed. The following sub sections summarized all the steps done.

This section discusses the data collected and the pre-processing done to obtain the flow estimates. The Yanze and Rusumo sub catchments were gauged. Additionally, the lake Muhazi sub catchment was also gauged and the entire Nyabugogo catchment at the Nemba gauging station. All other entities except the lake Muhazi sub catchment had few field measurements of discharge. However, the lake Muhazi outlet was a dimension fixed concrete dyke. Considering the smoothed response capability of the lake Muhazi (due to its large area), a different approach was adopted to estimate the lake outlet.

4.2.1. Data collected

The data collected on site for flow estimation were the available water stages which are recorded by local observers sending the readings to the RNRA/IWRM department every three times a day from their mobile phones to an online system. These data have shown to be of low quality and lots of incorrect readings were observed. Also, the existing field measurements of discharge and few information on the river geometries on site were collected. This sub section is organised in a case by case manner describing the gauged sub catchments.

- **Rusumo river sub catchment**

The sub catchment of Rusumo, on figure 3-2, is located in the far north upstream of the Nyabugogo river besides the lake Muhazi sub catchment outlet. Table 6-1 provides the major characteristics of this sub catchment. The Rusumo river cross section was measured on site using a current meter (C31 253194, propeller number 272477) and a tape as shown on figure 4-5. Very few field measurements of the river Rusumo discharge were available as illustrated on figure 4-6 (right). Rusumo riverbed is composed primarily of stones and few floating sediments. These sediments do not completely settle because of the disturbance of water resulting from the presence of a large water fall in the river.

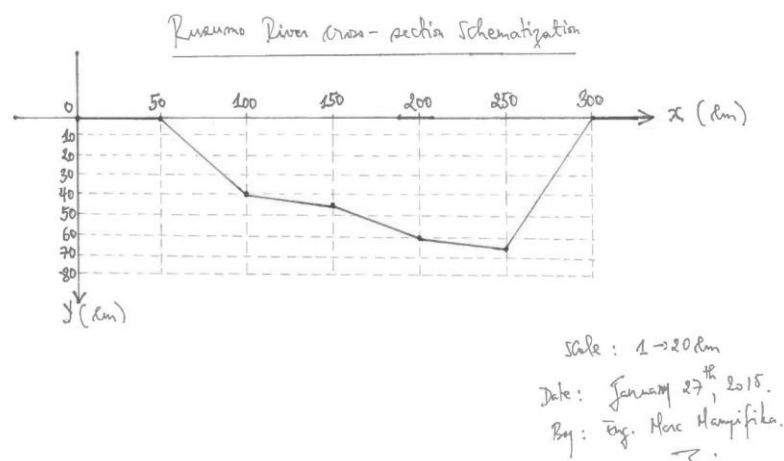


Figure 4-5: Rusumo River cross section measurement and manual schematization.

The Rusumo River water stages are illustrated in figure 4-6 (left). It can be seen that there are few missing data but also a systematic error is observed on the base flow (i.e. the base flow axis is inclined).

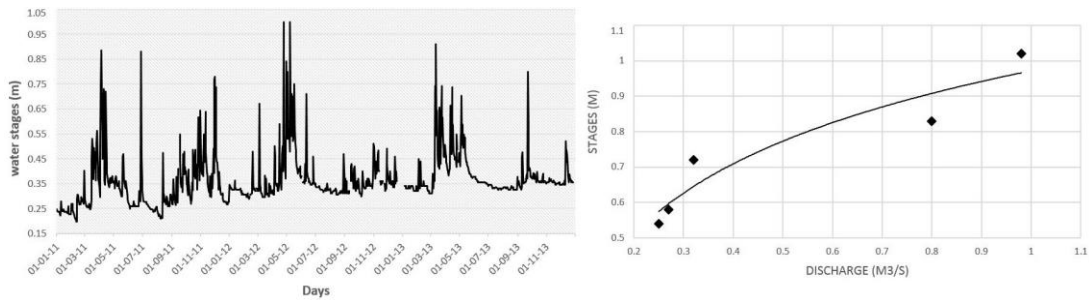


Figure 4-6: Rusumo River water stages (left) and Rusumo River stage discharge relationship (right).

- **Yanze river sub catchment**

The Yanze River is the most downstream tributary to the Nyabugogo River and as such contributes to the rainfall-runoff hydrograph which makes up upstream boundary conditions to the flood model (refer to figure 3-2 for the catchment location). The river serves as a major water supply to the city of Kigali. It is also the last contributing tributary before the Nyabugogo River flows into the Nyabarongo River. The catchment characteristics are provide in table 6-1. The river cross section (figure 4-7) was measured on site with a total station during the Nyabugogo floodplain topographical survey (more details are provided in the section 4.4). Very few field measurement of the discharge were available and are illustrated on figure 4-8.

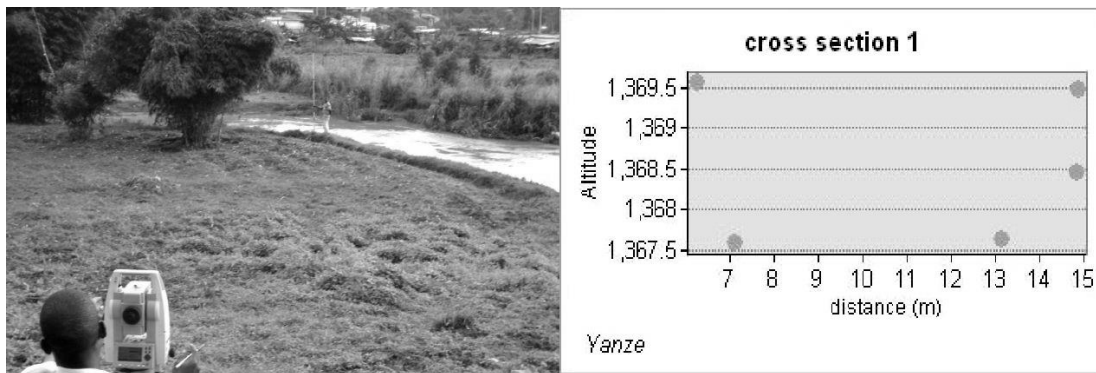


Figure 4-7: Yanze River cross section measurement and automatic schematization using ArcGIS software.

The collected Yanze River water stages are illustrated on figure 4-8 where few missing data and anomalies can be clearly seen.

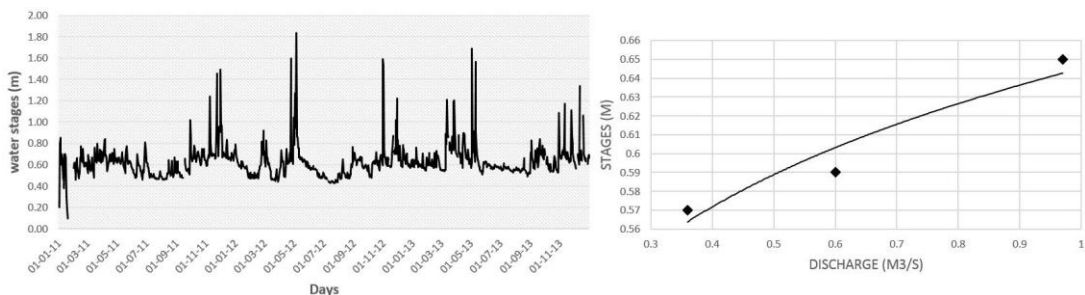


Figure 4-8: Yanze River water stages (left) and Yanze River stage discharge relationship (right).

- Nyabugogo river catchment

The Nyabugogo River is the main river in the study area. It originates from the Lake Muhazi upstream, crossing the entire catchment while receiving many inflows from its tributaries. Figure 3-2 provide an illustration. The river cross section was measured using an ADCP¹⁶ device as illustrated on figure 4-9 and in the annex D. Few field measurements of the discharge were available and are illustrated on figure 4-10.

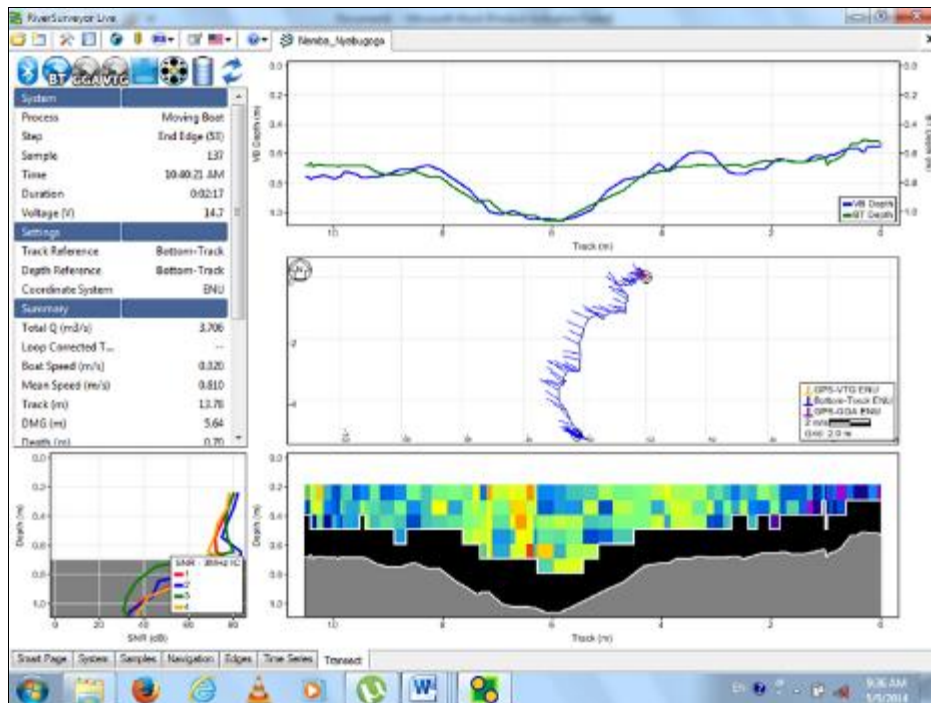


Figure 4-9: Nyabugogo River cross section measurement and automatic schematization using an ADCP device.

The first graph provides the river cross section in green, the second graph shows a top view of the ADCP device path on the river (refer to annex D) and the third graph shows the velocity distribution in the river with the blank band below indicating the riverbed level (as the ADCP waves cannot penetrate).

The collected Nyabugogo River water stages are illustrated on figure 4-10, where incorrect records are observed as well as missing records.

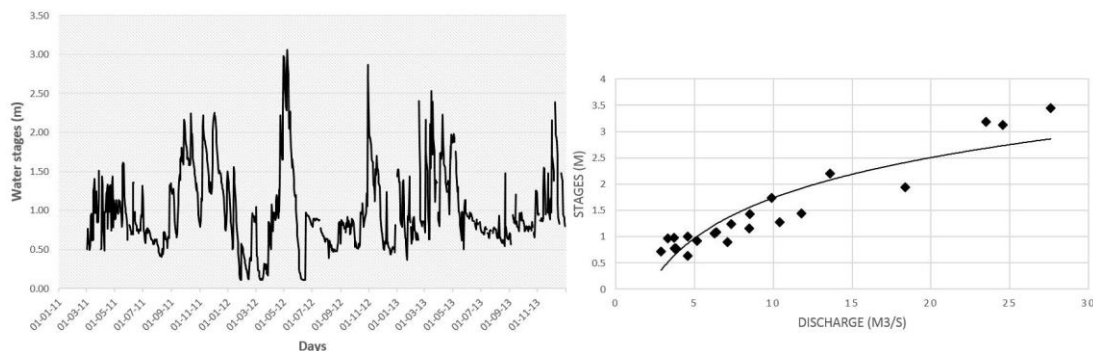


Figure 4-10: Nyabugogo River water stages (left) and Nyabugogo River stage discharge relationship (right).

¹⁶ Acoustic Doppler Current Profiler.

- **Lake Muhazi catchment**

This is the biggest sub catchment of the Nyabugogo catchment since its area is more than the half of Nyabugogo catchment area. It was observed on site that the lake discharges through a fixed weir which is part of a long dyke (>200m) to control the lake outflow. On the dyke there was a scale (figure 4-11) but unfortunately no record of stages were available. The lake Muhazi drains the entire sub catchment and smoothly release the water at the dyke where the Nyabugogo River starts. The lake outlet area was covered with lots of vegetation (figure 4-11) obstructing the flow and though increasing the smoothness of the lake outflow. It was also observed that the dyke scale had water marks on it as shown on figure 4-11, indicating minimum and maximum stages at 0.20 and 0.60 meters respectively. These water marks reflect on the lake surface fluctuations and allow for estimation of the lake outflow.



Figure 4-11: Lake Muhazi outlet dyke (top left), lake gauging scale (bottom left) and vegetation covering the outlet of the lake (right).

4.2.2. Stage discharge relationship

The collected water stages were converted into discharges after estimation of the rating curves of the gauged rivers. After this conversion, the missing and erroneous discharges were filled in and corrected. The simple rating curve fitting method was applied in this research to convert the available water stages into discharges using the available field measurements of discharge. This method was applied because the gauging stations observed on site are placed at locations where there is little scouring and no backwater effects. Mainly the flow at these stations is governed by the channel control (Braca & Futura, 2008). The methods used for filling in and correcting the flow data are the linear interpolation (for shorter period) and the interpolation between the logarithmically transformed values of the beginning and end of the gap (for longer gap on the recession part mostly) (Hydraulics, 1999). Since these methods are based on assumptions applied on discharges it was therefore advised to apply them directly on discharge rather than stages.

- **Rusumo sub catchment**

It was observed previously that the Rusumo River water stages had a systematic error such that the base flow was inclined progressively with time. In order to correct this error, a semi logarithmic plot of the base flow values was done to allow a slope estimation of the error. Once the slopes were identified, these were used to correct the data. On figure 4-12, the semi log plot is provided on the right and on the left, the corrected water stages are plotted against the raw water stages.

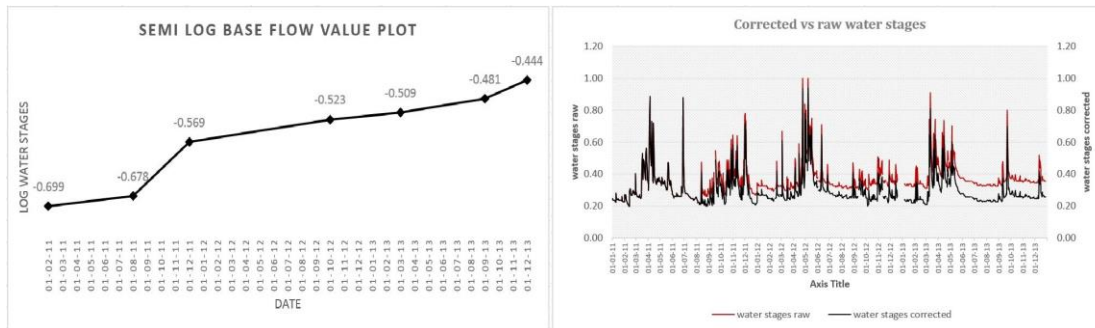


Figure 4-12: Rusumo River corrected water stages.

The stage-discharge relationship obtained for the Rusumo river was:

$$Q = 1.283448 * (h - 0.10)^{2.01592}, \tag{4-2}$$

The resulting hydrograph of the Rusumo River is illustrated on figure 4-13 where it is plotted against the corrected water stages on the left. The right side indicate the completed and corrected hydrograph.

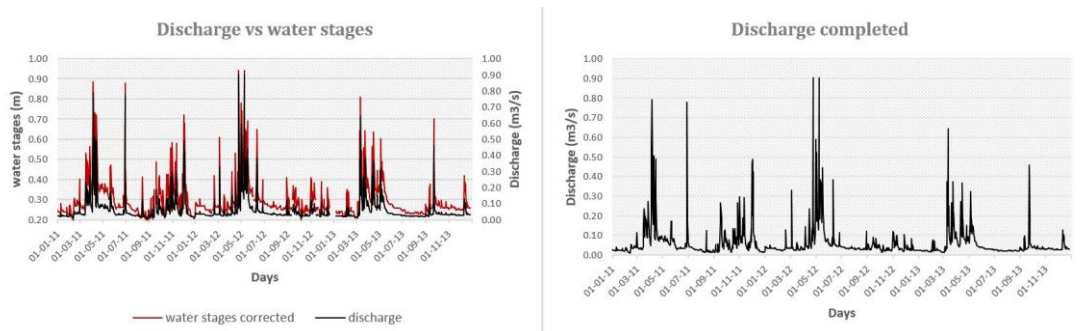


Figure 4-13: Rusumo River discharge.

- **Yanze sub catchment**

The same method was used to convert Yanze River stages into flow measurements. However, there was no necessity of correcting for systematic error in the stages collected. The main challenge with this sub catchment was that very few field measurements of discharge were available and that made the task very difficult in formulating its stage discharge relation. Nonetheless, the relation obtained was able to estimates the peaks but not the base flow. Since the research was about flooding, the relation was used, however more field measurements are required for proper representation of the stage discharge relationship of the Yanze River. The stage-discharge relationship obtained for the Yanze River was:

$$Q = 7.819934 * (h - 0.52)^{1.004906}, \tag{4-3}$$

Once the hydrograph was obtained using equation 4-3, the completion and correcting methods stated above were applied to end up with a complete hydrograph. Figure 4-14 illustrates the converted hydrograph against the water stages on the left and the completed hydrograph on the right.

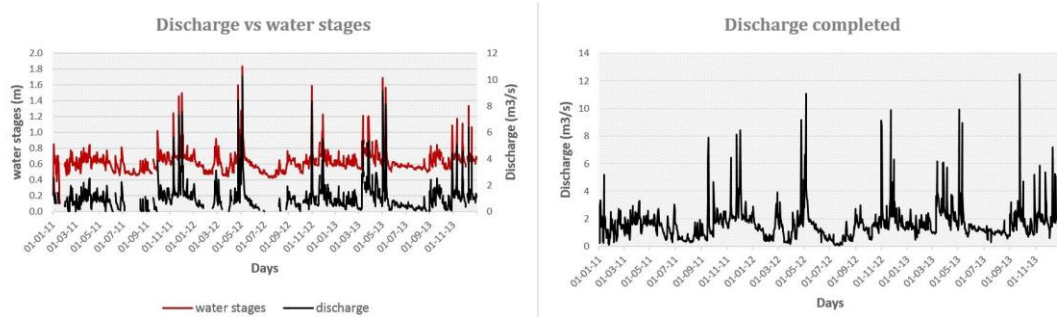


Figure 4-14: Yanze River discharge.

- **Nyabugogo catchment**

The stage-discharge relationship, obtained by applying the same methods described previously, used for the Nyabugogo River was:

$$Q = 8.1269 * (h - 0.3)^{0.97936}, \quad 4-4$$

Figure 4-15 illustrates the conversion of the stages into discharge on the left and on the right illustrates the filled in and corrected hydrograph.

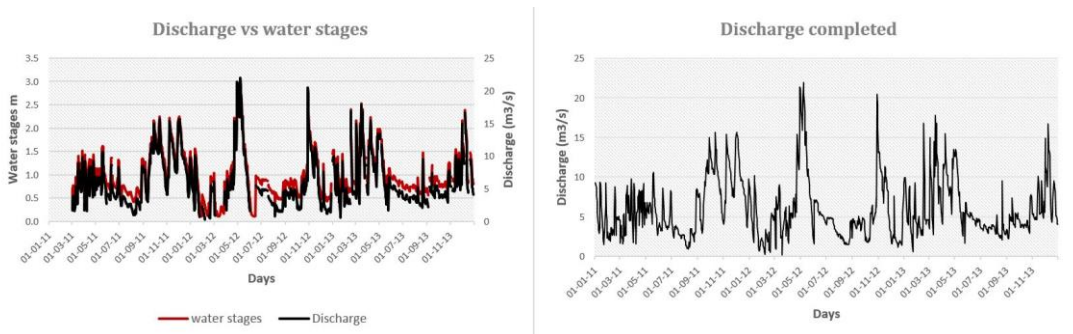


Figure 4-15: Nyabugogo River discharge.

4.2.3. Consistency check of discharge data

For better understanding of the catchment response to rainfall in terms of flow, the relation between the rainfall changes and flow changes were plotted. The logic behind this analysis is that an increase or decrease in rainfall should coincide with an increase or decrease in runoff. The change ratios are catchment specific and depend on the catchment topography, geology, soils, wetness, etc. According to Debru (2010), these ratios commonly ranges between +10 and -10 showing the system's response to rainfall. Values outside this range indicates abnormal catchment behaviour and therefore are considered errors in either the rainfall or runoff observations. The outlier correction method was applied for correction (Hoyos Goetz, 2011). The method consists of removing the outliers and replacing them by interpolated values in both the rainfall and discharge data of the corresponding date. The following equations were used to establish these ratios.

$$\Delta P = P_t - P_{t-1} \ \& \ \Delta Q = Q_t - Q_{t-1} \quad (mm), \quad 4-5$$

$$Ratio = \frac{|\Delta P|}{\Delta Q}$$

4-6

Few outliers were detected in Rusumo sub catchment data. Two outliers are in the range of -6000 to 6000 while the majority of the few outliers are in the range of -2000 to 2000. The following implied minor correction in the Rusumo sub catchment data. Figure 4-16 illustrates the ratios obtained for the Rusumo sub catchment data.

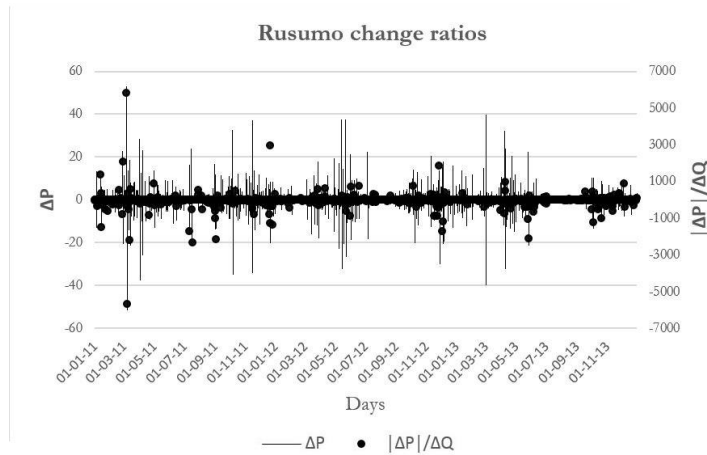


Figure 4-16: Rusumo sub catchment change ratios.

Few outliers were also observed in the ratios of the Yanze sub catchment data. One outlier was in the range of -1500. The majority of the few detected outliers were in the range of -600 to 600. The following is illustrated on figure 4-17. The outlier correction was also applied to correct for these.

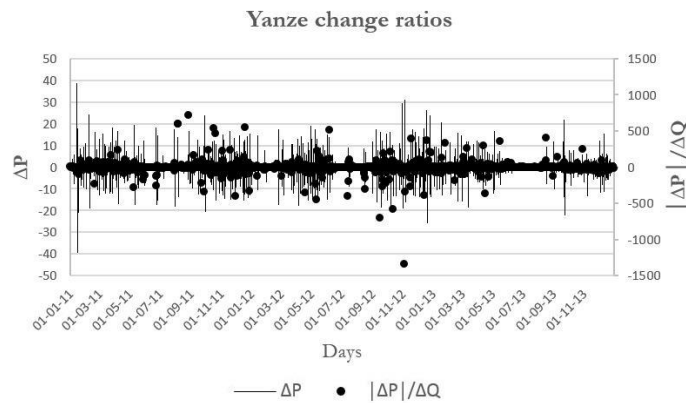


Figure 4-17: Yanze sub catchment change ratios.

The Nyabugogo catchment data ratios were observed with few outliers as well. Three outliers were in the range of 8000. The rest of the observed outliers were in the range of -4000 to 4000. Figure 4-18 illustrates these observations. The outlier correction method was applied for this case as well.

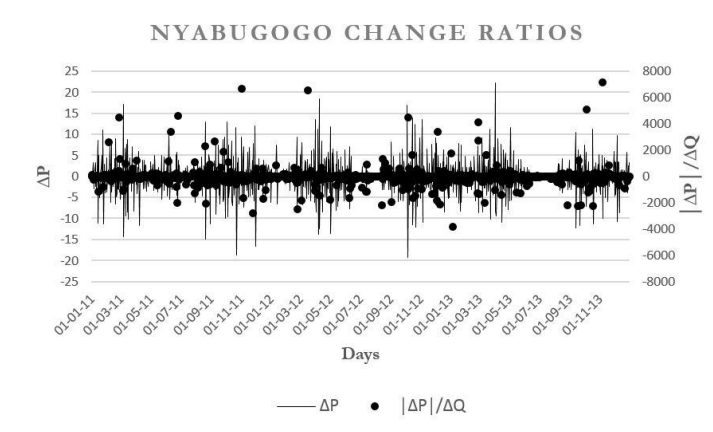


Figure 4-18: Nyabugogo catchment change ratios.

4.2.4. Corrected hydrographs

After identifying the outliers from the graphical analysis and correcting them as described above, the final hydrographs to be used in the Nyabugogo rainfall-runoff model were obtained. These are illustrated in the figure 4-19, 4-20 and 4-21.

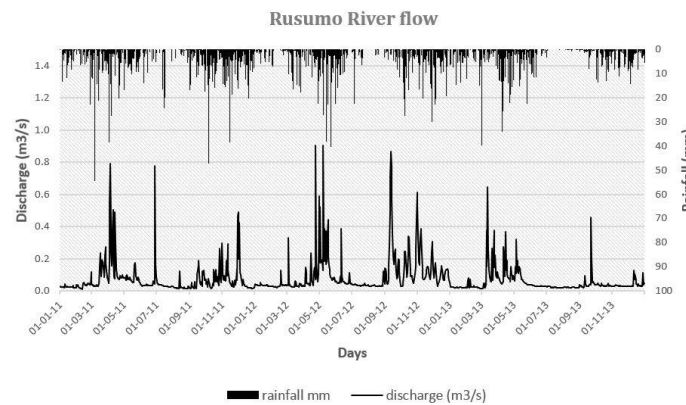


Figure 4-19: Rusumo River Hydrograph.

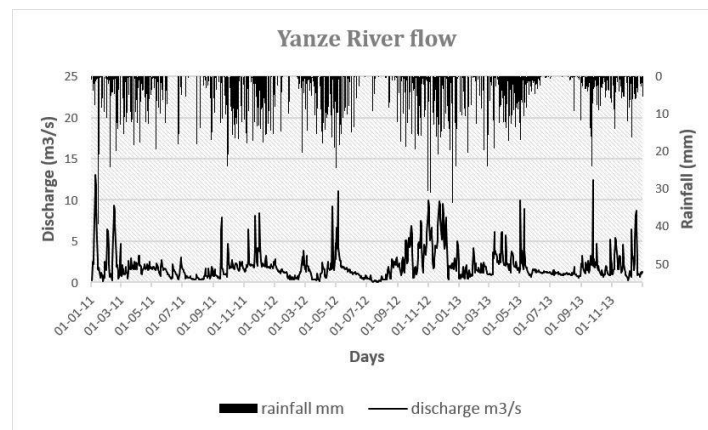


Figure 4-20: Yanze River hydrograph.

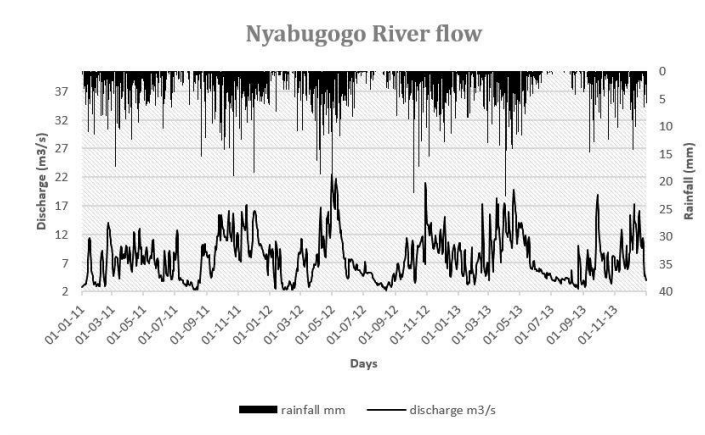


Figure 4-21: Nyabugogo River hydrograph.

4.2.5. Lake Muhazi sub catchment

A relatively simple approach based on hydrological reasoning and understanding was used to estimate the lake Muhazi outflow. Firstly, the water marks on the scale (figure 4-12) was considered to be the maximum and minimum stage limits of the lake response. In other words, these water marks represent the lake surface fluctuation due to rainfall (mostly effective rainfall draining to the lake). Secondly, the dimension fixed concrete outlet dyke was considered to be a no variable parameter in the output flow computation since everything about the dyke was fixed so that the manning's equation (Bray, 1979) could be applied. Thirdly, since the lake surface fluctuation influences the outflow and the latter is totally dependent on the runoff, a link between the runoff and the lake surface fluctuation was established. The computation of the runoff was done using the NRCS (SCS) CN method and the resulting runoff were normalized to the water marks in order to transform the lake surface fluctuations into stages. Lastly, using the manning's equation, the estimated stages were converted into discharges and resulted in the hydrograph provided in figure 4-22.

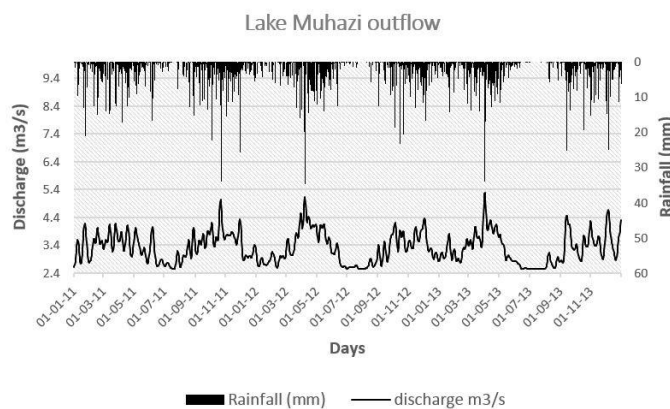


Figure 4-22: Lake Muhazi hydrograph.

4.3. Topographical data acquisition

Topographical data are very important for hydrologic modelling. The accuracy of these data in representing the terrain is of significant importance in modelling. Recent developments in topographical data acquisition have led to more reliable terrain representations that have contributed in improving the efficiency of hydrologic models. On one hand, for rainfall-runoff models, these data were used for catchment delineation, hydrological systems geomorphological parameters extraction, etc. And on the other hand, for flood models, these data were used for the terrain representation.

Two sources of topographical data were used in this research. The SRTM DEM¹⁷ was used to extract the geomorphological parameters of the Nyabugogo catchment and its sub catchments which were used in setting up the rainfall-runoff model in HEC-HMS and are summarized in the table 6-1. A 10 m spatial resolution DTM¹⁸ available locally at the RNRA was used to develop the 2D grid, at different resolution (5 m, 10 m, 15 m and 20 m), for the flood model in Sobek 1D2D.

The SRTM was an 11 days space shuttle flight mission in 1999 that used an IFSAR¹⁹ instrument to produce a near-global DEM of the earth's land surface with 16 m absolute vertical height accuracy at 30 m postings (Duren et al., 1998). The product is nowadays available with a horizontal spatial resolution of 90m and a vertical accuracy of 1m (Maathuis & Wang, 2006). This product was applied in this research, for extracting the catchments geomorphological characteristics, because of its vertical accuracy even for high altitudes.

The DTM collected from RNRA was obtained from the 0.25m spatial resolution digital orthophoto images that were produced as one of the outcomes of the Rwanda Land Use and Development Master Plan project. The resulting DTM had a spatial resolution of 10m while covering the entire country. The technique used (SWEDESURVEY, 2010) for producing the elevation data was considered with an acceptable accuracy for low lands but rather doubtful for high altitudes, therefore it was opted to use the SRTM data for the rainfall-runoff model and the national DTM for the flood model (which is a flood plain). A separate topographical survey, during fieldwork, was conducted by the researcher in order to obtain accurate information about the river geometry (more description is provided in the next section).

4.4. River geometry

An adequate representation of the river is of significant importance in flood modelling and especially in this study since a coupled 1D2D modelling approach was applied. It is common practice to collect information on the river geometry on site through topographical surveying as it was done in this research. The collection of these data was done using a total station instrument as illustrated on figure 4-7. The cross sections and longitudinal profile of the river were the main target of the topographical surveying done. Figure 4-23 illustrates the locations of the topographical data collection points. An example of the resulting cross section is illustrated in figure 4-7.

¹⁷ Shuttle Radar Topography Mission Digital Elevation Model.

¹⁸ Digital Terrain Model.

¹⁹ Interferometric Synthetic Aperture Radar.

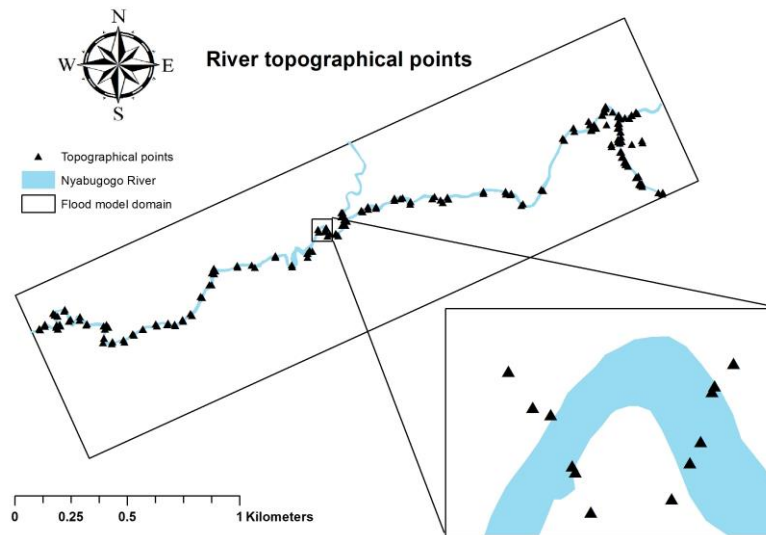


Figure 4-23: Nyabugogo River topographical points.

4.5. Observed flood depths

Flood depth observations on site are very helpful in assessing the efficiency of the flood model. Few observation points were collected during the fieldwork of this research. Since no measurements were available, interviews of the locals working and/or living in the Nyabugogo commercial hub was the main source of information about the flooding depth. The following source was supported and backed up with the identification of flood marks in the study area. The data were used in this research to assess the sensitivity of the flood model to surface roughness because the assessment of the efficiency requires more data about the flood characteristics in relation to a well captured event. Figure 4-24 illustrates the location of the collected observation points.

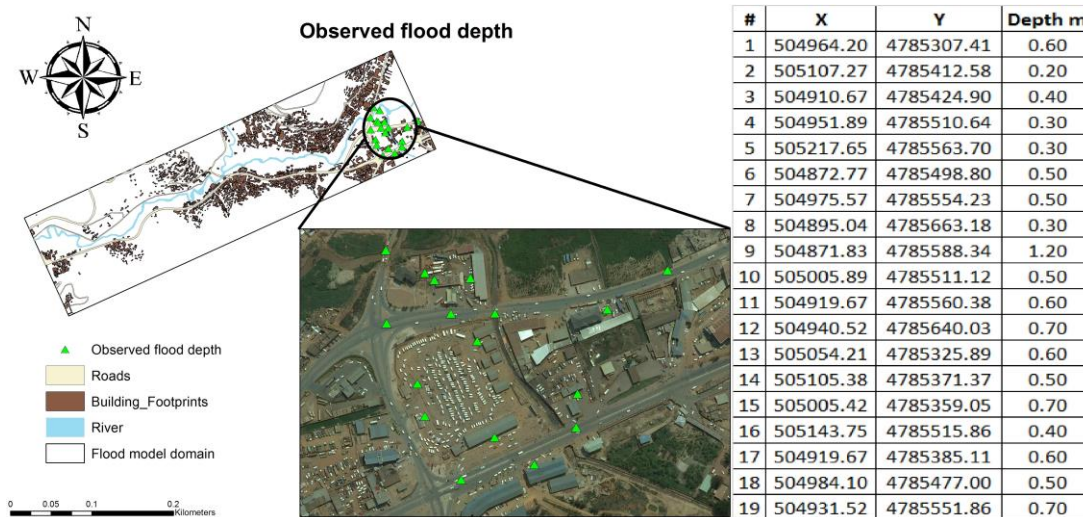


Figure 4-24: Flood depth observations.

4.6. Satellite rainfall data

High spatial and temporal resolution of rainfall observations were required in this study to enable analysis of the three to four hourly flood events frequently observed in the Nyabugogo commercial hub, downtown Kigali. The satellite rainfall product applied in this study to enable assessment of space-time

variability of the rainfall observations was the CMORPH²⁰ 8km X 8km product which is available every 30 minutes. The CMORPH rainfall estimates were obtained using the ISOD²¹ toolbox of the ILWIS²² software. A detailed description of the product is available on the NOAA²³ website. Figure 4-25 illustrates the toolbox used for accessing the product online.

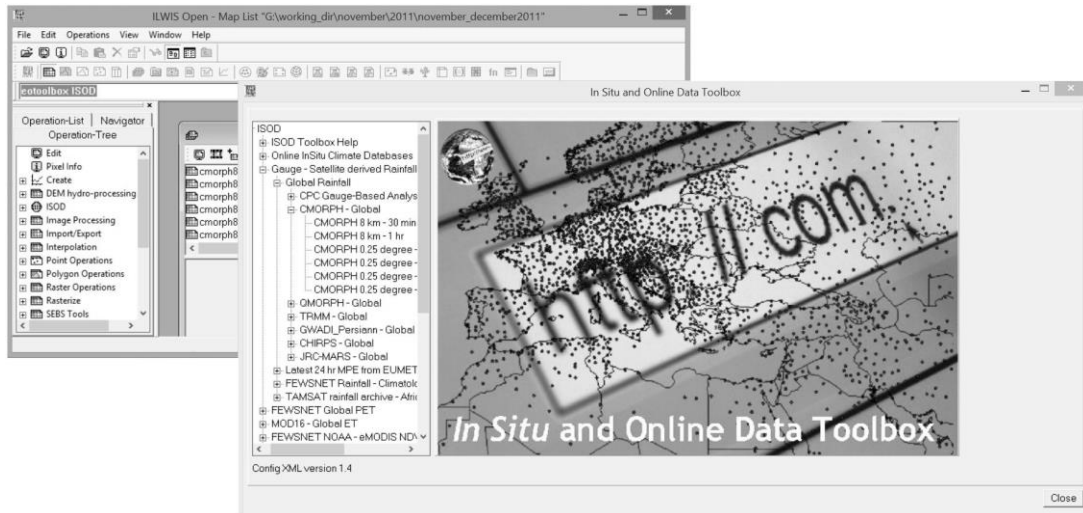


Figure 4-25: ISOD toolbox main screen.

²⁰ Climate prediction centre morphing technique.

²¹ In situ and Online Data toolbox.

²² Integrated Land and Water Information System.

²³ National Oceanic and Atmospheric Administration.

5. RESEARCH METHODOLOGY AND MATERIALS

5.1. Conceptual framework

This study used a hydrodynamic flood model to assess frequent flash floodings in the Nyabugogo commercial hub, downtown Kigali. The upstream inflows to the flood model were estimated using a rainfall-runoff model of the upstream area. To overcome the data scarcity problem, the model used for rainfall-runoff modelling required parameters which were estimated with some degree of certainty inherent from the available data. The unknown parameter values were locally regionalize (over the entire catchment) using those obtained from the gauged sub catchments calibrated rainfall-runoff model. The rainfall-runoff model was forced with extreme rainfall events obtained from satellite remote sensing. The space-time variability of the satellite rainfall estimates was used for rainfall representation. Figure 5-1 illustrates the main steps undertaken in this study.

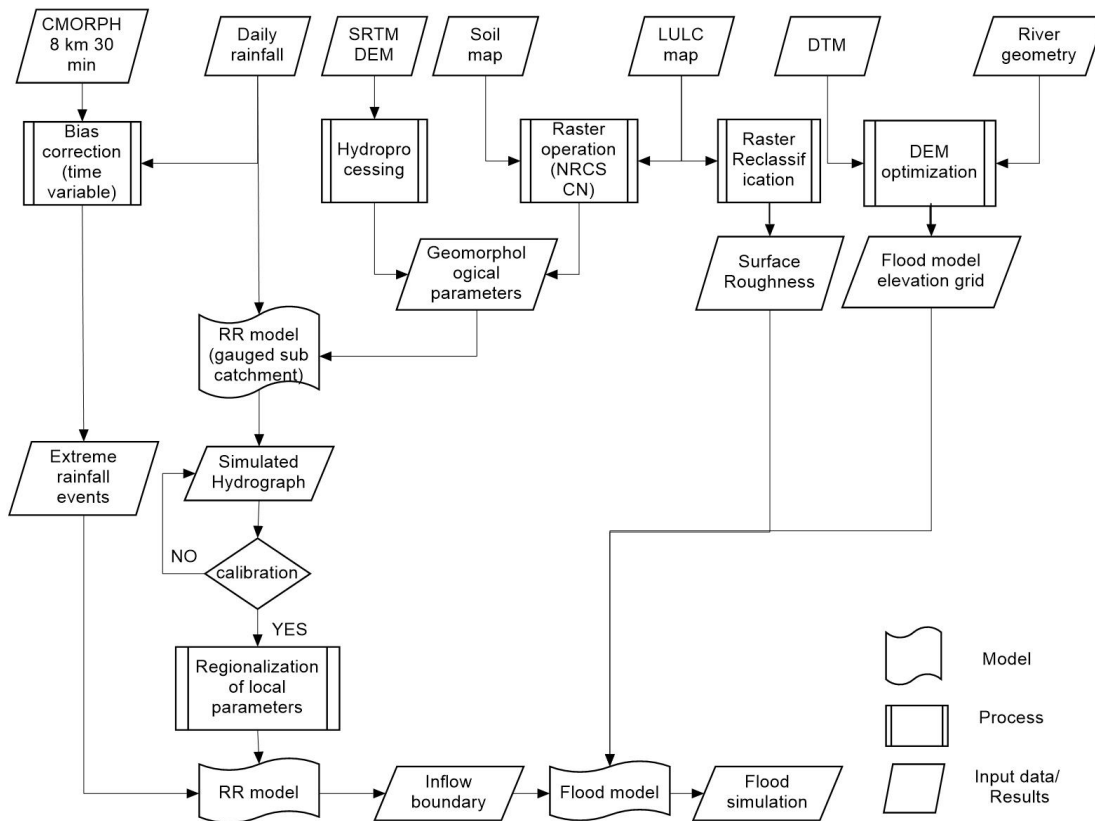


Figure 5-1: Conceptual framework.

5.2. Satellite rainfall estimates

5.2.1. Extreme rainfall events

The identification of the extreme rainfall events that may cause flooding was done based on the identification of hydrograph peaks and their corresponding recorded rainfall on figure 4-21, representing the entire Nyabugogo catchment response. A window of two weeks preceding and following the discharge peaks was taken in order to ensure that aspect of spatial-temporal rainfall variability were accounted for in analysing the relation between rainfall and related runoff. Rain event periods were selected:

- From November 28th, 2011 to December 7th, 2011;
- From May 3rd, 2012 to May 14th, 2012;
- From October 21st, 2012 to November 1st, 2012; and
- From March 11th, 2013 to March 20th, 2013.

The CMORPH rainfall estimates were used to represent the rainfall observations per sub catchments. Once this was done, the highest events were selected and considered to be the extreme rainfall events to serve flood model simulation in this study.

5.2.2. Bias correction

The CMORPH rainfall estimates have been tested and used in many hydrological applications. Many researchers like Alemseged Tamiru Haile, Habib, and Rientjes (2013) and Habib et al. (2014) have indicated the need of bias correction prior to application of the CMORPH 8km X 8km product for rainfall-runoff modelling. Bias correction on a daily time abse was applied to the satellite rainfall estimates used in this study to ensure adequate rainfall representation.

The method applied in this study was the time variable (TV) bias correction method as described by Habib et al. (2014). The space domain was fixed at sub catchments level and a daily window applied for the bias correction to ensure adequate rainfall representation. The mathematical form of the time variable bias correction is:

$$BF_{TV} = \frac{\sum_{t=d-l}^{t=d-1} \sum_{i=1}^n G_{(i,t)}}{\sum_{t=d-l}^{t=d-1} \sum_{i=1}^n S_{(i,t)}}, \quad 5-1$$

Where BF is the daily bias factor, G and S are the daily gauge and CMORPH rainfall estimates respectively, i is the gauge location, t is the time step number and l is the length of the time window for bias calculation.

The CMORPH rainfall fields were multiplied by the BF_{TV} for their respective time windows to result in a CMORPH set which is bias corrected and illustrated in figure 6-2.

5.3. Rainfall-runoff modelling

5.3.1. Sub catchments geomorphological parameters

A combination of different methods was used for estimating the geomorphological parameters required for rainfall-runoff modelling in this study. These methods include the NRCS CN²⁴ method as described by Arlen D. Feldman (2000) and the SRTM DEM Hydroprocessing as described by Maathuis and Wang (2006).

The CN parameter is estimated as a function of land use, soil type and antecedent soil moisture using the tables provided by the NRCS. The application of this method was done based on previous work by MUSONI (2009). From the soil texture component of the available soil map, the saturated hydraulic conductivities were obtained using the SPAW²⁵ model. The resulting saturated hydraulic conductivities were optimized using the soil depth component of the available soil map and were related to the

²⁴ National Resources Conservation Service Curve Number.

²⁵ Soil-Plant-Atmosphere-Water hydrologic budget model.

hydrologic soil groups (HSG) using the NRCS CN classification. The resulting HSG map was combined with the existing LULC map to produce the CN map based on the NRCS CN tables. Since the sub catchments consisted of several soil types and land uses, a composite CN was calculated per sub catchments, as:

$$CN_{composite} = \frac{\sum A_i CN_i}{\sum A_i}, \quad 5-2$$

Where A_i is the drainage area of the subdivision i , CN_i is the CN for the subdivision i and $CN_{composite}$ is the composite CN used for runoff volume computations.

According to Arlen D. Feldman (2000), the users of the NRCS CN model as implemented in HEC-HMS²⁶ must know that the CN table used include composite CN for urban districts, residential districts and newly graded areas. If these CN are used, no further accounting of directly-connected impervious area is required.

The SRTM DEM was hydroprocessed using the ILWIS DEM Hydroprocessing toolbox and ArcGIS hydrology toolbox. The steps undertaken for Hydroprocessing were provided by (Maathuis & Wang, 2006).

The resulting HSG and CN maps are illustrated on figure 6-1 and the geomorphological parameters are provided in table 6-1.

5.3.2. HEC-HMS model development

A detailed description of the HEC-HMS model is provided in the technical reference manual edited by Arlen D. Feldman (2000). HEC-HMS is a conceptual model which represents the watershed components in separate sub models and simulate the watershed behavior using the sub models in an uncoupled manner (Hoyos Goez, 2011). A simpler approach, proposed and available in HEC-HMS, was adopted in this study because it is a flood study. For this case, a detailed accounting and reporting of the water amount stored in the upper soil layers was not required since the model only served to estimate the peak runoff discharge for selected event periods. Simpler representations of the watershed behaviour were used, shown in figure 5-2, where only the necessary components for predicting runoff were detailed while the rest were lumped (Arlen D. Feldman, 2000).

²⁶ Hydrologic Engineering Center-Hydrologic Modelling System from the U.S. Army Corps of Engineers.

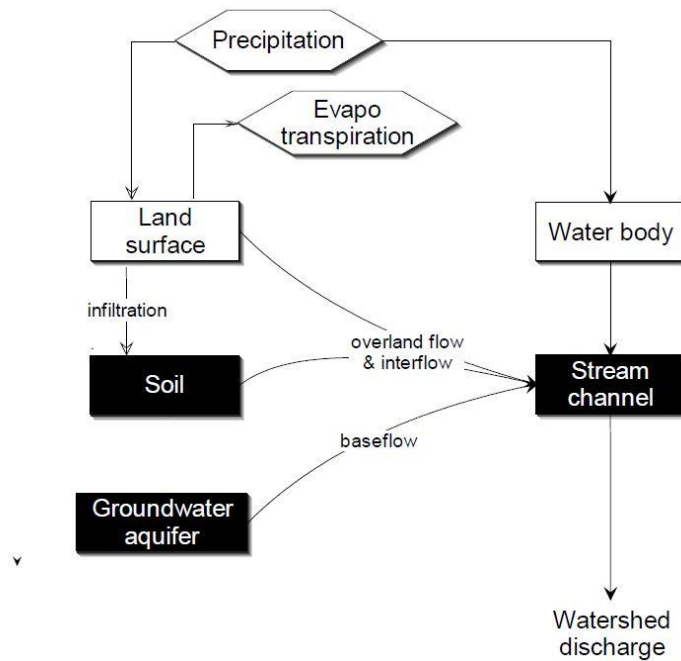


Figure 5-2: Typical watershed runoff representation (Arlen D. Feldman, 2000).

For the runoff components on figure 5-2, separate models in HEC-HMS are provided. These are classified as a direct runoff, a base flow and a channel flow model. An overview of these models are provided in the HEC-HMS technical reference manual. The choice of the methods used in this study, was based on their suitability for event modelling but also the data availability and limitations. The aim was to apply a combination of models in HEC-HMS in such a way that all the required parameters values may be estimated from the available data with a certain degree of accuracy inherent to these data and the remaining unknown values estimated from calibration of the gauged sub catchment models and regionalize locally to the entire catchment. The selected models for this study are illustrated in figure 5-3.

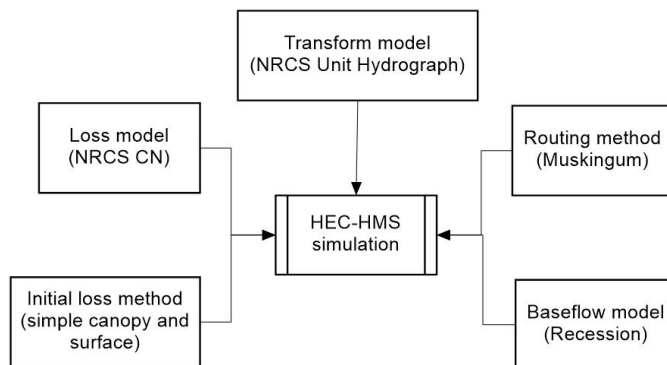


Figure 5-3: HEC-HMS applied components.

The setting of the HEC-HMS model was done in 4 stages. Firstly, a definition of the basin model manager comprising all the sub models discussed above was done. Secondly, all the required time series (precipitation, discharge, etc.) were defined and stored in the time series data manager. Then a meteorological model manager regulating the distribution of the time series over the sub catchments was defined. Finally, the control specifications were established specifying the simulation time step as well as the beginning and end time of the simulation in the control specification manager. The description of the HEC-HMS sub models in this study adopted from the HEC-HMS manual is as follows:

- **Runoff volume computation:**

The NRCS CN model was used to estimate the excess precipitation which is done as a function of cumulative precipitation, soil cover, land use and antecedent moisture. Its mathematical expression is:

$$P_e = \frac{(P-0.2S)^2}{P+0.8S}, \quad 5-3$$

Where P_e is the accumulated precipitation excess at time t , P is the accumulated rainfall depth at time t , I_a is the initial abstraction (initial loss) and S is the potential maximum retention (watershed ability to abstract and retain storm precipitation). Excess precipitation is activated when rainfall exceeds the initial abstraction. An empirical relationship between I_a and S was developed from analysis of the results of small experimental watersheds by the NRCS. It resulted in $I_a = 0.2S$.

The parameter S is related to the watershed characteristics through the curve number (CN) as:

$$S = \begin{cases} \frac{1000-10CN}{CN} & \text{(foot - pound system)} \\ \frac{25400-254CN}{CN} & \text{(SI)} \end{cases}, \quad 5-4$$

- **Direct runoff modelling:**

The NRCS Unit Hydrograph, a parametric UH model, was used in this study. The NRCS technical report 55 provides a detailed description of this model. The basic concept of this model is a dimensionless, single peaked UH which peak discharge (U_p) is expressed as the ratio of the watershed area (A) and the time to peak (or time of rise t_p). The model is mathematically expressed as:

$$U_p = c \frac{A}{T_p}, \quad 5-5$$

Where C is the conversion constant (2.08 in S.I. and 484 in foot-pound system). The time to peak is expressed in terms of the unit of excess precipitation as:

$$T_p = \frac{\Delta t}{2} + t_{lag}, \quad 5-6$$

Where Δt is the excess precipitation duration (computational run interval) and t_{lag} is the basin lag time. It is suggested that the lag time be related to the time of concentration (t_c) as:

$$t_{lag} = 0.6t_c, \quad 5-7$$

For this research, based on the available data, the Bransby William equation as reported by (Wanielista et al., 1997) was applied. The equation is as follows:

$$t_c = 21.3L \frac{1}{A^{0.15^{0.2}}}, \quad 5-8$$

Where t_c is the time of concentration (T), L is the main channel length (L), S is the longitudinal slope of the channel and A is the watershed area (L^2). The equation is described appropriate for terrain with steep slopes like hilly or mountainous terrain.

- **Base flow modelling:**

In this research, the exponential recession model was used for base flow modelling. It is commonly used to explain the natural storage drainage in a watershed. The base flow at any time t is related to an initial value as:

$$Q_t = Q_0 k^t, \quad 5-9$$

Where Q_t and Q_0 are the base flow at time t and initial base flow (at time zero) respectively and k is the exponential decay constant. The decay constant is defined as a ratio of the base flow at time t to the base flow one day earlier. The initial base flow can be specified as flow rate (L^3T^{-1}) or as a flow per unit area (L^5T^{-1}). Since the recession base flow model is applied at the beginning of a storm event and later in the event as the subsurface flow reduces up to the channel level, a user-defined threshold flow is to be defined. This threshold can be defined as a flow rate or as a ratio to the computed peak flow and serves to define the time the total flow is to be computed after the peak of the direct runoff. The parameters required for this model include the initial flow, recession ratio and the threshold flow.

- **Channel flow modelling:**

These models are also known as routing models in HEC-HMS. They compute downstream hydrographs by solving the continuity and momentum equations which are the basic equations behind the open channel flow. These equations constitute the Saint-Venant equations or dynamic wave equations and are based on assumptions like constant velocity and horizontal water surface across the channel section, gradual variation of flow with hydrostatic pressure prevailing at all points in the flow, also no lateral and secondary circulation considered and finally fixed channel boundaries.

For this research, the Muskingum routing model was used. A simple finite difference approximation of the continuity equation is used in this model and it is written as:

$$\left(\frac{I_{t-1}+I_t}{2}\right) - \left(\frac{O_{t-1}+O_t}{2}\right) = \left(\frac{S_t-S_{t-1}}{\Delta t}\right), \quad 5-10$$

The reach storage in figure 5-4 is modelled as the sum or the difference of the prism storage and the wedge storage depending on the flood rising and falling stage respectively.

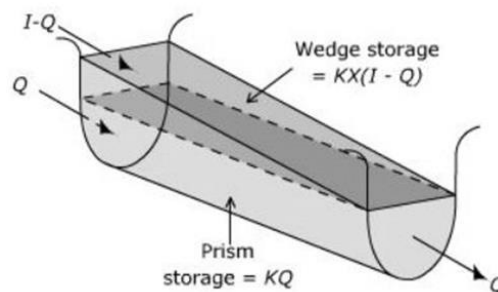


Figure 5-4: Muskingum reach schematization.

Considering that the prism storage is the outflow rate (Q) multiplied by the travel time k and that the wedge storage is an inflow-outflow weighted difference multiplied by the travel time k , the following equation is obtained.

$$S_t = kQ_t + kX(I_t - Q_t) = k[XI_t + (1 - X)Q_t], \quad 5-11$$

Where k is the travel time of the flood wave in the reach, X is a dimensionless weight ($0 \leq X \leq 0.5$).

5.3.3. Calibration of the HEC-HMS model

“**Model calibration:** the procedure of adjustment of parameters values of a model to reproduce the response of reality within the range of accuracy specified in the performance criteria.”

(Refsgaard & Henriksen, 2004)

There are many performance criteria that can be used for calibration. In this study, three performance criteria have been used to assess the efficiency of the rainfall-runoff model, these were set to control the peak, volume and hydrograph simulation. These are mathematically shown in the table 5-1.

#	Performance criteria	Equation
1	Peak-weighted root mean square error.	$PWRMSE = \left\{ \frac{1}{NQ} \left[\sum_{i=1}^{NQ} (q_o(i) - q_s(i))^2 \left(\frac{q_o(i) + q_o(mean)}{2q_o(mean)} \right) \right] \right\}^{\frac{1}{2}}$
2	The Nash-Sutcliffe coefficient of efficiency.	$NS = 1 - \frac{\sum_{i=1}^n (Q_{obs} - Q_{sim})^2}{\sum_{i=1}^n (Q_{obs} - \bar{Q})^2}$
3	The Relative Volumetric Error.	$RVE = \left(\frac{\sum_{i=1}^n Q_{sim(i)} - \sum_{i=1}^n Q_{obs(i)}}{\sum_{i=1}^n Q_{obs(i)}} \right) * 100$

Table 5-1: Performance criteria.

5.3.4. Regionalization of the local parameters

In this study, the gauged sub catchment rainfall-runoff models were set up first. The aim was to determine through calibration the value of the parameters that are unknown for the ungauged sub catchments. These parameters were the Muskingum K and X and the Initial base flow, recession constant and threshold base flow. Their optimum values, obtained after calibration, were used through rationing to estimates the values of the ungauged sub catchments parameters based on the assumption that the sub catchments of one mesoscale catchment have similar properties.

The rationing of the parameters K and X was done based on the river length conversion. The obtained ratios were then used for the ungauged sub catchments based on the proximity factor with respect to the gauged sub catchments.

The average of the recession constants of the two gauged sub catchments was used as the estimate of the ungauged sub catchments recession coefficient. The area conversion was then applied to determine the initial base flow and threshold base flow ratios per gauged sub catchments. These ratios were then averaged as well before application as estimates for the ungauged sub catchments.

5.4. Flood modelling

5.4.1. Digital terrain modelling

The comparison of DEM interpolation methods is necessary for flood modelling since it provides information on the most accurate representation of the topography for a particular study area (A.T. Haile, 2005). This statement indicates that 2 kinds of assessments are required for producing an adequate and accurate topographical representation. However, in this research, a pre-processing of the available topographical data revealed that the interpolation methods assessment was of less importance since their effects were considered negligible. This was due to the study area set up and its features (natural and artificial) representation. Firstly, the flood model domain is a flat river flood plain. In addition to that, the

existing features (river, roads and buildings) were out of the assessment since these were brought in from field measurements (refer to the river geometry section 4.4) and available features footprints (buildings and roads). Secondly, the pre-processing of the available DTM consisted of using different interpolation methods (with different weights wherever required) and comparing the resulting DEMs among them using the raster differentiation. The obtained differences were negligible and located in high altitudes at the edges of the flood model domain where less priority in accurate representation was required. After pre-processing of the DTM used for the flood model domain topographical representation, the IDW²⁷ method with the weight 2 was used for the interpolation of the flood model elevation grid.

Four spatial resolution of the elevation grid were produced from the DTM collected as illustrated on figure 5-5. These resolutions were 5, 10, 15 and 20m; and where tested with the preliminary flood simulations to enable assessment of the one close to representing the reality so to be used for further analysis.

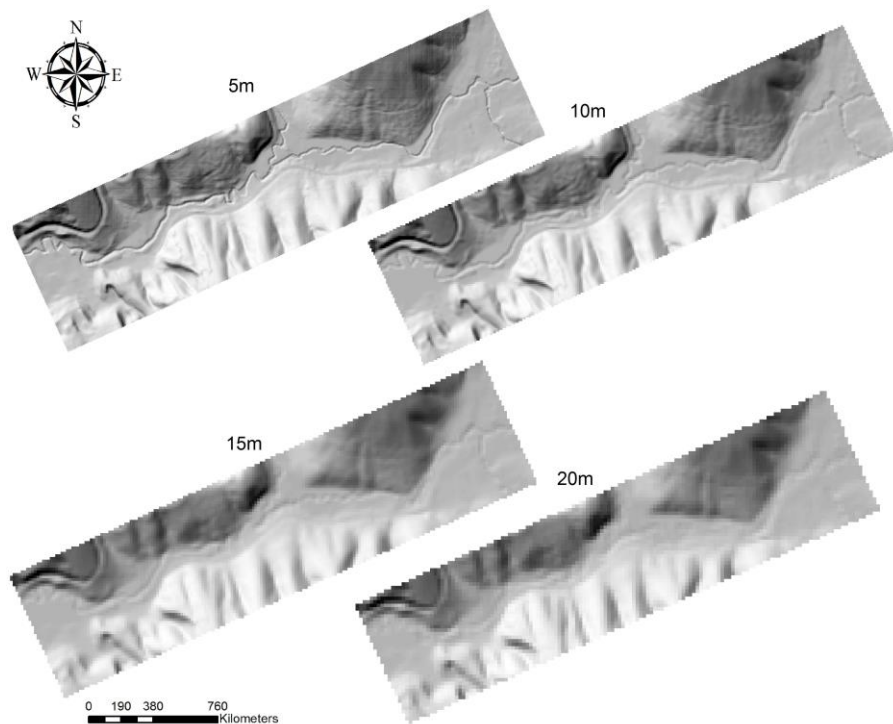


Figure 5-5: Hill shades of the elevation grid at different resolutions.

5.4.2. River geometry

The topographical points illustrated on figure 4-24 were used to interpolate the river geometry. Two different steps were done in order to represent the river geometry in this study. Firstly, the longitudinal profile of the river was interpolated at the real world riverbed elevation (as collected on the field). Secondly, the river cross sections (more than fifty) were used in the flood model as shown on figure 5-6. The interpolation method used was the IDW with weight 2. This was done with 2 rows of points measured on site with a total station at the riverbed level. The effects of different interpolation methods were found negligible in this case as well. Considerable efforts were put in setting the 1D network in the flood model as shown on figure 5-6.

²⁷ Inverse Distance Weighting.

5.4.3. Sobek 1D2D model development

- **Model approach and equations**

Sobek 1D2D model was developed by WL/Delft hydraulics. A complete description of the governing equations used in Sobek is provided in the user's manual, chapter six (Delft/Hydraulics, 2014). Sobek combines 1D and 2D approaches to simulate water flow in river reaches, riverbank overflow and flow in floodplains, using a finite difference approximation allowing the use of rectangular grids only (A.T. Haile, 2005). The combined 1D and 2D Sobek is used when the channel width is narrower than the size of the grid cells. The computation of water flow is done by solving the complete Saint-Venant equation using the Delft-scheme numerical solver.

For 1D flow, two equations are solved. These are:

- Continuity equation (1D):

$$\frac{\partial A_f}{\partial t} + \frac{\partial Q}{\partial x} = q_{lat}, \quad 5-12$$

- Momentum equation (1D):

$$\frac{\partial Q}{\partial t} + \frac{\partial}{\partial x} \left(\frac{Q^2}{A_f} \right) + g A_f \frac{\partial h}{\partial x} + \frac{g Q |Q|}{C^2 R A_f} - w_f \frac{\tau_{wind}}{\rho_w} = 0, \quad 5-13$$

The first term describes the inertia, the second describes the convection, the third describes the water level gradient, the fourth describes the bed friction and the last term describes the wind friction.

Where: A_f is the cross sectional flow area (L^2), Q is the discharge (L^3T^{-1}), q_{lat} is the lateral discharge per unit length (L^2T^{-1}), g acceleration due to gravity (LT^{-2}), x is the distance (L), t is the time (T), h is the water level (L), w_f is the cross sectional width at the water level (L), C is the Chezy coefficient ($L^{1/2}T^{-1}$), R is the hydraulic radius (L), ρ_w is the water density (ML^{-3}) and τ_{wind} is the wind shear stress ($LT^{-2}M^{-1}$).

For 2D flow, three equations are solved. These are:

- Continuity equation (2D):

$$\frac{\partial \zeta}{\partial t} + \frac{\partial(uh)}{\partial x} + \frac{\partial(vh)}{\partial y} = 0, \quad 5-14$$

- Momentum equations (2D) in (the x- and y-direction):

$$\frac{\partial u}{\partial t} + u \frac{\partial u}{\partial x} + v \frac{\partial u}{\partial y} + g \frac{\partial \zeta}{\partial x} + g \frac{u|\bar{u}|}{C^2 h} + au|u| = 0, \quad 5-15$$

$$\frac{\partial v}{\partial t} + u \frac{\partial v}{\partial x} + v \frac{\partial v}{\partial y} + g \frac{\partial \zeta}{\partial y} + g \frac{v|\bar{v}|}{C^2 h} + av|v| = 0, \quad 5-16$$

The terms in the equations above are respectively the acceleration terms, horizontal pressure gradient terms, convective terms, bottom friction terms and wall friction terms.

Where: \mathbf{u} is the velocity in x-direction (LT^{-1}), \mathbf{v} is the velocity in y-direction (LT^{-1}), $|\bar{\mathbf{u}}|$ is the velocity magnitude ($=\sqrt{u^2 + v^2}$) (LT^{-1}), ζ is the water level above plane of reference (L), \mathbf{C} is the Chezy coefficient ($L^{1/2}T^{-1}$), \mathbf{h} is the total water depth ($= d + \zeta$) (L), \mathbf{d} is the depth below plane of reference (L), \mathbf{a} is the wall friction coefficient (L^{-1}).

The 2D equations in Sobek differ from the 1D because the 2D do not incorporate the turbulent stress terms (considered unimportant for flood flow computations) but rather have wall friction terms (to account for the resistance of vertical obstacles like houses, trees, etc.).

The calculation procedure in Sobek 1D2D is based on the momentum equation for calculating the velocity at future time for the overland flow (A.T. Haile, 2005). The fractional time step method is used for solving the momentum balance. In the first fractional time step the advection is calculated then the friction and pressure gradient terms are calculated in the second fractional time step. Substituting the first fractional time step velocity in the discretized momentum balance results in the equation 5-17.

$$\mathbf{u}_m^{t+1} = \mathbf{u}_m^t + \Delta t \left\{ g \frac{\theta(\zeta_{Cm,1}^{t+1} - \zeta_{Cm,2}^{t+1})}{dm} + g \frac{(1-\theta)(\zeta_{Cm,1}^t - \zeta_{Cm,2}^t)}{dm} + \frac{g \mathbf{u}_m^{t+1} |\mathbf{u}_m^t|}{C^2 (\zeta_m^t - b_m)} \right\} \quad 5-17$$

Where \mathbf{u}_m is the velocity orthogonal to the edge which is calculated in advection, \mathbf{C} is the Chezy coefficient, $\mathbf{C}_{m,1}$ and $\mathbf{C}_{m,2}$ are cells centres, ζ_m and $\zeta_{m,1}$ are the water surface levels above some reference level at m and $\mathbf{C}_{m,1}$, b_m is the bottom level (above the reference level) of line m .

In Sobek, the equation 5-17 is rewritten with the coefficients $\mathbf{r}(\mathbf{u})$ and $\mathbf{f}(\mathbf{u})$:

$$\mathbf{u}_m^{t+1} = \mathbf{r}(\mathbf{u})_{(m)} + \mathbf{f}(\mathbf{u})_{(m)} (\zeta_{Cm,1}^{t+1} - \zeta_{Cm,2}^{t+1}), \quad 5-18$$

Where:

$$\mathbf{r}(\mathbf{u})_{(m)} = \left(\frac{1}{\Delta t} - \frac{g |\mathbf{u}_m^t|}{(\zeta_m^t - b_m) C^2} \right)^{-1} \left(\frac{\mathbf{u}_m^t}{\Delta t} + (1 - \theta) \frac{g}{dm} (\zeta_{Cm,1}^t - \zeta_{Cm,2}^t) \right), \quad 5-19$$

$$\mathbf{f}(\mathbf{u})_{(m)} = \left(\frac{1}{\Delta t} - \frac{g |\mathbf{u}_m^t|}{(\zeta_m^t - b_m) C^2 \Delta t} \right)^{-1} \left(\theta \frac{g}{dm} \right), \quad 5-20$$

The term $(\zeta_m^t - b_m)$ is the water depth at line m taken from the outflow cell.

The velocity substitution in the mass balance equation in terms of $\mathbf{f}(\mathbf{u})$ and $\mathbf{r}(\mathbf{u})$ results in a linear equation for the water levels in each cell, written in a matrix as shown below. This linear system of equations is calculated by the iterative method known as conjugate gradient.

$$\mathbf{A} \begin{pmatrix} \zeta_1^{t+1} \\ \zeta_2^{t+1} \\ \zeta_3^{t+1} \\ \vdots \\ \zeta_n^{t+1} \end{pmatrix} = \mathbf{b}, \quad 5-21$$

\mathbf{A} is the wetted cross section and it is explicitly calculated in Sobek.

- **Model schematization**

In Sobek 1D2D, the user interface called NETTER provides possibilities of data input and editing as well as tools for viewing the model results. The schematization of the 1D channel was done separately from the 2D grid. The latter was imported in the NETTER as an ASCII file already prepared in ArcGIS. Different tools provided in NETTER were used to schematize the 1D network. A series of reaches were used to represent the 1D network, these were connected by connection nodes and their geometries were defined using cross-section nodes. Structures like bridges, culverts, etc. were defined using special nodes. Upstream inflows to the flood model were input using 2D boundary nodes placed at the edges of the 1D network. In the 1D2D setup in Sobek, the 1D channel is firstly filled with water before the overflow is simulated on the 2D grid. An illustration of the above is provided on figure 5-6.

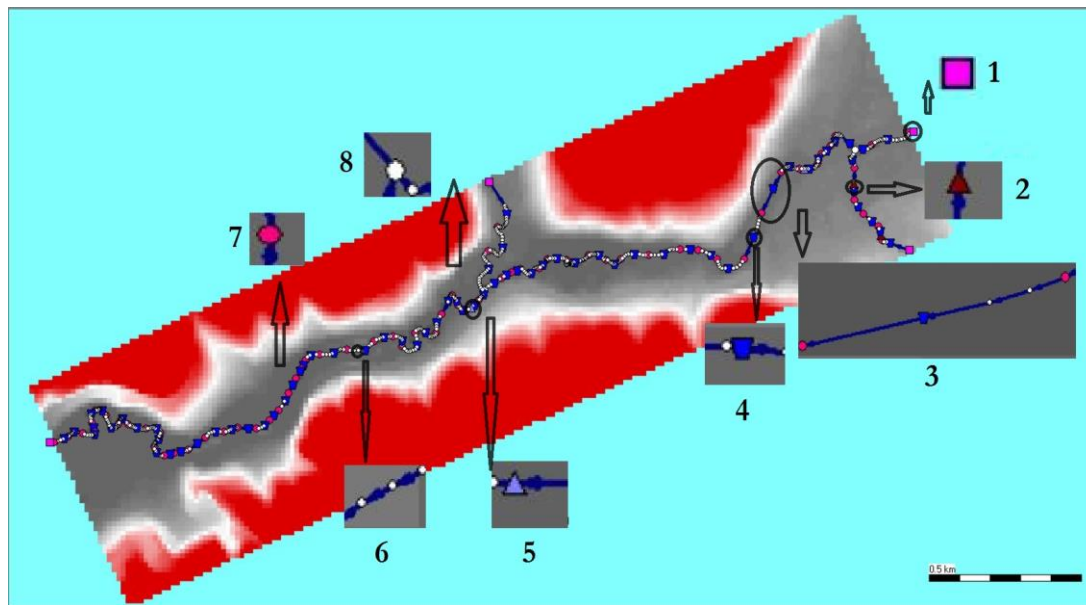


Figure 5-6: schematization in Sobek 1D2D.

On figure 5-6 the numbers indicate the following:

1. 2D boundary nodes
2. Culvert node
3. Reach
4. Cross section node
5. Bridge node
6. Calculation points
7. Connection node
8. Linkage node

Channel characteristics like cross section, water surface level, riverbed and friction factor defining the flow were input in the NETTER through the cross section nodes (refer to figure 5-7). These nodes were specified for all the reaches. These cross sections were obtained from the topographical survey described previously in the section 4.4.

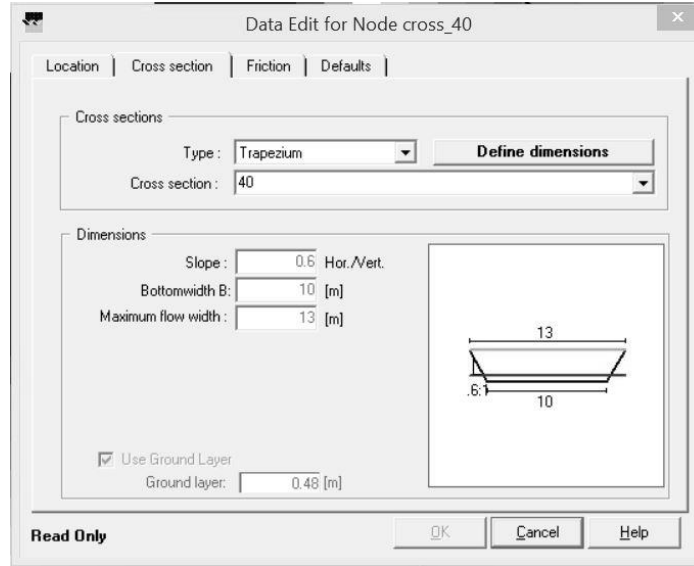


Figure 5-7: Cross section input window in NETTER.

A setp wise calibration was adopted in this study to overcome the problem of data scarcity. This was based on the researcher's study area knowledge and the observed flood depths. The parameters used during this process for assessing the setting up of the flood model were the maximum flood depth, maximum velocity, inundation area and flood duration.

5.4.4. Surface roughness

The surface roughness, which indicates the resistance to the flow of water in the flood model domain, was defined using the Manning's coefficients. This is one of many ways of defining the surface roughness in Sobek. Tabulated values of the Manning's coefficients are available in many reference books. Since the surface roughness is significantly related to the land cover, the available orthophoto (0.25 m resolution) of the study area was used to define the surface roughness. A classification of the study area land cover was done and resulted in five classes that were used to define the roughness coefficients. These classes were the green areas (forest, agriculture, etc.), the commercial areas, the roads and parkings, the residential areas and the river channel. The definition of the surface roughness resulted in a map showing the distribution of the roughness coefficients over the entire flood model domain. The map was given a same spatial resolution as the elevation grid used in sobek as required by the model. The latter is done in Sobek so that a roughness and height is defined for every grid in the flood model domain.

#	Land Cover	Manning's coefficients
1	Green areas	0.025
2	Commercial zones	0.03
3	Residential zones	0.032
4	Roads and parkings	0.035
5	River channel	0.04

Table 5-2: Roughness coefficient adapted from Tennakoon (2004).

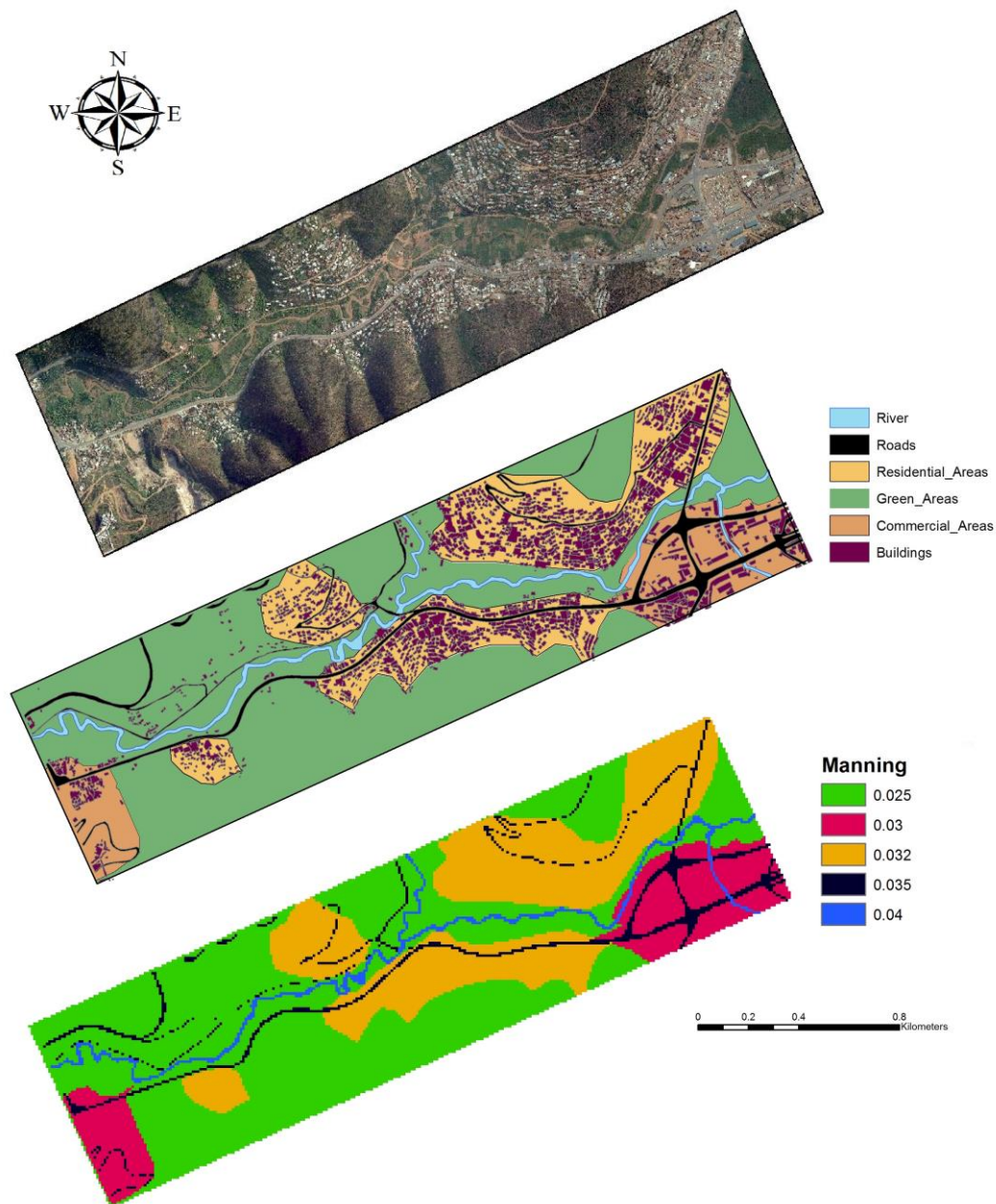


Figure 5-8: Roughness coefficient map.

The buildings roughness coefficients representation was done using their footprints. Three possible ways of representations exist and are dependent on the specification of the surface roughness values during the flood model parameterization. The buildings can be solid objects in this case blocking completely the flow of water where their pixels are assigned a roughness value of 1, other features like roads for example, act as the conveying and storage structures of the flooding water. Buildings can also be partially solids objects where their pixels are assigned larger roughness values (in this case 0.7) which act as storage structures of the flooding water during the flood event to release the excess water after the event with a larger delay. Finally, buildings can be hollow objects where a relatively small and single roughness value for the entire domain is specified, in this case their pixels simultaneously act as conveying and storage structures of the flooding water. Solid objects representation for buildings requires the DEM to include the heights of buildings on their pixels (A.T. Haile, 2005).

6. RESULTS AND DISCUSSION

6.1. Geomorphological parameters

Figure 6-1 illustrates the HSG and CN maps used in this research and indicates that A and D were the dominant Hydrological Soil Groups. Also the CN were found in the range of 85 - 88 with the exception of the floodplain area with a CN of 65 and the sub catchment of Gatare with a value of 92.5.

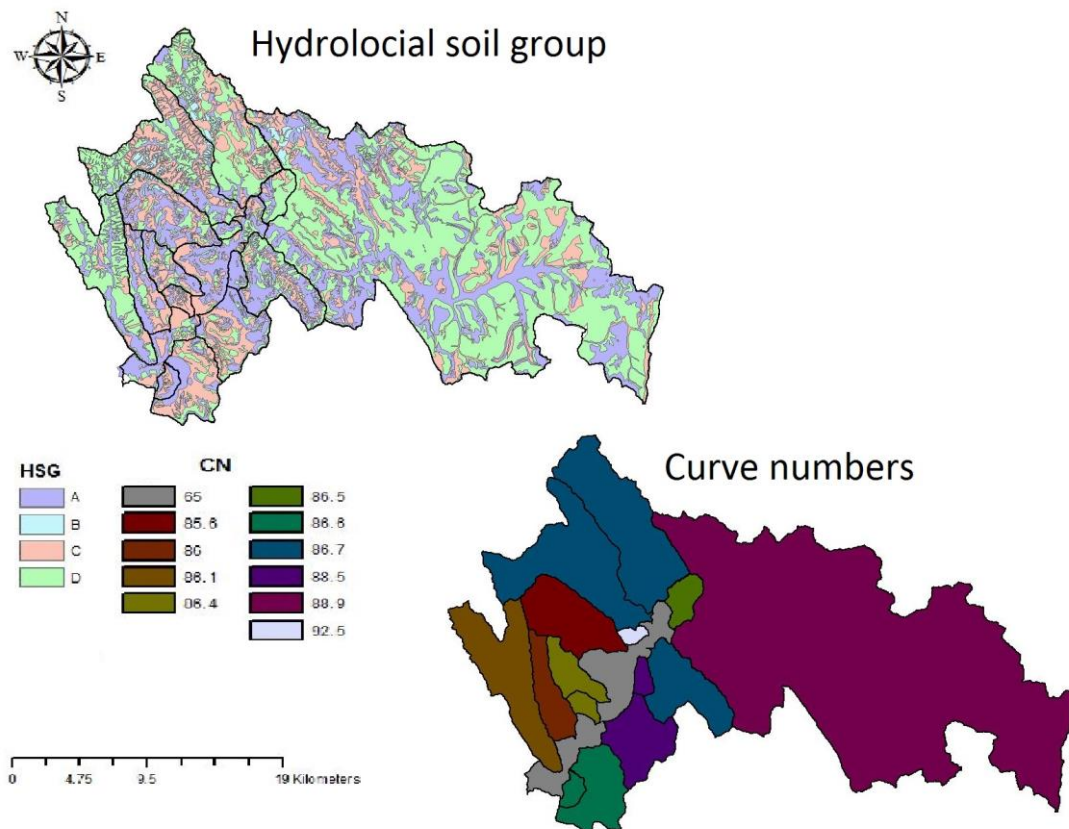


Figure 6-1: HSG and CN maps.

The Hydroprocessing results provided characteristics of the sub catchments which indicated that the majority of sub catchments delineated have relatively small areas with steep slopes. The floodplain and the Lake Muhazi sub catchment were found with flat slopes and large areas. A combination of these information resulted in the production of the table 6-1 which was the basis of setting up the rainfall-runoff model in HEC-HMS.

#	Sub Catchments	Channel length (km)	Channel slope (%)	area (km ²)	Time of concentration (min)	Lag time (min)	CN	Impervious area (%)
1	Mpazi	2.8	2.96	8.43	26.5	15.9	86.6	78.4
2	Rugunga	9.35	0.62	52.85	100.714	60.43	86.6	72
3	Rufigiza	12.45	0.79	54	127.49	76.49	88.5	0.14
4	Misare	3.24	1.19	8.14	36.93	22.16	88.5	0
5	Kajevuba	13.27	0.85	60.04	135.5	79.5	86.7	0.162
6	Murama	6.04	3.7	18.2	50.64	30.4	86.5	0
7	Rusumo	22.02	2.11	129	169.81	101.89	86.7	2.0431
8	Mwange	14.88	1.78	126.68	118.93	71.36	86.7	0.14
9	Gatare	1.48	1.1	5.39	17.86	10.72	92.5	0
10	Rusine	17.7	2.14	67.02	145.32	87.19	85.6	0.22
11	Nyacyonga	8.84	2.76	25.77	75.9	45.57	86.4	2
12	Byabagabo	3.24	2.05	8.48	32.99	19.8	86.4	2.45
13	Karuruma	12.6	2.64	35.06	105.83	63.5	86	1.45
14	Yanze	16.08	2.03	96.63	128.63	77.18	86.1	0.13
15	Muhazi	N/A	N/A	878.69	N/A	N/A	88.9	0.015
Floodplain								
16	reach 1	30.61	0.304	62.748	373.76	224.25	65	6.74
	reach 2	2.08	0.1	3.78	42.012	25.21		
	reach 3	4.3	0.58	9.072	55.99	33.59		

Table 6-1: Sub catchments geomorphological parameters.

6.2. Extreme rainfall events

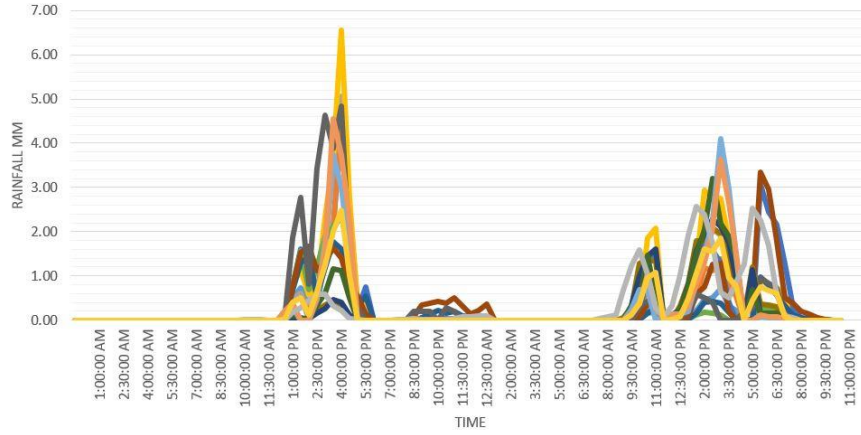
6.2.1. Rainfall coverage per sub catchments

Figure 6-2 illustrates the amount of water received by every sub catchments of the Nyabugogo catchment during the extreme rainfall events obtained from the approach described in section 5.2. An important aspects of these extreme events was that they extended over a two days period (i.e. for all the four cases a succession of two rainfall events within a period less than a day were observed). With a rainfall patterns like the ones observed on figure 6-2, it was expected that the first events would fill the rivers and soils of the catchment and the second would lead to flooding (mostly flash floods considering the time duration of these events and the rapid catchment responses observed in the Nyabugogo catchment).

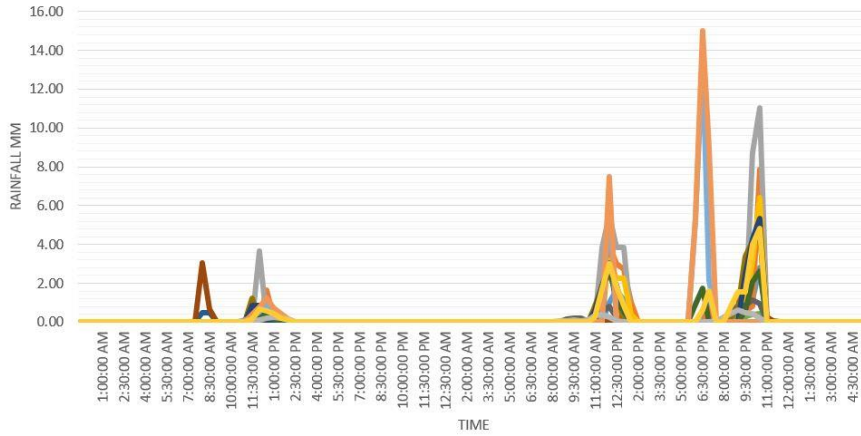
For clarity purposes, figure 6-2 was illustrated using lines but it is important to know that the appropriate representation would have been histogram based, since satellite records are not continuous over time. It was found unpractical to use histograms for illustrating the extreme rainfall events in figure 6-2 for 16 sub catchments over two days period divided in 30 min intervals.



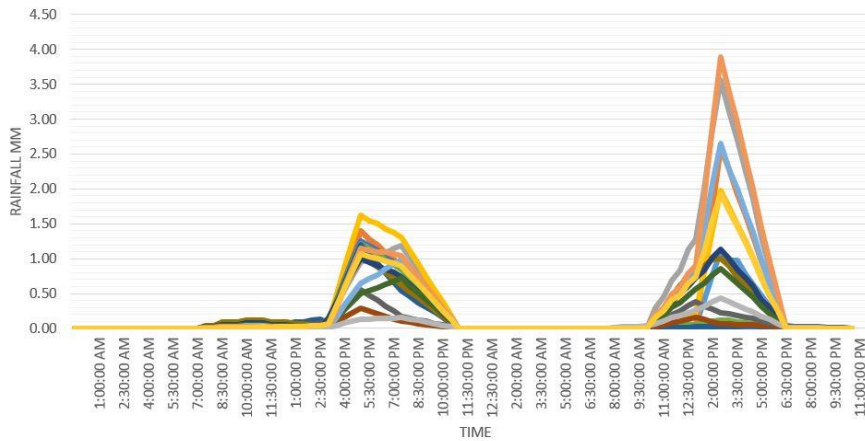
Event 1



Event 2



Event 3



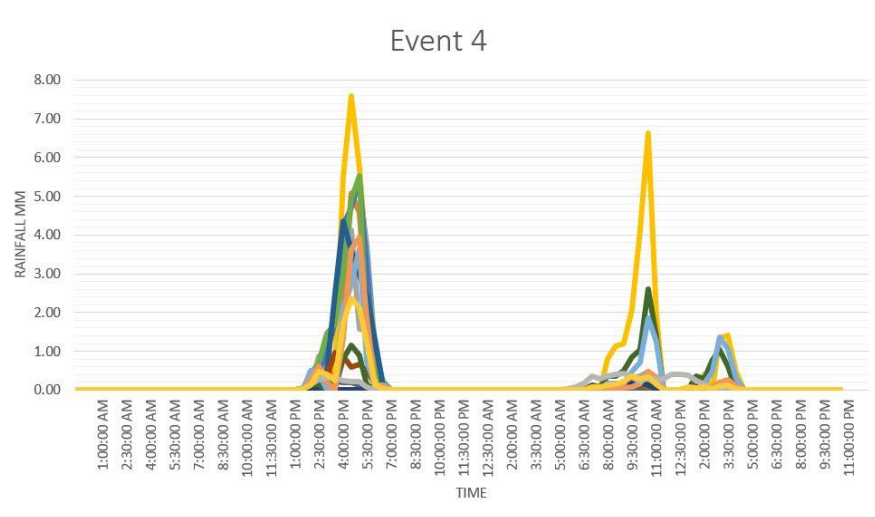


Figure 6-2: Extreme rainfall events susceptible of causing floods in the Nyabugogo commercial hub, downtown Kigali.

A classification of the sub catchments that received more water during these extreme rainfall events is shown in the table 6-2. The classification was done in two groups for every extreme events and was based on the heights of peaks per sub catchments with respect to the highest peak per extreme event.

#	Sub catchmensts	Event 1		Event 2		Event 3		Event 4	
		much water	little water	much water	littlt water	much water	littlr water	much water	little water
1	<i>Byangabo</i>	<i>X</i>		<i>X</i>		<i>X</i>		<i>X</i>	
2	Floodplain		X		X	X			X
3	Gatare		X		X		X	X	
4	Kajevuba		X		X		X		X
5	<i>Karuruma</i>	<i>X</i>		<i>X</i>		<i>X</i>		<i>X</i>	
6	Misare		X		X		X		X
7	<i>Mpazi</i>	<i>X</i>		<i>X</i>		<i>X</i>		<i>X</i>	
8	Muhazi		X		X		X		X
9	Murama	X			X		X		X
10	Mwange		X		X		X	X	
11	<i>Nyacyonga</i>	<i>X</i>			<i>X</i>	<i>X</i>		<i>X</i>	
12	Rufiziga	X			X		X		X
13	<i>Rugunga</i>	<i>X</i>		<i>X</i>		<i>X</i>		<i>X</i>	
14	<i>Rusine</i>	<i>X</i>			<i>X</i>		<i>X</i>	<i>X</i>	
15	Rusumo	X			X		X		X
16	<i>Yanze</i>	<i>X</i>			<i>X</i>		<i>X</i>	<i>X</i>	

Table 6-2: Sub catchments receiving much water.

The sub catchments represented in a bold italic with a grey background are the ones which were classified as those which received much water from the selected extreme rainfall events. These sub catchments were considered as sub catchments potentially receiving much water usually.

6.2.2. Extreme rainfall pattern

Few observations were made on the extreme rainfall patterns using the collected satellite images. These observations were found to be in accordance with the observations made by Gamoyo, Reason, and Obura (2014). The main observations done were of three different aspects as follows:

- The period of March to May and October to December are more likely to have extreme rainfall events. This was based on the regional observations of Gamoyo et al. (2014) over the East Africa region where two rainy seasons were reported as spread over March-April-May (constituting the heavy rainy season with mostly longer rainfall events as the inter tropical convergence zone moves northwards) and October-November-December (constituting the small rainy season as the inter tropical convergence zone moves southwards).
- The rainfall intensities exhibited abrupt changes in intensity. This was based on the reported interannual variability in the rainfall totals of these seasons over the region related to the El Nino southern oscillation and the Indian ocean dipole events as well as the shift of the Walker circulation over the East Africa coast with strong uplift inducing very wet conditions.
- A horizontal movement of the rainfall events pattern from east to west was observed. This is due to the reported marine air mass movement advected from the western tropical Indian ocean towards East Africa.

An example of a typical pattern of rainfall event is illustrated on figure 6-3 as adapted from the second extreme rainfall event selected in this study.

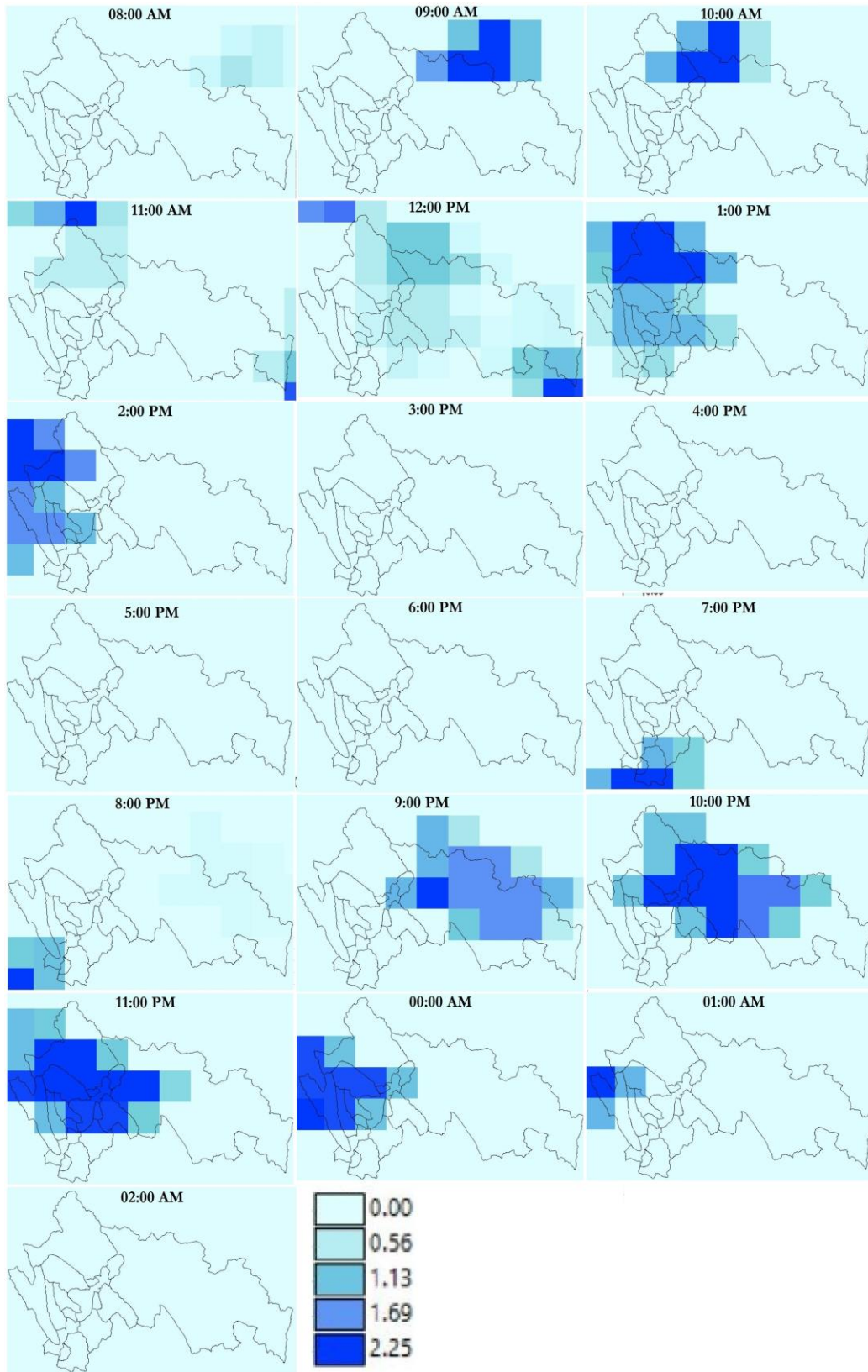


Figure 6-3: Typical rainfall event pattern.

6.3. Rainfall-runoff model

6.3.1. Gauged sub catchments rainfall-runoff model outputs

The set up main screens of HEC-HMS for the Rusumo and Yanze sub catchments are illustrated on figure 6-4.

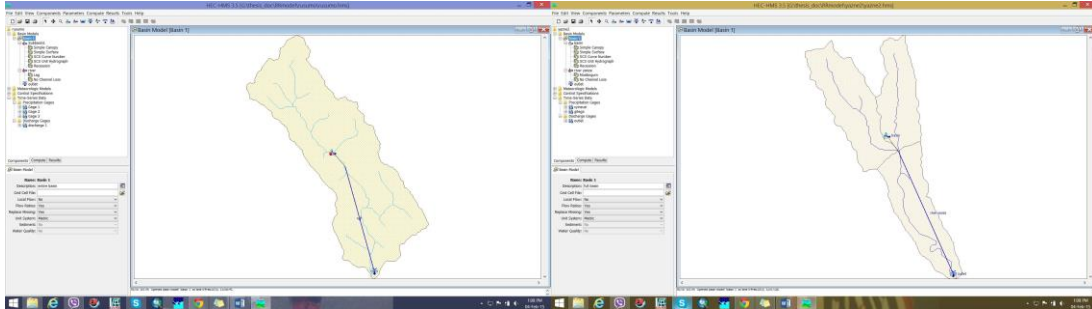


Figure 6-4: Set up screens of Rusumo and Yanze sub catchments.

The simulated hydrographs are illustrated on figure 6-5. It can be seen that the adopted methods were weak in simulating the base flow.

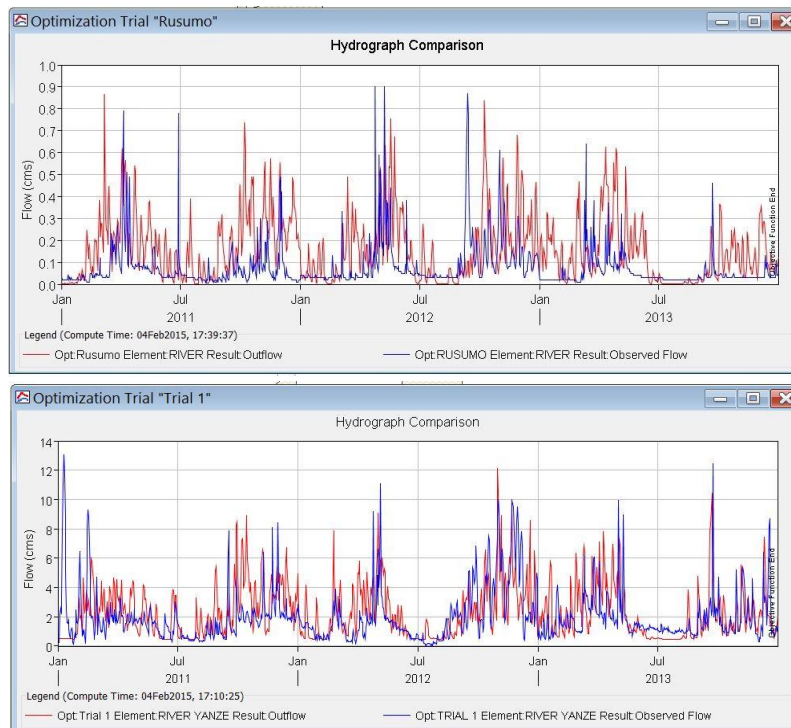


Figure 6-5: Rusumo (top) and Yanze (bottom) simulated hydrograph.

The limitations of the available data restricted the application of other methods and therefore the model discussed previously were applied. The target was to simulate the hydrographs peaks as well as possible while keeping an overall acceptable hydrograph simulation. Also the methods applied were suitable for event modelling for a maximum of 14 days recommended by Arlen D. Feldman (2000), unfortunately the available data were daily based without a possibility of disaggregation up to two weeks unless further appropriate site measurements which was not possible due to lack of time and finance. The application of the objective functions described in the section 5.3.3 were therefore applied to ensure acceptable results.

The obtained optimum parameters for the Rusumo and Yanze sub catchments models and the corresponding objective function values were as indicated in table 6-3.

#	Parameters	sub catchments	
		Rusumo	Yanze
1	X	0.0010052	0.00078471
2	K (hr.)	29.311	25
3	Recession constant	0.95411	0.995
4	Initial base flow (m ³ /s)	0.031849	1.0276
5	Threshold base flow (m ³ /s)	0.0752987	1
Objective functions		Values	
1	PWRMSE	0.2	0.6
2	NS	0.55	0.6
3	RVE	32.5	18.4

Table 6-3: Optimum parameters and Objective functions values for Rusumo and Yanze sub catchments rainfall-runoff models.

Table 6-3 exhibits the weakness of the methods applied and inaccuracies in the collected data in terms of objective function values. The peak simulation is better for the Rusumo than the Yanze model, however the latter has proven to be more efficient especially in modelling the volume of water released. The collected data of the Rusumo river flow were believed to have poor quality based on the high volumetric error (>30) that were observed after multiple calibration of the model. The optimum parameters in table 6-2 were used for the estimation the missing parameter values of ungauged sub catchments.

6.3.2. Regionalization of local parameters

The optimum parameters obtained from the Yanze and Rusumo rainfall-runoff models were used to determine the estimating ratios applied for estimating the missing parameter values of the ungauged sub catchments before applying any calibration of the entire Nyabugogo catchment set up. These rationing were based on the area and length conversion as well as the proximity factor as described previously. The results are summarised in table 6-4.

ratios	K (hr/km)	X (/km)	Recession coefficient	Initial base flow (m ³ /s/km ²)	Threshold base flow (m ³ /s/km ²)	Sub catchments within proximity
sub catchments						
Rusumo sub catchment	1.331	0.00004565	0.95411	0.0002469	0.0005837	Mwange, Rusine, Murama, Kajevuba, Gatara, Misara and Nyabugogo reach 1
Yanze sub catchment	1.555	0.0000488	0.995	0.0106	0.01035	Rugunga, Nyacyonga, Karuruma, Rufigiza, Byangabo, Nyabugogo reach 2 and Nyabugogo reach 3
Applied ratios	length conversion proximity factor applied		Average	Surface conversion		
			0.974555	0.00542345	0.00546685	

Table 6-4: Ratios used for estimating missing parameters.

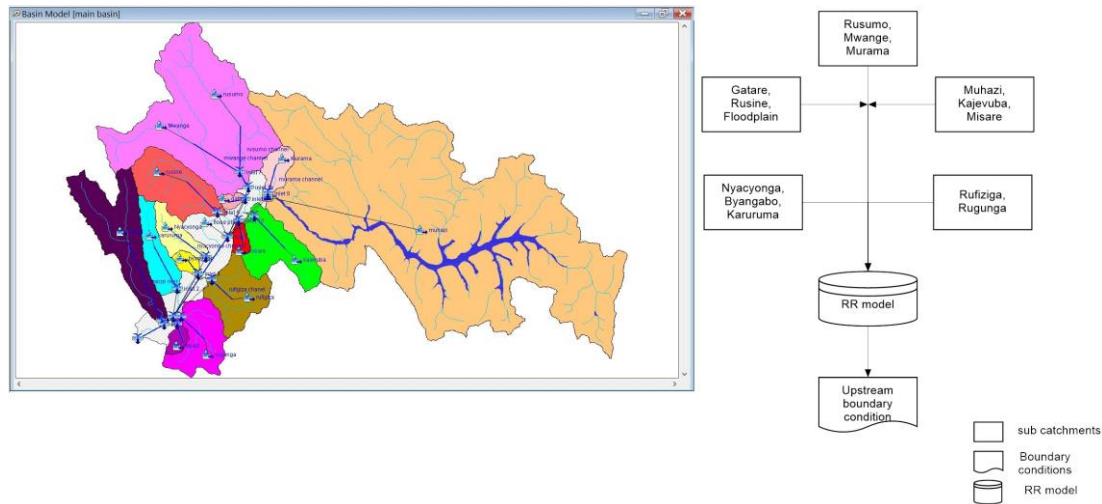


Figure 6-7: Nyabugogo catchment schematization in HEC-HMS.

The unvariant gradient solver was used for the calibration in all the models setups. The efficiency of the Nyabugogo model adopted, expressed in terms of objective function values, was found to be of a PWRMSE equal to 3.4, a NS equal to 0.6 and a RVE equal to -4.9. Figure 6-8 illustrates the overall simulated hydrograph at the Nyabugogo catchment outlet.

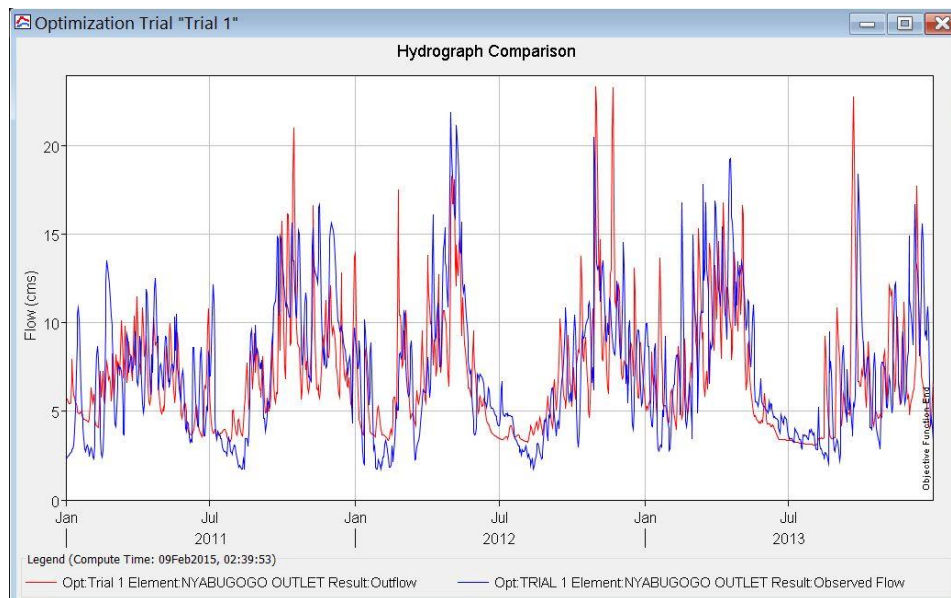
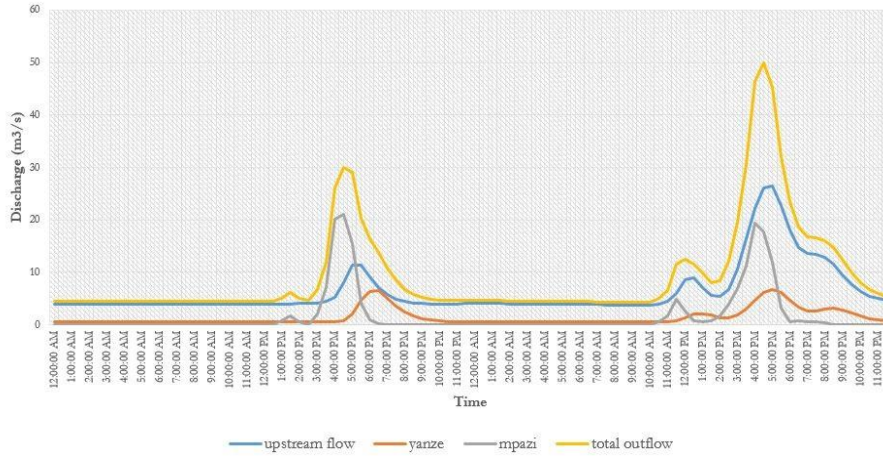


Figure 6-8: Nyabugogo catchment simulated hydrograph.

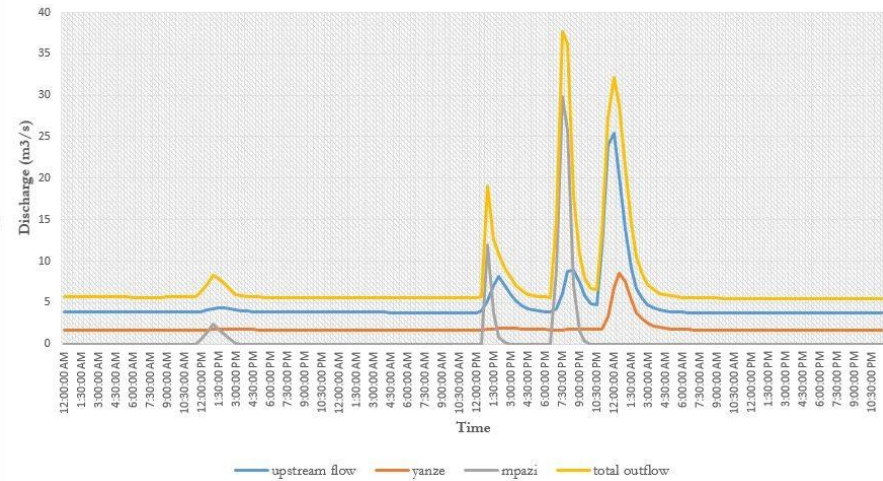
6.3.5. Inflow boundaries of the flood model

As stated previously, the main objective of setting up the rainfall-runoff model using HEC-HMS was to enable estimation of upstream area inflows. These inflow estimations were used as input to the flood model. Figure 6-9 illustrates the boundary flow hydrographs estimated for every selected extreme rainfall events. The upstream area contribution, the Mpazi and Yanze sub catchments contribution are shown as these constitutes the upstream inflow boundary hydrographs to the flood model. The total outflow is also shown as aggregated from all upstream inputs.

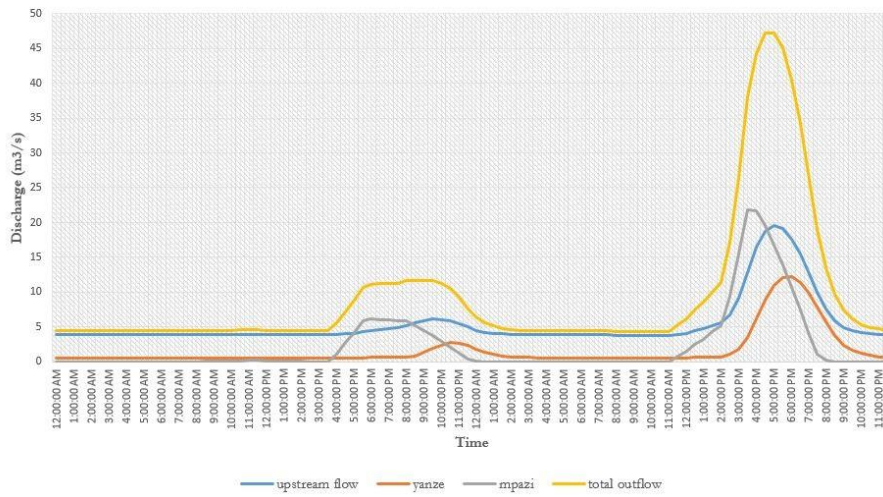
Event 1 (November 29th-30th, 2011)



Event 2 (May 3rd-5th, 2012)



Event 3 (October 31st-November 1st, 2013)



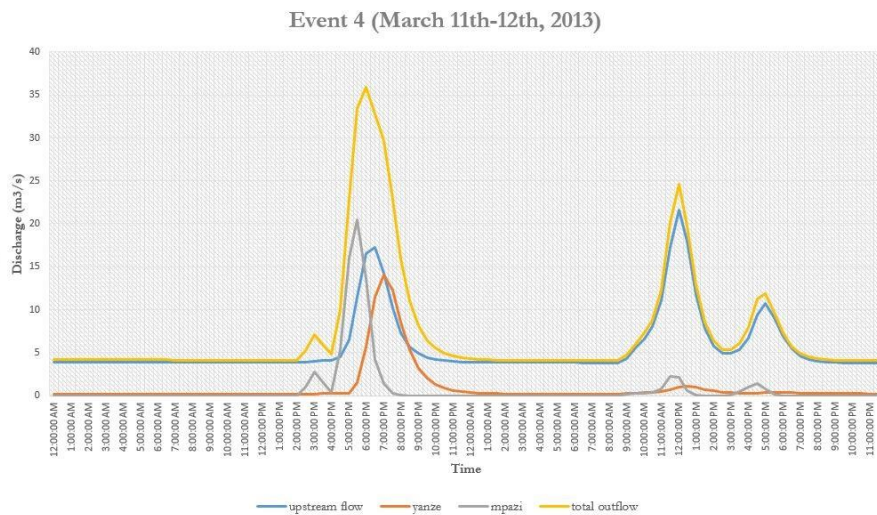


Figure 6-9: Upstream inflow boundary hydrograph to the flood model.

The analysis of the inflow contribution per sub catchments per extreme rainfall events revealed a classification of the sub catchments contributing much water to the flooding. Table 6-5 illustrates, in bold and italic scripture on a grey background, the sub catchments that contributed much water to flooding during the selected extreme rainfall events. The sub catchments of Yanze and Mpazi have a high contribution compared to others, however also the sub catchments of Karuruma, Nyacyonga, Ruzizi and Rugunga contributed much water to flooding. The sub catchment of Muhazi is also flagged as a higher water contributor but it is mostly keeping the river wet since its response to extreme rainfall event is hardly observed in its hydrograph.

#	Sub catchmensts	Events 1		Events 2		Events 3		Events 4	
		much water	little water						
1	Byangabo		X	X		X			X
2	Floodplain		X		X		X		X
3	Gatare		X		X		X		X
4	Kajevuba		X		X		X		X
5	<i>Karuruma</i>		X	X		X		X	
6	Misare		X		X		X		X
7	<i>Mpazi</i>	X		X		X		X	
8	<i>Muhazi</i>	X		X		X		X	
9	Murama		X		X		X		X
10	Mwange		X		X		X		X
11	<i>Nyacyonga</i>	X		X		X		X	
12	<i>Rufiziga</i>	X		X		X		X	
13	<i>Rugunga</i>	X		X		X		X	
14	Rusine		X		X		X		X
15	Rusumo		X		X		X		X
16	<i>Yanze</i>	X			X	X		X	

Table 6-5: Sub catchment contributing much water to flooding.

6.4. Flood model

The setting up of the flood model was done in a stepwise manner based on the researcher study area knowledge and the collected flow depth from interview of locals. The following section summarizes all the steps and findings obtained from the flood model.

6.4.1. River profile

Figure 6-10 shows the longitudinal profiles of the river Nyabugogo obtained from the different DEM resolutions used in this study. It was observed that the river longitudinal profile was not strongly affected by the increase in spatial resolution from 5m to 20m. The fact that only the topographical points measured at the river bottom were used may have led to this observation. The measured profile on site is also plotted (using the total station surveying points) on figure 6-10 for comparison.

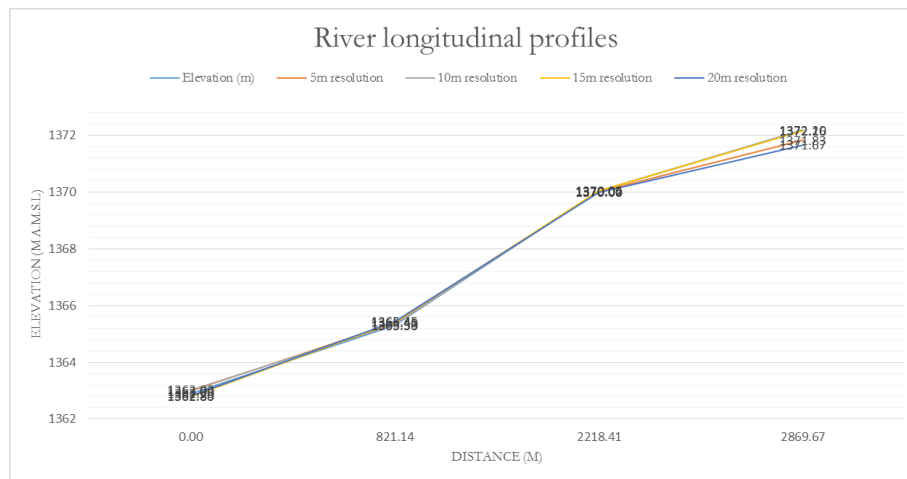


Figure 6-10: Nyabugogo river longitudinal profiles for different spatial resolutions.

6.4.2. Effect of DEM resolution

In various studies it is shown that flood wave propagation is strongly affected by topography. Flood model outputs like flood depth, flow velocity, flood extent, etc. are dependent on the DEM resolution used for the modelling. Difficulties often arise when defining appropriate DEM resolution to represent complex topography of a catchment. In this study a DEM with rectangular grid structure was applied and every grid cell was defined as a lumped entity represented by a single value of elevation for the entire grid cell's area. This required different model inputs from DEMs differing in magnitude and resolution, resulting in different model outputs.

An increase in DEM resolution implies that averaging domains covering the pixel area increases which always affects the representation of terrain features and obstacles. As such selection of coarser DEM resolution affects the dynamics of flow. The analysis of this effect is of great importance in flood modelling. The selection of a resolution also may be affected by aspects like computational time (which is excessive for fine resolution) and loss of detailed on site information which is larger for coarser resolution. A compromise between the two has to be found for generating acceptable model outputs.

In this study, the maximum flood depths and velocities stored in the Sobek outputs as well as the duration and inundation areas were used to assess the effects of the different DEM resolutions used. The model outputs for different DEM resolutions is illustrated in figure 6-11 with table 6-6 providing the statistical values of these outputs as obtained in ILWIS.

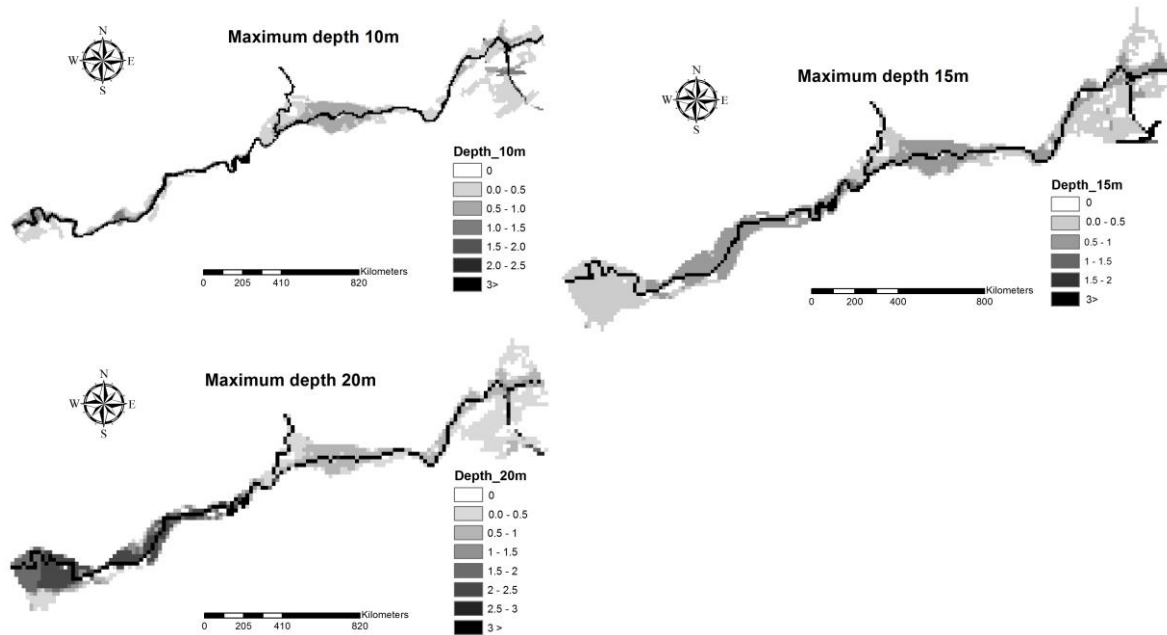


Figure 6-11: Maximum depth maps for different DEM resolutions.

#	DEM resolutions	Depth (m)			Velocity (m/s)			Duration (hours)			Innundation area (m ²)	Computation time (hours)
		Max	Mean	STD.	Max	Mean	STD.	Max	Mean	STD.		
1	10 m	5.524	1.315	1.519	3.579	0.465	0.453	24	14.1	6.7	280100	25
2	15m	4.266	1.034	1.232	3.301	0.415	0.358	24	14.3	6.3	430650	10
3	20m	5.398	1.511	1.489	4.4	0.579	0.55	24	14.4	6.1	444800	4

Table 6-6: Model outputs for different resolutions.

Three maximum flood depth maps are provided in figure 6-11 for three different DEM resolutions. The simulation conditions (boundary conditions, simulation periods and settings) were kept similar for each of the DEMs in order to enable a comparison between them. The observations obtained from the model outputs of these setups are shown in table 6-6. An increase in maximum depth, maximum velocity and innundation area from fine to coarser resolutions was observed. Also a decrease in computation time from fine to coarser resolutions was observed.

The increments observed for the maximum depth, maximum velocity and innundation area with increasing grid resolution were associated to the effect of averaging of the coarser resolution grid elements and the flow direction definition of the rectangular grid DEM structure used in Sobek. Coarser resolution grids simplify the definition of the grid elements. This simplification affects not only the elevation values, channel slopes, channel dimensions but also the roughness distribution which results in less energy loss and obstructions to the flow. Additionally, the flow assignment is less accurate for coarser resolution. For example, in Sobek the flow is allowed from one element to only one of its four neighbours depending on the head distribution. The difficulty introduced in this case is the depiction of the flow path at reasonable accuracy. The significance of the flow path heterogeneities and small scale processes is minimized with coarser resolution grids. From the analysis of the model outputs at different resolutions, it can be concluded that the topographical representation as well as the spatial discretization used for flood modelling significantly affected the model outputs. A similar conclusion was also reported in studies by Tennakoon (2004), A.T. Haile (2005), Md Ali et al. (2015), Zhang et al. (2014), etc.

The flood duration provided by the model outputs were found to be increasing with the decrease of the grid resolution. Generally, higher mean and standard deviations were observed due to the fact that the river was constantly wet for the entire 24 hours simulation period, leading the model to mark the river pixels as 24 hours flooded while the rest across the model domain had relatively small values of flood duration. The smaller values of the flood duration distributed across the model domain and the river values produced, resulted in higher mean and standard deviation values when these were combined. An increase in the mean value indicated an increase in the flood duration across the model domain and a decrease in the standard deviation value indicated a higher number of pixels being constantly flooded throughout the simulation period and across the model domain. In this study, it was observed that the mean value was increasing while the standard deviation value was decreasing from the simulation outputs obtained using a fine to a coarser grid resolution respectively as illustrated in table 6-6.

A significant increase in computation time was observed for model runs using fine resolution grids compared to model runs using coarser resolution grids as shown in table 6-6. The simulations were performed using a core i7 PC. Due to the internet network instability, the 5 m resolution simulation was interrupted after two and half days at multiple occasions. Due to the time limit of the report submission, the 5 m resolution was unfortunately not incorporated in this report.

6.4.3. Surface roughness

The parameterization of the surface roughness was done by assigning Manning's roughness coefficients to different land covers (see table 5-2) and its assesment was done based on the comparison of observed flood depths and simulated ones as well as the researcher's study area knowledge. The first run was performed with a spatially invariant roughness coefficient value for all the pixels that make up the model domain. For the second run spatially variant roughness values were used to reflect on the terrain properties at the scale of the pixels. A map showing the grid based distributed roughness values is shown in figure 5-8. Many trials have been executed, the change in roughness values were done manually until a satisfactory value of the root mean square error and a more or less realistic flood extent were obtained. In flood modelling surface roughness is mostly obtained through calibration but the data scarcity on flood characteristics in this study led to the investigation of the model's sensitivity to surface roughness. An estimation of the model sensitivity was determined using the observed flood depths collected during the fieldwork. The constraints imposed by the time and computer facilities limitations led to a limited number of simulations. The main finding from the simulation was that the model outputs were highly sensitive to the river channel roughness. In his study, DeChant (2014) reported similar findings. Figure 6-12 illustrates the sensitivity analysis results of the flood model to surface roughness.

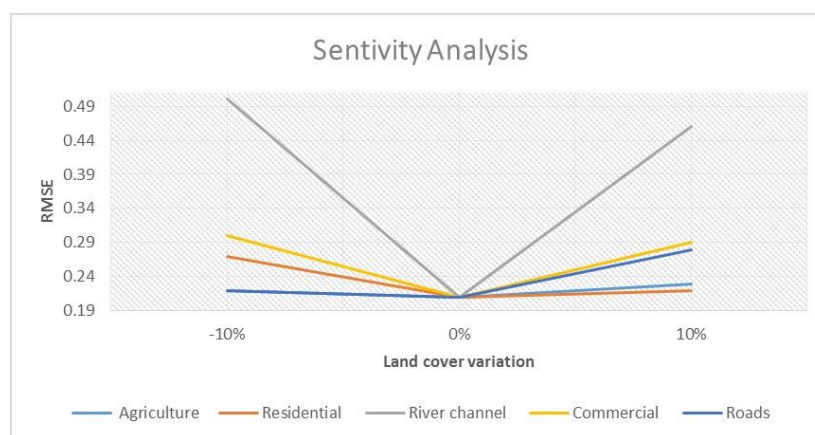


Figure 6-12: Surface roughness sensitivity analysis plot.

6.4.4. Building representation

In this study, the available buildings footprints (which were digitized from the available 0.25m resolution orthophoto of the flood model domain) were used to extract and elevate the building pixels in the DEM. The data scarcity did not allow for further assessment on the roughness values assignment per building since these were not available. A single roughness value per representation was used for all the buildings roughness assignment. Figure 6-13 provides the simulation outputs for the three buildings representations.

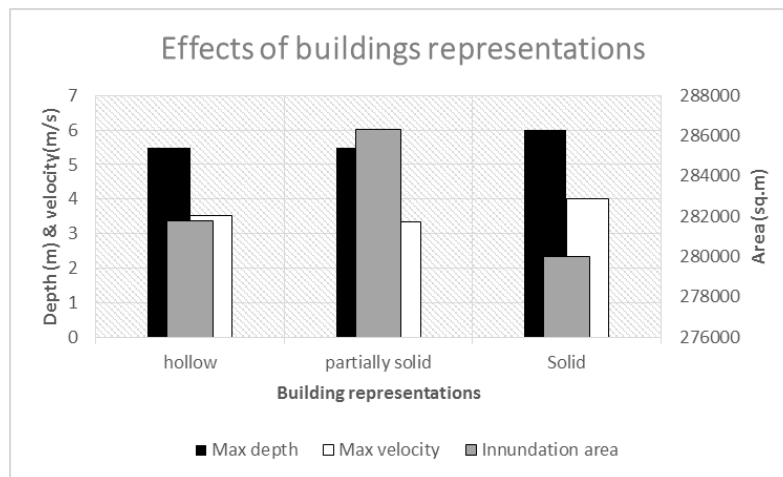


Figure 6-13: Building representations effects on the model outputs. A similar figure is shown in A.T. Haile (2005).

Higher values of maximum depth and maximum velocity were observed in the representation of buildings as solid objects. This may be associated to the fact that this representation do not allow water to enter the buildings resulting in increasing depths and velocities in the model domain. The complexity of urban areas hydrodynamics made this phenomenon difficult to explain and that is why only the flow characteristics shown in figure 6-13 were considered to highlight these effects in the flood model. However, the partially solid representation gave a large inundation area which is associated to its large delay in releasing water after the flood event.

6.4.5. Simulation results

The flood model results were observed from the Sobek simulations and revealed the following. The Nyabugogo river is filled with water coming from the upstream sub catchments runoff before receiving runoff from Mpazi and Yanze sub catchments. By the time these two sub catchments discharge in the Nyabugogo river, the water level in the main river is already high causing significant backwater effects. High velocities were observed at the points of confluence in all the simulations that were done. An illustration is provided clearly on figure 6-14 and figure 6-15. Simulation videos are also available for more clarification.

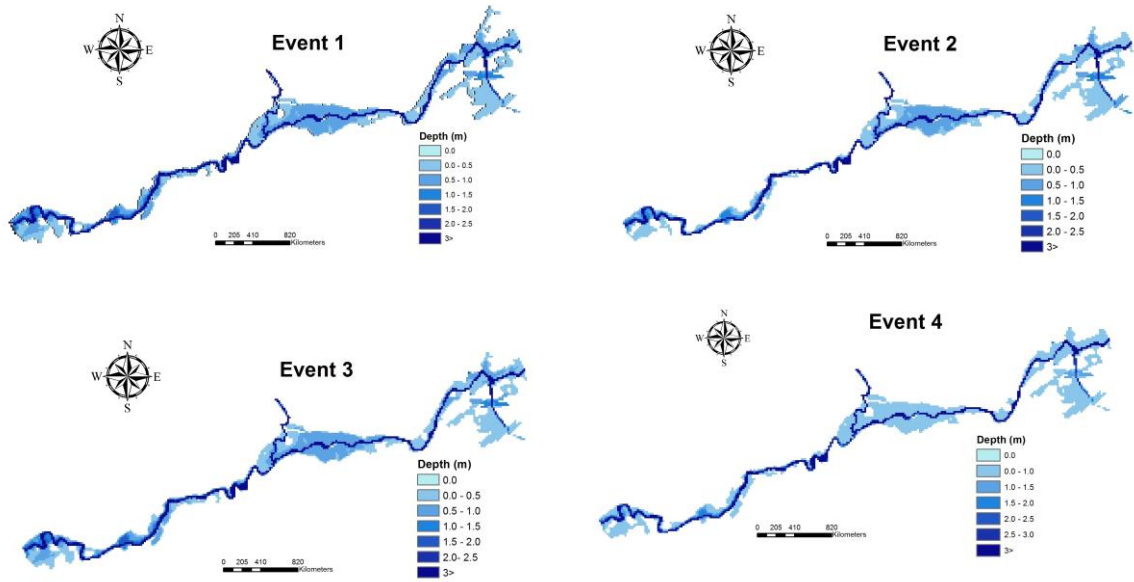


Figure 6-14: Maximum flood depth per event.

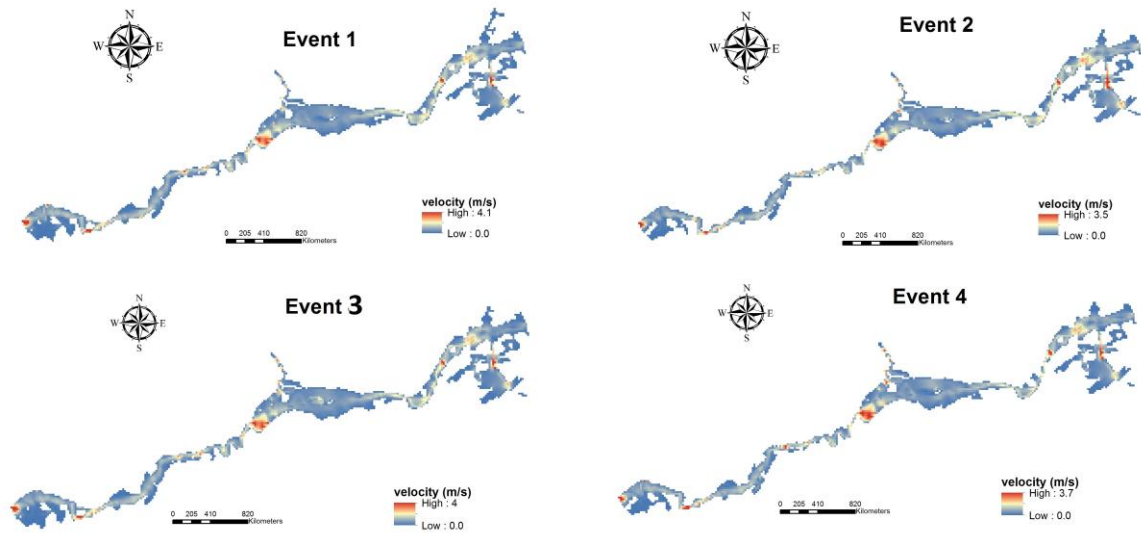


Figure 6-15: Maximum velocity per event.

7. CONCLUSION AND RECOMMENDATIONS

7.1. Conclusion

The main objective of this study is to develop a flash flood model of the data scarce Nyabugogo commercial hub in Kigali city, using remote sensing data, a rainfall-runoff and a 1D2D hydrodynamic flood model. important issue in this study was the data scarcity and their integration in the hydrologic models used, was considered as a scientific challenge in this study. Satellite data and rainfall-runoff model was applied in order to overcome the problem of data scarcity and estimate the upstream inflows. In this study, the rainfall-runoff model was effectively used to estimate the runoff hydrographs from the extreme events which make up the upstream boundary inflow which served as boundary inflows to the flood model. The satellite rainfall estimates were used for their space-time variability to allow representation and identification of extreme rainfall events which caused floods.

The study area conceptualization was done firstly in such a way that the estimation of the spatially and temporally rainfall distribution and related catchment runoff per sub catchments would allow to link rainfall patterns in upstream catchments to actual floodings in the downstream area. The use of satellite based rainfall enabled event based rainfall-runoff modelling and was done in a way to allow analysis of the upstream effects in the flood model domain.

The first step in this study consisted of preparing the available collected data from fieldwork and online in order to know the missing data and to define a methodology to overcome problems of data scarcity. Ten rainfall stations with daily data were used after being filled in and corrected. Four gauging stations (Yanze, Rusumo, the Lake Muhazi and the entire Nyabugogo at the Nemba station) were available with time series at daily interval. Except the Lake Muhazi gauge, the other stations had few discharge measurements which were used to estimate their stage-discharge relationships. The estimations of the Lake Muhazi surface fluctuations were normalized to the observed water marks visible on its gauge (herewith considered as maximum 0.60m and minimum 0.20m water stages) and the Manning's equation was applied to convert the normalized water stages to the lake outflow. The consistency and quality of all the flow data were assessed before using them for modelling.

The second step of this study consisted of setting up the rainfall-runoff model. The HEC-HMS software was used where the NRCS CN model, the Muskingum routing model and the baseflow recession model were applied. The choice of these models was based on their data requirement. The available SRTM DEM, the study area orthophoto, the LULC map and a soil map were used to determined the geomorphological parameters which were used for parameterising the rainfall runoff model. For every gauged hydrological systems in the study area, a rainfall-runoff model was set up and calibrated to estimate the unknown values of the parameters K and X of the Muskingum method as well as the initial and threshold baseflow and the recession coefficient. These parameters were locally regionalized over the entire Nyabugogo catchment using the area conversion, the proximity factor and the main channel length conversion. In this particular steps, the lake Muhazi sub catchment was considered as a separate entity. The entire Nyabugogo catchment set up in HEC-HMS was done and calibrated following the Nyabugogo river parameters only. It was also observed that the entire catchment set up was significantly sensitive to the Nyabugogo river parameterization.

The third step of this study consisted of identifying the extreme rainfall events at fine space-time resolution in order to estimate the high catchment runoff discharges. The CMORPH rainfall product available at 8km X 8km every 30minutes was used. The time variable bias correction method at a daily window was applied to these estimates. The identification of the extreme rainfall events was based on the analysis of where the extreme rainfall events corresponded to the peaks in the entire catchment hydrograph. Windows of two weeks spread over the peaks were selected to ensure the capturing of the extreme rainfall events. Four periods were determined and the maximum rainfall events in those periods were selected and considered as extreme.

The main findings from these steps were as follow. The rainfall pattern which cause flood events as simulated in this study was found to be moving from east towards west over the region. Also the climate of the region was found to have two rainy seasons per year in March-April-May and October-November-December constituting high risk zones of having extreme rainfall events. It was found that the sub catchments of Byangabo, Karuruma, Mpazi, Nyacyonga, Rugunga, Rusine and Yanze received most of the rainfall water compared to other sub catchments, however upon rainfall-runoff model simulations only the sub catchments of Karuruma, Mpazi, Muhazi, Nyacyonga, Rufigiza, Rugunga and Yanze contributed high amounts of runoff water in the Nyabugogo river. Based on the satellite observations, it was also seen that the sub catchments of Yanze and Mpazi mostly received rainfall water after the others.

The last step of this study was about setting up the flood model. Sobek 1D2D was used for this purpose. The setting up of Sobek was done in a stepwise manner to overcome the problem of data scarcity. The effects of DEM spatial resolutions, buildings representation and surface roughness were assessed. It was found that coarser resolutions led to larger inundation areas, maximum depths and higher flood durations. Also buildings represented as solid objects led to higher maximum depths and maximum velocities while the partially solid buildings led to larger innundation areas. It was also found that the model was significantly sensitive to the main channel roughness. The Sobek simulations indicated strong backwater effects on the confluence points of Mpazi and Yanze tributaries with the Nyabugogo river.

This study is the first of its kind in the country of Rwanda. Advanced hydrologic models were applied in this study despite the limitation of poor data availability. This indicates that simple network apparatus and configurations for data collection are sufficient to allow suitable hydrological analysis in Rwanda. The only requirement is only to improve the collection techniques and densify the existing network.

7.2. Recommendations

The major limitation in this study was the poor availability of data of the extreme rainfall events and flood characteristics. Even though this was a scientific challenge to this study, a calibration and validation of the flood model could not be performed. This limitation led to the methology that was presented in this study, however an improvement of this entire set up is recommended in order to enable further analysis and learn more about the Nyabugogo commercial hub frequent flash flooding causes. The following recommendation were therefore made in this study.

- The measurements daily time interval of rainfall does not fully capture the extreme rainfall events patterns. This should be improved and a more dense network should also be installed. Instalment of on-line automated procedres are recommended.
- The actual flow measurement practices using local observers have proven to be weak in terms of quality and quantity (poor network) and measurements time scale. Solutions like datalogger

should be looked at as well as a network densification. Recurrent field measurements of discharges are required to validate the stage-discharge relationships applied in this model.

- A significant quality and quantity check as well as update of the existing meteorological and hydrological databases in Rwanda is recommended. The data collection techniques are also recommended to be improved.
- In this study, only one satellite product was applied for the detection of the extreme rainfall events based on literatures. The application of satellite rainfall products for flood modelling was found not common and therefore the assessment of more satellite products is recommended in order to ensure the best possible representation of extreme rainfall events in the study area.
- The improvement of the flood model requires some additions to what the rainfall-runoff model requires. Flood characteristics measurements are required for calibration and validation. If financial possibilities permit, the acquisition of LIDAR data for topographical representation is very much recommended.
- Due to time limitation only two hydrologic models were used fro this study. It is recommended, once the required data made available, to apply different hydrologic models approach in order to assess their differences but mostly benefit from their strengths and gain advanced knowledge on the frequent flooding causes in the Nyabugogo commercial hub, downtown Kigali.

LIST OF REFERENCES

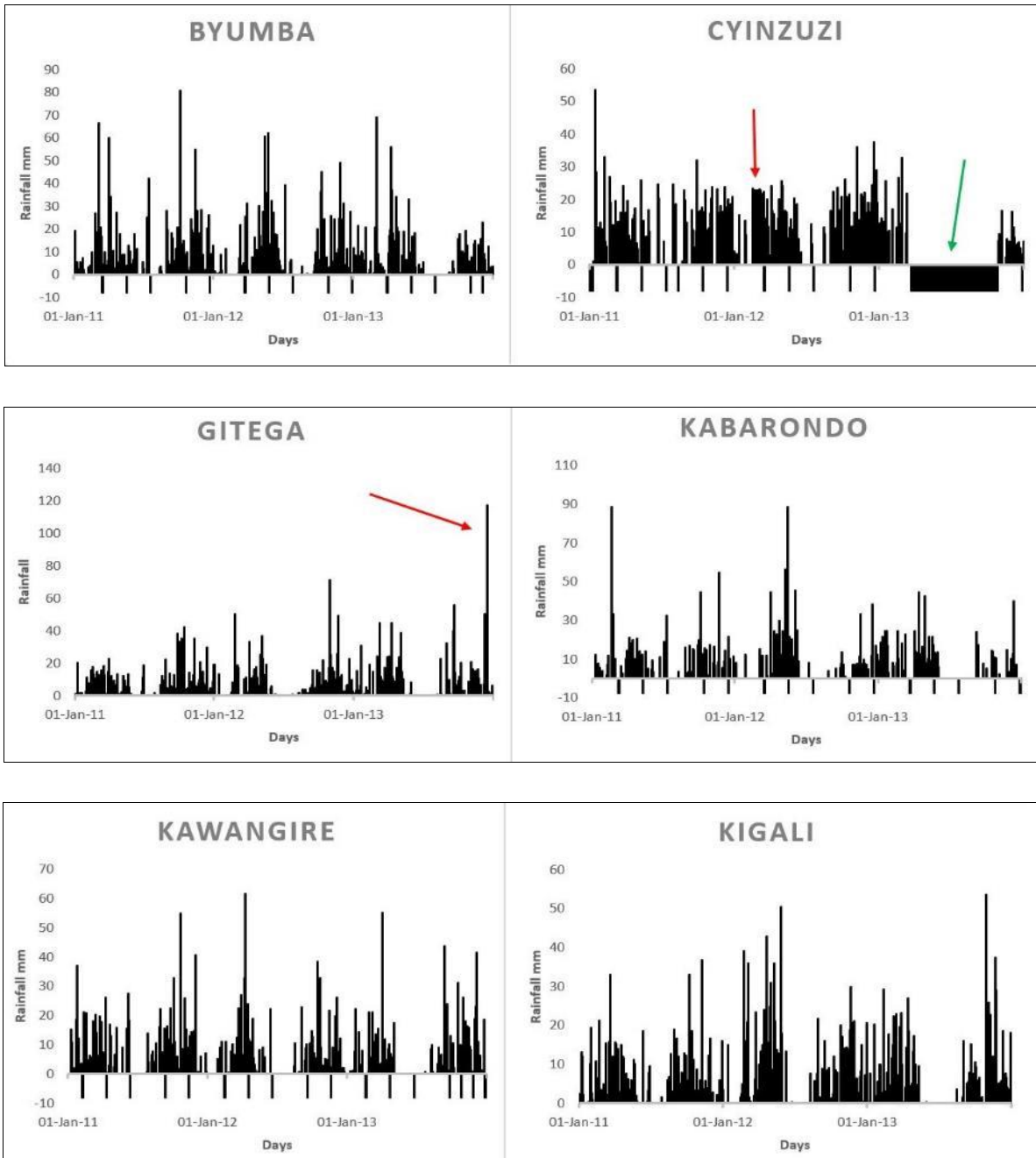
- Abushandi, E., & Merkel, B. (2013). Modelling rainfall runoff relations using HEC-HMS and IHACRES for a single rain event in an arid region of Jordan. *Water Resources Management*, 27(7), 2391-2409.
- Alemseged, T., & Rientjes, T. (2007). *Uncertainty issues in hydrodynamic flood modeling*. Paper presented at the Proceedings of the 5th international symposium on spatial data quality SDQ.
- Arlen D. Feldman, E. (2000). *Hydrologic Engineering Center, Hydrologic Modeling System HEC-HMS, Technical Reference Manual*, : U.S. Army corps of Engineers.
- Artan, G., Gadain, H., Smith, J. L., Asante, K., Bandaragoda, C. J., & Verdin, J. P. (2007). Adequacy of satellite derived rainfall data for stream flow modeling. *Natural Hazards*, 43(2), 167-185.
- Band, L. E., & Moore, I. D. (1995). Scale: Landscape attributes and geographical information systems. *Hydrological Processes*, 9(3-4), 401-422. doi: 10.1002/hyp.3360090312
- Bizimana, J., & Schilling, M. (2010). Geo-Information Technology for Infrastructural Flood Risk Analysis in Unplanned Settlements: A Case Study of Informal Settlement Flood Risk in the Nyabugogo Flood Plain, Kigali City, Rwanda. In P. S. Showalter & Y. Lu (Eds.), *Geospatial Techniques in Urban Hazard and Disaster Analysis* (Vol. 2, pp. 99-124): Springer Netherlands.
- Bladé, E., Gómez-Valentín, M., Dolz, J., Aragón-Hernández, J. L., Corestein, G., & Sánchez-Juny, M. (2012). Integration of 1D and 2D finite volume schemes for computations of water flow in natural channels. *Advances in Water Resources*, 42(0), 17-29. doi: <http://dx.doi.org/10.1016/j.advwatres.2012.03.021>
- Braca, G., & Futura, G. (2008). *Stage-discharge relationships in open channels: Practices and problems*: Univ. degli Studi di Trento, Dipartimento di Ingegneria Civile e Ambientale.
- Bray, D. I. (1979). Estimating average velocity in gravel-bed rivers. *Journal of the Hydraulics Division*, 105(9), 1103-1122.
- Casas, A., Lane, S. N., Yu, D., & Benito, G. (2010). A method for parameterising roughness and topographic sub-grid scale effects in hydraulic modelling from LiDAR data.
- Debru, T. H. (2010). *Rainfall-runoff modelling in Kobo Valley, Amhara regional state, Ethiopia*. (Master of Science MSc.), University of Twente, ITC Faculty, Enschede, The Netherlands.
- DeChant, C. M. (2014). Quantifying the Impacts of Initial Condition and Model Uncertainty on Hydrological Forecasts.
- Delft/Hydraulics. (2014). *SOBEK 2.13: User's Manual*. The Netherlands.
- Douben, K.-J. (2006). Characteristics of river floods and flooding: a global overview, 1985–2003. *Irrigation and Drainage*, 55(S1), S9-S21. doi: 10.1002/ird.239
- Duren, R. M., Wong, E., Breckenridge, B., Shaffer, S. J., Duncan, C., Tubbs, E. F., & Salomon, P. M. (1998). *Metrology, attitude, and orbit determination for spaceborne interferometric synthetic aperture radar*. Paper presented at the Aerospace/Defense Sensing and Controls.
- Fernández-Nieto, E. D., Marin, J., & Monnier, J. (2010). Coupling superposed 1D and 2D shallow-water models: Source terms in finite volume schemes. *Computers & Fluids*, 39(6), 1070-1082. doi: <http://dx.doi.org/10.1016/j.compfluid.2010.01.016>
- Finaud-Guyot, P., Delenne, C., Guinot, V., & Llovel, C. (2011). 1D–2D coupling for river flow modeling. *Comptes Rendus Mécanique*, 339(4), 226-234. doi: <http://dx.doi.org/10.1016/j.crme.2011.02.001>
- Gamoyo, M., Reason, C., & Obura, D. (2014). Rainfall variability over the East African coast. *Theoretical and Applied Climatology*, 1-12.
- Gumindoga, W. (2010). *Hydrologic Impact of Land-Use Change in The Upper Gilgel Abay River Basin, Ethiopia; TOPMODEL Application*. M. Sc. Thesis, ITC Netherlands.
- Gupta, S. K. (2010). *Modern Hydrology and Sustainable Water Development* Retrieved from <http://itc.ebib.com/patron/FullRecord.aspx?p=792631>
- Habib, E., Haile, A. T., Sazib, N., Zhang, Y., & Rientjes, T. (2014). Effect of Bias Correction of Satellite-Rainfall Estimates on Runoff Simulations at the Source of the Upper Blue Nile. *Remote Sensing*, 6(7), 6688-6708.

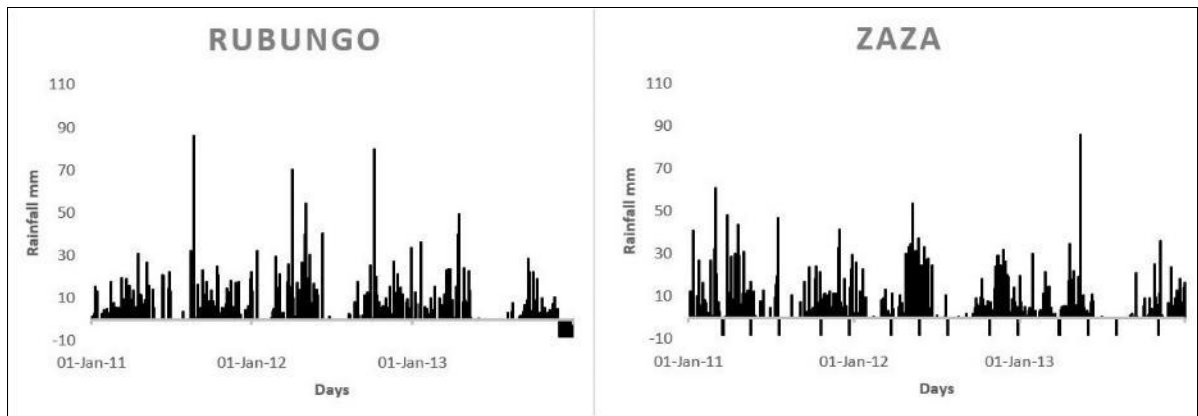
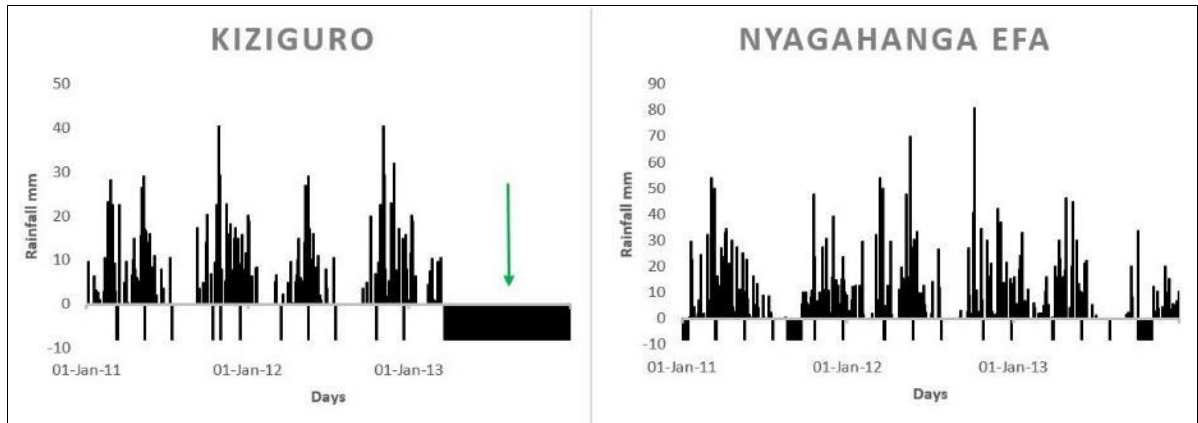
- Habib, E., Haile, A. T., Tian, Y., & Joyce, R. J. (2012). Evaluation of the high-resolution CMORPH satellite rainfall product using dense rain gauge observations and radar-based estimates. *Journal of Hydrometeorology*, 13(6), 1784-1798.
- Haile, A. T. (2005). *Integrating hydrodynamic models and high resolution DEM LIDAR for flood modelling*. ITC, Enschede. Retrieved from http://www.itc.nl/library/papers_2005/msc/wrem/haile.pdf
- Haile, A. T., Habib, E., Elsaadani, M., & Rientjes, T. (2013). Inter-comparison of satellite rainfall products for representing rainfall diurnal cycle over the Nile basin. *International Journal of Applied Earth Observation and Geoinformation*, 21, 230-240.
- Haile, A. T., Habib, E., & Rientjes, T. (2013). Evaluation of the climate prediction center (CPC) morphing technique (CMORPH) rainfall product on hourly time scales over the source of the Blue Nile River. *Hydrological Processes*, 27(12), 1829-1839.
- Helsel, D. R., & Hirsch, R. M. (1992). *Statistical methods in water resources* (Vol. 49): Elsevier.
- Hoyos Goetz, H. (2011). *Runoff modelling of the upper Cabra river basin Panama*. University of Twente Faculty of Geo-Information and Earth Observation (ITC), Enschede.
- Hunter, N. M., Bates, P. D., Horritt, M. S., & Wilson, M. D. (2007). Simple spatially-distributed models for predicting flood inundation: A review. *Geomorphology*, 90(3-4), 208-225. doi: <http://dx.doi.org/10.1016/j.geomorph.2006.10.021>
- Hydraulics, D. C. B. D. (1999). Training module # SWDP-39 How to correct and complete discharge data. New Delhi: Worldbank and the government of The Netherlands.
- Jury, M. (2013). A return to wet conditions over Africa: 1995–2010. *Theoretical and Applied Climatology*, 111(3-4), 471-481. doi: 10.1007/s00704-012-0677-z
- Laouacheria, F., & Mansouri, R. (2015). Combination of Hydrological Modelling and Gis for Runoff Hydrograph Prediction in Small Urban Catchment *Engineering Geology for Society and Territory-Volume 3* (pp. 453-458): Springer.
- Leauthaud, C., Belaud, G., Duvail, S., Moussa, R., Grünberger, O., & Albergel, J. (2013). Characterizing floods in the poorly gauged wetlands of the Tana River Delta, Kenya, using a water balance model and satellite data. *Hydrology and Earth System Sciences*, 17(8), 3059-3075. doi: 10.5194/hess-17-3059-2013
- Lloyd, C. D. (2005). Assessing the effect of integrating elevation data into the estimation of monthly precipitation in Great Britain. *Journal of Hydrology*, 308(1-4), 128-150. doi: <http://dx.doi.org/10.1016/j.jhydrol.2004.10.026>
- Maathuis, B. H. P., & Wang, L. (2006). Digital Elevation Model Based Hydro-processing. *Geocarto International*, 21(1), 21-26. doi: 10.1080/10106040608542370
- Maggioni, V., Vergara, H. J., Anagnostou, E. N., Gourley, J. J., Hong, Y., & Stampoulis, D. (2013). Investigating the Applicability of Error Correction Ensembles of Satellite Rainfall Products in River Flow Simulations. *Journal of Hydrometeorology*, 14(4), 1194-1211. doi: 10.1175/jhm-d-12-074.1
- Md Ali, A., Solomatine, D., & Di Baldassarre, G. (2015). Assessing the impact of different sources of topographic data on 1-D hydraulic modelling of floods. *Hydrology and Earth System Sciences*, 19(1), 631-643.
- Mikova, K., Wali, U. G., & Nhapi, I. (2010). Infilling of Missing Rainfall Data from a Long Term Monitoring Records. *International Journal of Ecology & Development™*, 16(S10), 89-99.
- Mukherjee, S., Joshi, P. K., Mukherjee, S., Ghosh, A., Garg, R. D., & Mukhopadhyay, A. (2013). Evaluation of vertical accuracy of open source Digital Elevation Model (DEM). *International Journal of Applied Earth Observation and Geoinformation*, 21(0), 205-217. doi: <http://dx.doi.org/10.1016/j.jag.2012.09.004>
- Munyaneza, O. (2014). *Space-time variation of hydrological processes and water resources in Rwanda. Focus on the Migina catchment*. (Doctor Phd Thesis), TU Delft and UNESCO-IHE, The Netherlands. Retrieved from http://www.unesco-ihe.org/sites/default/files/2014_unesco-ihe_phd_thesis_munyaneza.pdf
- MUSONI, J. P. (2009). *Runoff Coefficient Classification on Nyabugogo Catchment*. (Master of Science Master of science), NUR and UNESCO-IHE, Rwanda.
- Padi, P. T., Baldassarre, G. D., & Castellarin, A. (2011). Floodplain management in Africa: Large scale analysis of flood data. *Physics and Chemistry of the Earth, Parts A/B/C*, 36(7-8), 292-298. doi: <http://dx.doi.org/10.1016/j.pce.2011.02.002>

- Paiva, R. C. D., Collischonn, W., & Tucci, C. E. M. (2011). Large scale hydrologic and hydrodynamic modeling using limited data and a GIS based approach. *Journal of Hydrology*, 406(3-4), 170-181. doi: 10.1016/j.jhydrol.2011.06.007
- Palmino-Reganit, M. (2005). *Analysis of community's coping mechanisms in relation to floods : a case study in Naga city, Philippines*. (Msc Thesis), ITC, Enschede. Retrieved from http://www.itc.nl/library/papers_2005/msc/ereg/reganit.pdf
- Perera, B. U. J. (2009). *Ungauged Catchment Hydrology: The case of Lake Tana*. (Master of science), University of Twente, Enschede, The Netherlands.
- Refsgaard, J. C., & Henriksen, H. J. (2004). Modelling guidelines—terminology and guiding principles. *Advances in Water Resources*, 27(1), 71-82.
- REMA. (2009). Rwanda State of Environment and Outlook Report. Kigali, Rwanda: Rwanda Environment Management Authority.
- Rientjes, T. (2014). *Modelling in Hydrology (lecturer notes)*. lecturer notes. Water Resources and Environmental Management department. ITC/ Utwente. Enschede, The Netherlands.
- Rientjes, T., Perera, B., Haile, A., Reggiani, P., & Muthuwatta, L. (2011). Regionalisation for lake level simulation—the case of Lake Tana in the Upper Blue Nile, Ethiopia. *Hydrology and Earth System Sciences*, 15(4), 1167-1183.
- Sanders, B. F. (2007). Evaluation of on-line DEMs for flood inundation modeling. *Advances in Water Resources*, 30(8), 1831-1843. doi: <http://dx.doi.org/10.1016/j.advwatres.2007.02.005>
- Sanyal, J., Densmore, A. L., & Carbonneau, P. (2014). Analysing the effect of land-use/cover changes at sub-catchment levels on downstream flood peaks: A semi-distributed modelling approach with sparse data. *CATENA*, 118(0), 28-40. doi: <http://dx.doi.org/10.1016/j.catena.2014.01.015>
- Searcy, J. K., & Hardison, C. H. (1950). MANUAL OF HYDROLOGY: PART I, GENERAL SURFACE-WATER TECHNIQUES. *Geological Survey Water-supply Paper*, 31.
- SHERIngénieurs-Conseils. (2013). Consultancy services for Development of Rwanda National Water Resources Master Plan Technical Note (I. W. R. Management, Trans.): RWANDA NATURAL RESOURCES AUTHORITY.
- SHERIngénieurs-Conseils. (2014). Consultancy services for Development of Rwanda National Water Resources Master Plan Appendix 05NNYL Catchment Master Plan (I. W. R. Management, Trans.): RWANDA NATURAL RESOURCES AUTHORITY.
- Smithers, J., Chetty, K., Frezghi, M., Knoesen, D., & Tewelde, M. (2013). Development and assessment of a daily time-step continuous simulation modelling approach for design flood estimation at ungauged locations: ACRU model and Thukela Catchment case study. *Water SA*, 39(4), 00-00.
- Straatsma, M., & Huthoff, F. (2011). Uncertainty in 2D hydrodynamic models from errors in roughness parameterization based on aerial images. *Physics and Chemistry of the Earth, Parts A/B/C*, 36(7-8), 324-334. doi: <http://dx.doi.org/10.1016/j.pce.2011.02.009>
- SWEDESURVEY. (2010). *Project Rwanda National Land Use and Development Master Plan Report for Production of Ortho Photo in Rwanda*. Rwanda: SWEDESURVEY.
- Tang, W. Y., Kassim, A. H. M., & Abubakar, S. H. (1996). Comparative studies of various missing data treatment methods - Malaysian experience. *Atmospheric Research*, 42(1-4), 247-262. doi: [http://dx.doi.org/10.1016/0169-8095\(95\)00067-4](http://dx.doi.org/10.1016/0169-8095(95)00067-4)
- Tarekegn, T. H. (2009). *Two - dimensional hydrodynamic modelling of flooding, using ASTER DEM in ribb catchment, Ethiopia*. (Msc thesis), ITC, Enschede. Retrieved from http://www.itc.nl/library/papers_2009/msc/gem/tarekegn.pdf
- Tarekegn, T. H., Haile, A. T., Rientjes, T., Reggiani, P., & Alkema, D. (2010). Assessment of an ASTER-generated DEM for 2D hydrodynamic flood modeling. *International Journal of Applied Earth Observation and Geoinformation*, 12(6), 457-465. doi: <http://dx.doi.org/10.1016/j.jag.2010.05.007>
- Tennakoon, K. B. M. (2004). *Parameterisation of 2D hydrodynamic models and flood hazard mapping for Naga city, Philippines*. ITC, Enschede. Retrieved from http://www.itc.nl/library/papers_2004/msc/upla/tennakoon.pDF
- Wanielista, M., Kersten, R., & Eaglin, R. (1997). *Hydrology: Water quantity and quality control*. John Wiley and Sons.
- Zhang, F., Han, L., Wang, M., & Huang, R. (2014). Flood routing model with lateral coupling one-dimensional channel and two-dimensional floodplain simulation. *Shuikexue Jinzhan/Advances in Water Science*, 25(4), 560-566.

ANNEX

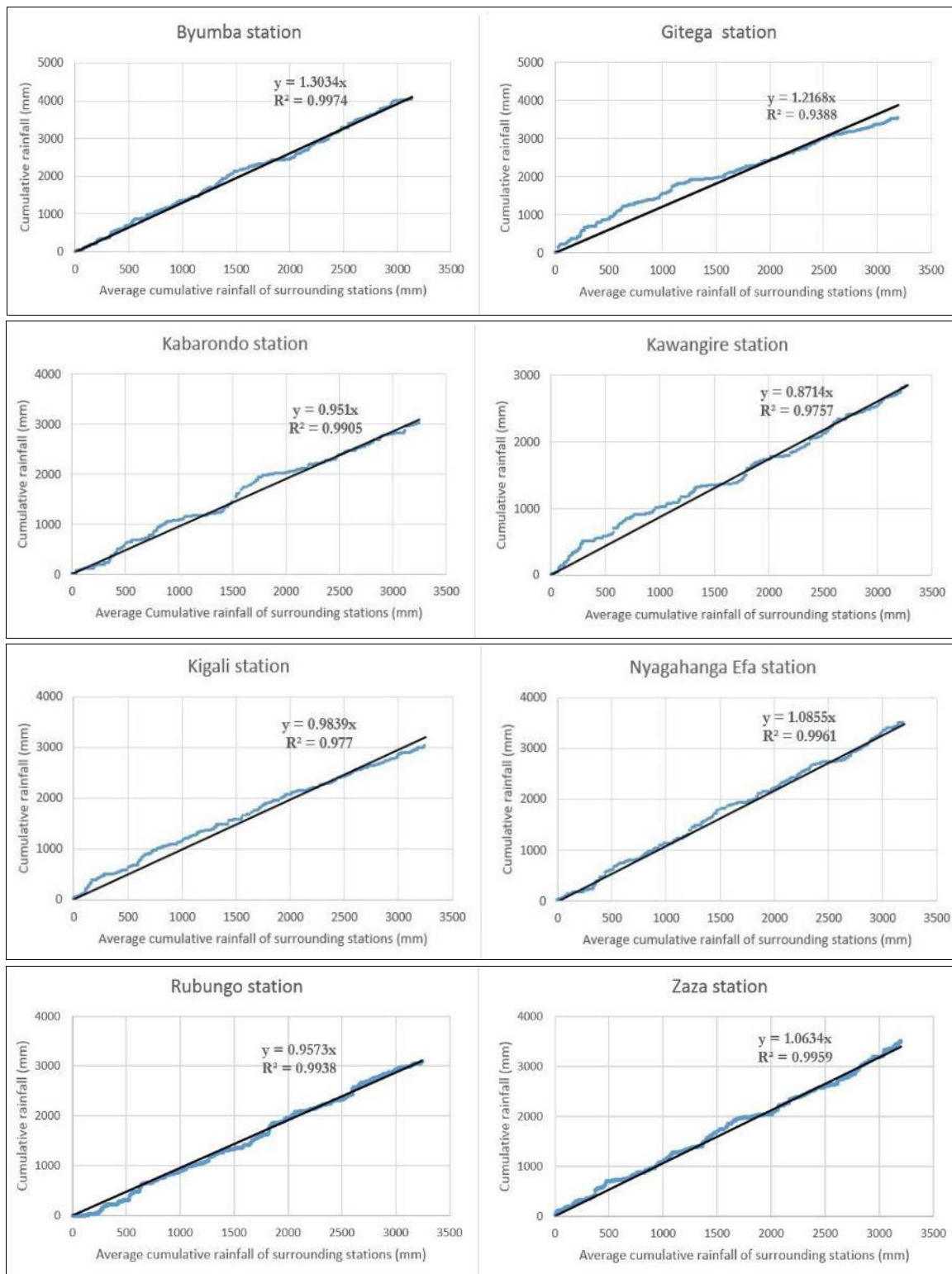
Annex A: Collected Rainfall data





Gitega meteorological station.

Annex B: Double Mass Curve of rainfall stations.



Annex C:

1. Simple linear regression

This method is used separately for the wet and dry seasons. It is adequate for rainfall data exhibiting strong correlation coefficients (refer to annex B). This method is known to operate on a pair of stations where one must be complete and the other incomplete must be strongly correlated to the complete one. The relation between these two stations is computed by linear regression as:

$$\mathbf{y}_t = \mathbf{a} + \mathbf{b}\mathbf{x}_t + \mathbf{a}\theta(1 - \rho)^{1/2}\sigma_y\boldsymbol{\varepsilon}_t, \quad 7-1$$

Where \mathbf{y}_t is the dependent variable (rainfall from the dependent station), \mathbf{x}_t is the dependent variable (rainfall from the independent station), \mathbf{a} & \mathbf{b} are the population parameters for the regression, σ_y is the population standard deviation, ρ is the cross correlation of two time series and $\boldsymbol{\varepsilon}_t$ is the normal uncorrected variable with mean 0 and variance 1 which is uncorrected with x_t .

The estimation of the parameters \mathbf{a} and \mathbf{b} are given by

$$\mathbf{a} = \bar{\mathbf{y}}_t - \mathbf{b}\bar{\mathbf{x}}, \quad 7-2$$

$$\mathbf{b} = r \frac{S_1(\mathbf{y})}{S_1(\mathbf{x})}, \quad 7-3$$

When just few records are missing, equation 31 without noise may be used for filling in the data i.e. $\boldsymbol{\varepsilon}_t$ ($\theta=0$), as was the case in this research. Since r is the cross correlation coefficient of the sample, it is then expressed as:

$$r = \frac{\sum(x_i - \bar{x})(y_i - \bar{y})}{\sqrt{\sum(x_i - \bar{x})^2 \sum(y_i - \bar{y})^2}} \quad 7-4$$

Where \mathbf{x}_i and \mathbf{y}_i are the rainfall records of the independent and the dependent stations, $\bar{\mathbf{y}}$ and $\bar{\mathbf{x}}$ are the estimated mean of the variable y_i and x_i ; and $S_1(\mathbf{y})$ and $S_1(\mathbf{x})$ are the corresponding estimated standard deviation of y_i and x_i .

2. Modified normal ratio

This a modified version of the normal ratio method. The normal ratio method is an aerial interpolation method used for daily rainfall filling in in case the inter station annual variation of rainfall is large (i.e. > 10%). It is suitable for regions with orographic effects. For this method, the erroneous or missing rainfall at the station under consideration is estimated as the weighted average of adjoining stations. Its mathematical form is:

$$\mathbf{y}_t = \left(\frac{\mu_y}{m}\right) \sum_{i=1}^m \frac{x_t^i}{\mu_x^i}, \quad 7-5$$

Where μ_y and μ_x are the sample mean with missing records and m series of completed records, respectively. X_i are some sample series with complete records at m nearby stations.

The modified normal ratio method incorporates the effects of distance between the stations to the equation 35. The resulting equation, which was applied in this research for gaps of more than a week, is of the form:

$$y_t = \frac{\sum_{i=1}^m D_i^{\frac{1}{b}} x_t^i \left(\frac{\mu_y}{\mu_x} \right)}{\sum_{i=1}^m D_i^{\frac{1}{b}}}, \quad 7-6$$

Where D_i is the distance between the indexed stations i and the base station with missing data. b is the distance weight and varies normally between 1.5 and 2 as reported by (Tang et al., 1996). The adequate value of b can be estimated through calibration and validation.

3. Simple rating curve fitting

The river section mostly plays a very important role in the shape of the rating curve, an explanation to that is the fact that at rising water stage different channel controls will govern the flow. The gauging stations locations observed on site were placed at locations of little scouring and no backwater effects, where in most cases the flow at the gauging stations are governed by the channel control. This situation led to opting for the simple rating curve fitting method. The principles underlining this method are simple to understand and apply. The power form equation of this method was selected as it is described to be the most commonly used form of the stage discharge relation. The power form equation is:

$$Q = c * (h + a)^b, \quad 7-7$$

Where Q is the discharge (L3T-1), h is the water level (L), a is the water level corresponding to zero flow and C and b are calibration coefficients. C is the discharge when the effective depth of flow ($h+a$) is equal to 1 and b is the rating curve slope on a logarithmic paper.

The following power equation can be transformed to a linear form using the logarithmic function to be:

$$\log Q = \log c + b \log(h + a), \quad 7-8$$

Or else $Y = \alpha + \beta X,$ 7-9

- Estimation of the parameter a :

The water level at zero flow is estimated in three different manner. In this case the arithmetic method (i.e. the Johnson method) was combined with the trial and error method to estimate the parameter a . The arithmetic method is based on the assumption that the product of a high flow and low flow is equal to the square of a medium flow. Mathematically it is written as:

$$Q_2^2 = Q_1 * Q_3, \quad 7-10$$

$$\frac{Q_2}{Q_1} = \frac{Q_3}{Q_2}, \quad 7-11$$

Where Q_1 is the low flow, Q_3 the high flow and Q_2 the median flow.

Replacing every flow in equation 7-11 by their value from equation 7-7, and applying simple arithmetical operations, the following relation is obtained:

$$\mathbf{a} = \frac{h_2^2 - h_1 h_3}{h_1 + h_3 - 2h_2} \quad 7-12$$

With the above formula, an estimate of the water level at zero flow is obtained. The latter is optimized with trial and error method consisting of fine tuning the value of \mathbf{a} until the double logarithmic plot of the rating curve becomes a straight line. If it is a curved line, the value of \mathbf{a} is increased or decreased depending on if the concavity of the curved line is negative or positive respectively.

- Estimation of the parameters \mathbf{c} and \mathbf{b} :

The least square method is used for estimating the parameters \mathbf{c} and \mathbf{b} from the equation 7-8. The least square method minimizes the sum of square of deviations between the logarithms of measured discharges (\mathbf{Y}_i) and the estimated discharges ($\widehat{\mathbf{Y}}_i$) obtained from the fitted rating curve. Since this error is to be minimum, therefore the partial derivatives slope of this error with respect to the constants must also be zero. Mathematically, this is expressed as follows:

$$E = \sum_{i=1}^N (\mathbf{Y}_i - \widehat{\mathbf{Y}}_i)^2 = \sum_{i=1}^N (\mathbf{Y}_i - \alpha - \beta \mathbf{X}_i)^2, \quad 7-13$$

$$\frac{\partial E}{\partial \alpha} = \frac{\partial \{\sum_{i=1}^N (\mathbf{Y}_i - \alpha - \beta \mathbf{X}_i)^2\}}{\partial \alpha} = \mathbf{0}, \quad 7-14$$

And

$$\frac{\partial E}{\partial \beta} = \frac{\partial \{\sum_{i=1}^N (\mathbf{Y}_i - \alpha - \beta \mathbf{X}_i)^2\}}{\partial \beta} = \mathbf{0}, \quad 7-15$$

The above expressions result in the two algebraic equations shown below:

$$\sum_{i=1}^N \mathbf{Y}_i - \alpha N - \beta \sum_{i=1}^N \mathbf{X}_i = \mathbf{0}, \quad 7-16$$

And

$$\sum_{i=1}^N (\mathbf{X}_i \mathbf{Y}_i) - \alpha \sum_{i=1}^N \mathbf{X}_i - \beta \sum_{i=1}^N (\mathbf{X}_i)^2 = \mathbf{0}, \quad 7-17$$

Since α and β are the only unknown in the equations above, they can easily be determined as:

$$\beta = \frac{N \sum_{i=1}^N (\mathbf{X}_i \mathbf{Y}_i) - (\sum_{i=1}^N \mathbf{X}_i)(\sum_{i=1}^N \mathbf{Y}_i)}{N \sum_{i=1}^N (\mathbf{X}_i)^2 - (\sum_{i=1}^N \mathbf{X}_i)^2}, \quad 7-18$$

And

$$\alpha = \frac{\sum_{i=1}^N \mathbf{Y}_i - \beta \sum_{i=1}^N \mathbf{X}_i}{N}, \quad 7-19$$

The coefficients \mathbf{c} and \mathbf{b} of the power equation can then finally be obtained as:

$$\mathbf{c} = 10^\alpha \text{ and } \mathbf{b} = \beta \quad 7-20$$

Annex D



Flow measurement using an ADCP device.



Confluence Nyabugogo-Nyabarongo River (free flow condition is observed).



Nyabugogo gauging station.